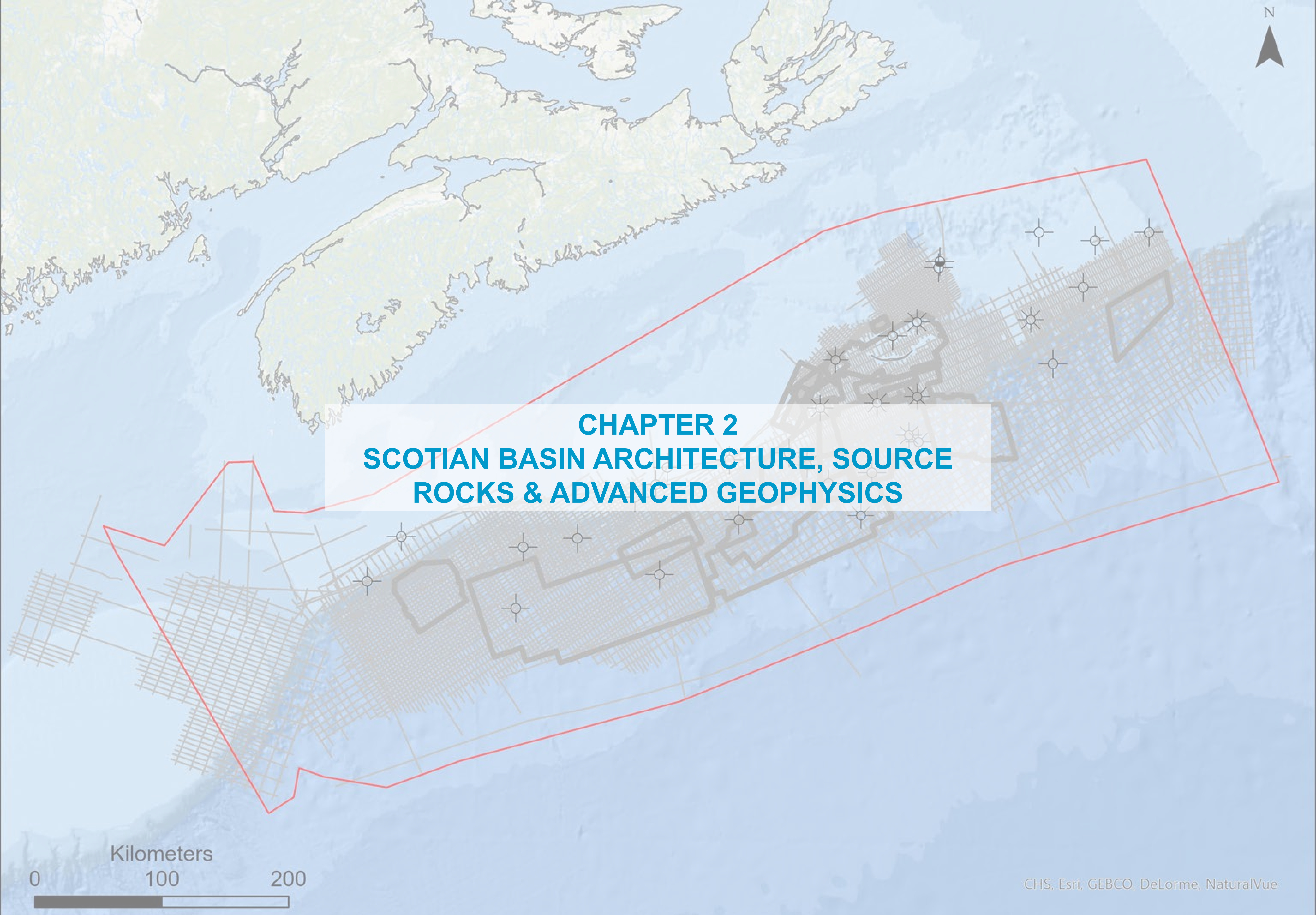

CHAPTER 2

SCOTIAN BASIN ARCHITECTURE, SOURCE ROCKS & ADVANCED GEOPHYSICS

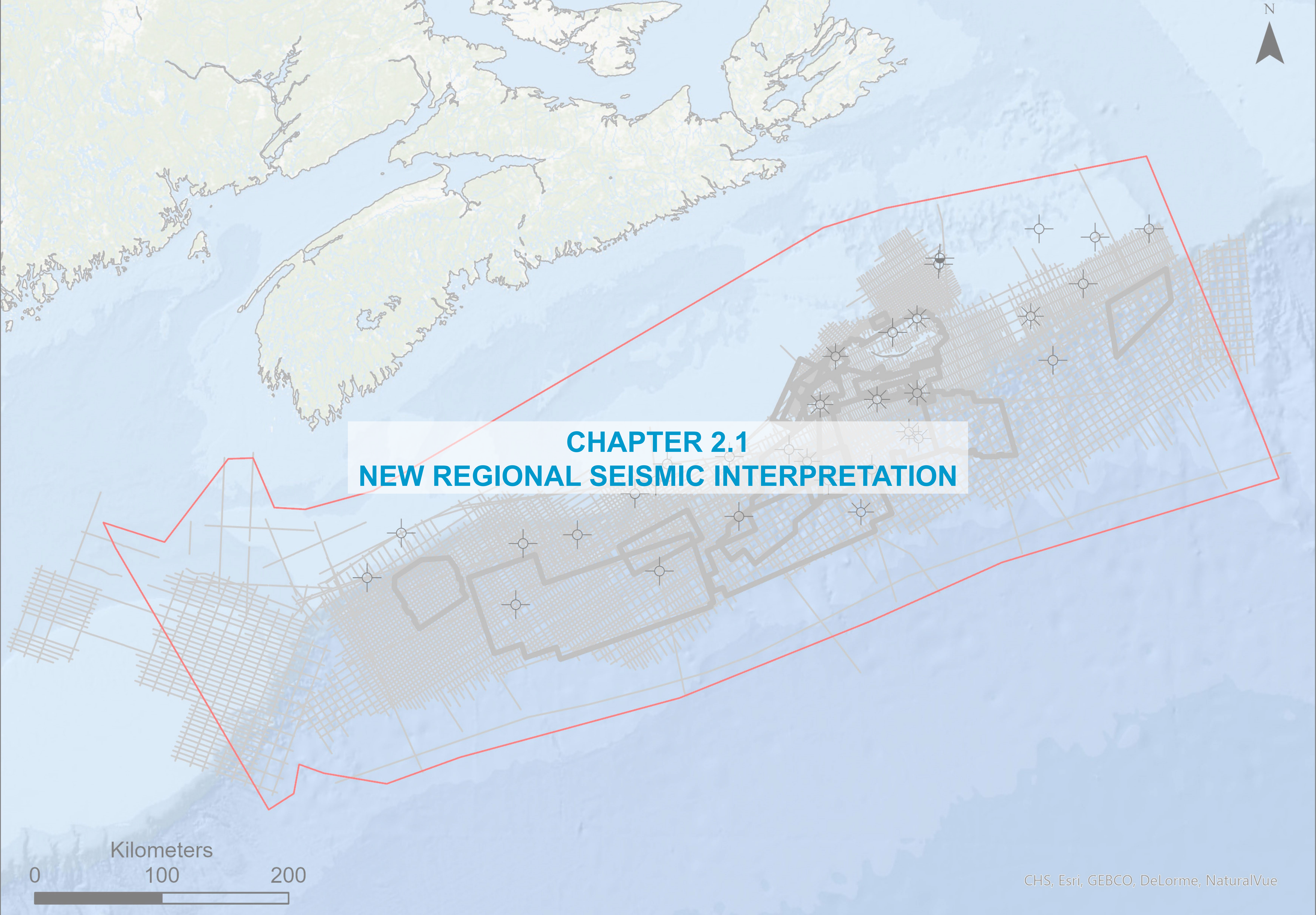

CHAPTER 2.1
NEW REGIONAL SEISMIC INTERPRETATION

Study Area

A broad spectrum of reflection seismic data-sets collected over the past five decades provides extensive coverage across the Scotian Basin. Notably, renewed exploration interest since 2012 resulted in the acquisition of two large wide-azimuth 3D reflection seismic volumes on the central to western Scotian Slope (Shelburne 3D and Tangier 3D), and the drilling of three wildcat exploration wells (Cheshire L-97/L-97A, Monterey Jack E-43/E-43A, and Aspy D-11/D-11A). These modern seismic surveys, coupled with seven older 3D seismic volumes, provided more than 29 000 km2 of near-continuous 3D seismic coverage for the SCOPE Atlas published in 2020 (Deptuck and Kendell 2020). The atlas presents an updated view of the seismic stratigraphy of the Shelburne and western Sable Subbasins, with new well control enabling, for the first time, high-confidence correlation of post-Bajocian strata across wide areas of the continental slope.

In this study, the framework markers presented in the SCOPE Atlas were expanded into surrounding areas, using all available data. Direct ties to Monterey Jack E-43 and Cheshire L-97 made it possible to correlate the seismic stratigraphic framework onto the slope seaward of the salt basin, where the absence of salt diapirs enabled seismic markers to be correlated towards the northeast. This provided an additional constraint on the age of seismic markers for areas like the eastern Scotian Slope where there is very little well calibration, and where correlations across the shelf (where more well control is available), are hindered by densely spaced listric faults and poor seismic imaging.

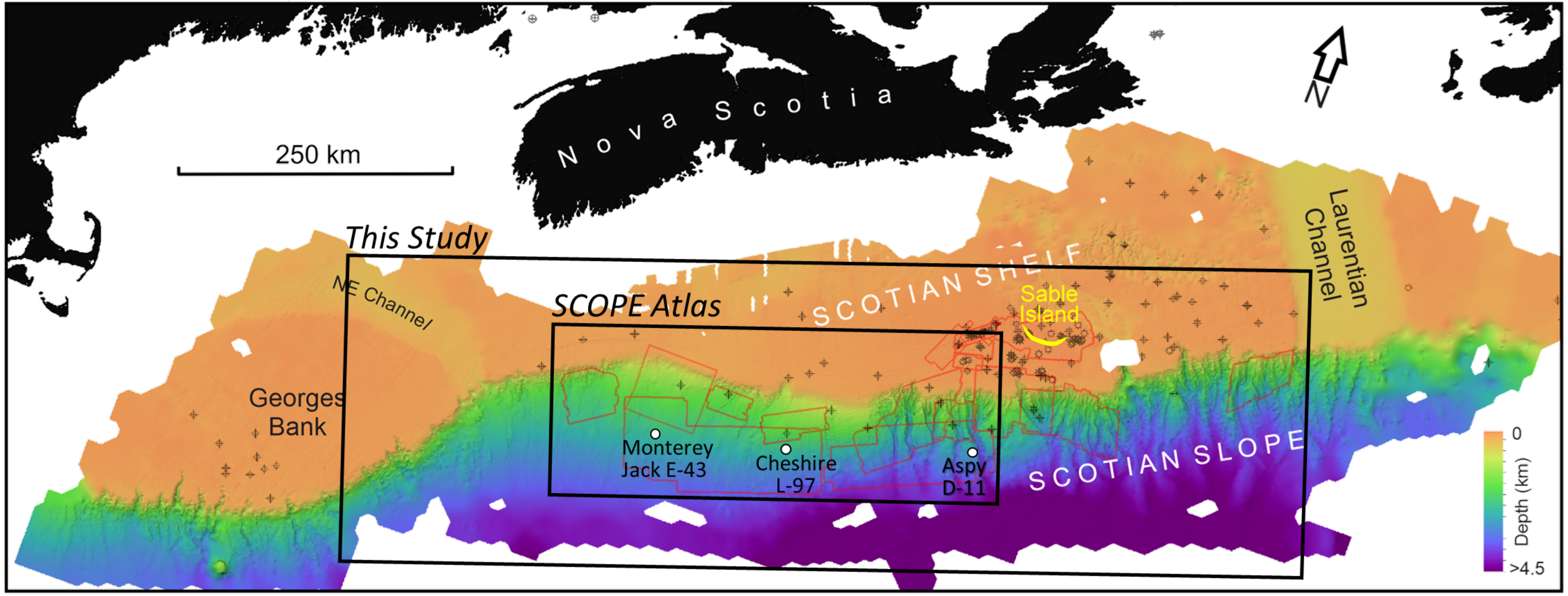

▽ Seafloor structure (3D seismic volumes shown in red)

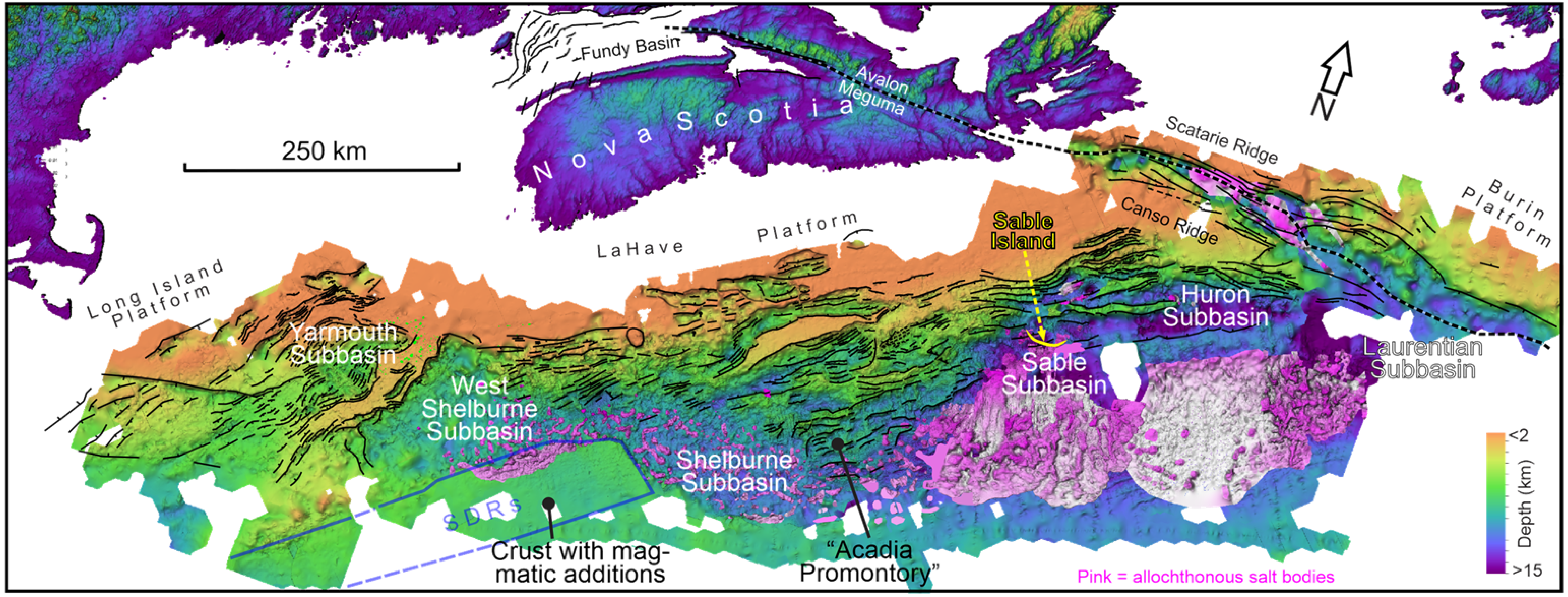

▽ Top basement structure showing basement faults and the top allochthonous salt grid

Figure 1: Study area in relation to the top basement structure map (*lower*) and the modern seabed (*upper*).

New Regional Seismic Interpretation

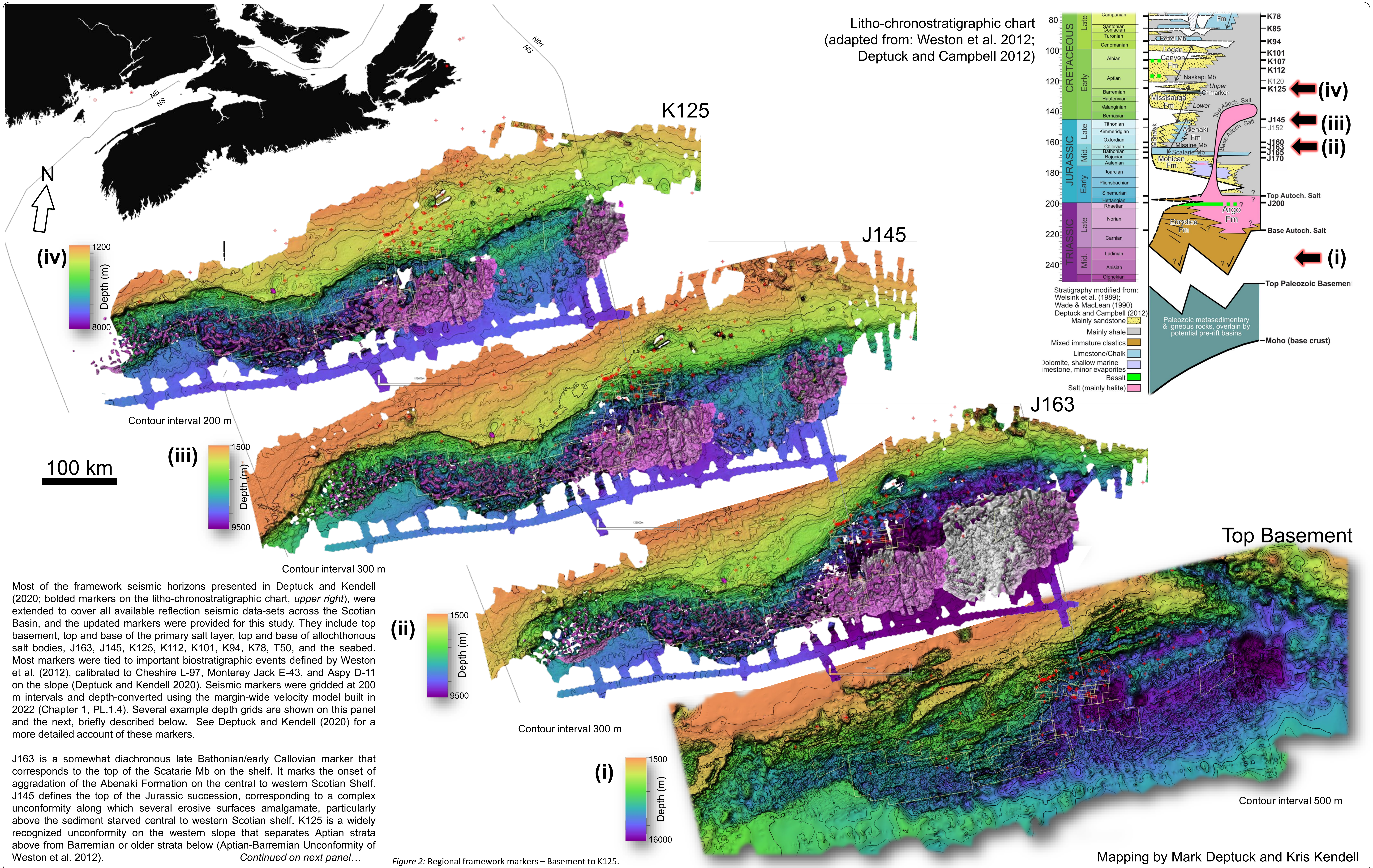

Most of the framework seismic horizons presented in Deptuck and Kendell (2020; bolded markers on the litho-chronostratigraphic chart, *upper right*), were extended to cover all available reflection seismic data-sets across the Scotian Basin, and the updated markers were provided for this study. They include top basement, top and base of the primary salt layer, top and base of allochthonous salt bodies, J163, J145, K125, K112, K101, K94, K78, T50, and the seabed. Most markers were tied to important biostratigraphic events defined by Weston et al. (2012), calibrated to Cheshire L-97, Monterey Jack E-43, and Aspy D-11 on the slope (Deptuck and Kendell 2020). Seismic markers were gridded at 200 m intervals and depth-converted using the margin-wide velocity model built in 2022 (Chapter 1, PL.1.4). Several example depth grids are shown on this panel and the next, briefly described below. See Deptuck and Kendell (2020) for a more detailed account of these markers.

J163 is a somewhat diachronous late Bathonian/early Callovian marker that corresponds to the top of the Scatarie Mb on the shelf. It marks the onset of aggradation of the Abenaki Formation on the central to western Scotian Shelf. J145 defines the top of the Jurassic succession, corresponding to a complex unconformity along which several erosive surfaces amalgamate, particularly above the sediment starved central to western Scotian shelf. K125 is a widely recognized unconformity on the western slope that separates Aptian strata above from Barremian or older strata below (Aptian-Barremian Unconformity of Weston et al. 2012).

Continued on next panel…

Figure 2: Regional framework markers – Basement to K125.

Mapping by Mark Deptuck and Kris Kendell

Regional Framework Markers

New Regional Seismic Interpretation

Scotian Basin Integration Atlas 2023 – CANADA – June 2023

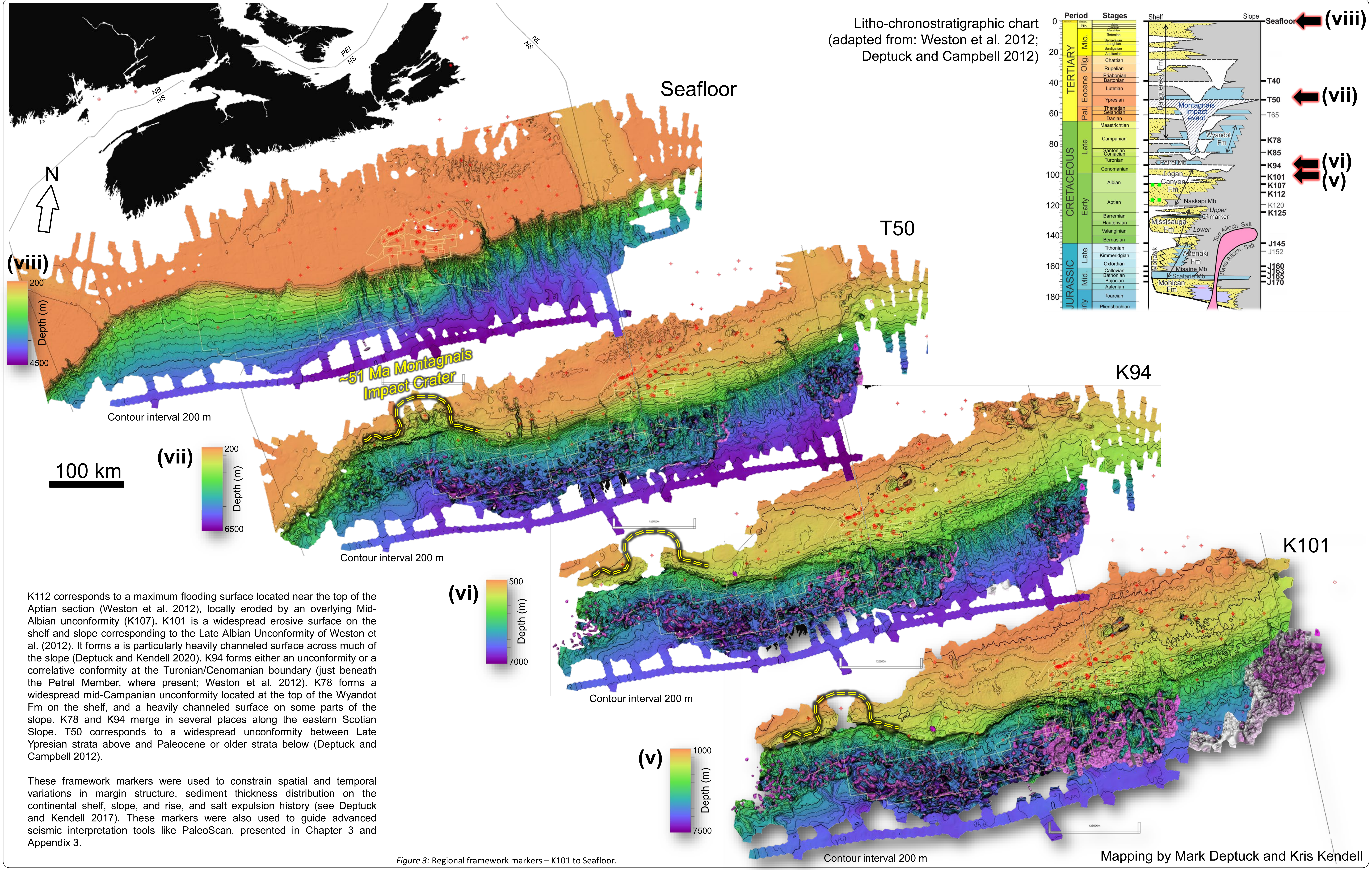

K112 corresponds to a maximum flooding surface located near the top of the Aptian section (Weston et al. 2012), locally eroded by an overlying Mid-Albian unconformity (K107). K101 is a widespread erosive surface on the shelf and slope corresponding to the Late Albian Unconformity of Weston et al. (2012). It forms a is particularly heavily channeled surface across much of the slope (Deptuck and Kendell 2020). K94 forms either an unconformity or a correlative conformity at the Turonian/Cenomanian boundary (just beneath the Petrel Member, where present; Weston et al. 2012). K78 forms a widespread mid-Campanian unconformity located at the top of the Wyandot Fm on the shelf, and a heavily channeled surface on some parts of the slope. K78 and K94 merge in several places along the eastern Scotian Slope. T50 corresponds to a widespread unconformity between Late Ypresian strata above and Paleocene or older strata below (Deptuck and Campbell 2012).

These framework markers were used to constrain spatial and temporal variations in margin structure, sediment thickness distribution on the continental shelf, slope, and rise, and salt expulsion history (see Deptuck and Kendell 2017). These markers were also used to guide advanced seismic interpretation tools like PaleoScan, presented in Chapter 3 and Appendix 3.

Figure 3: Regional framework markers – K101 to Seafloor.

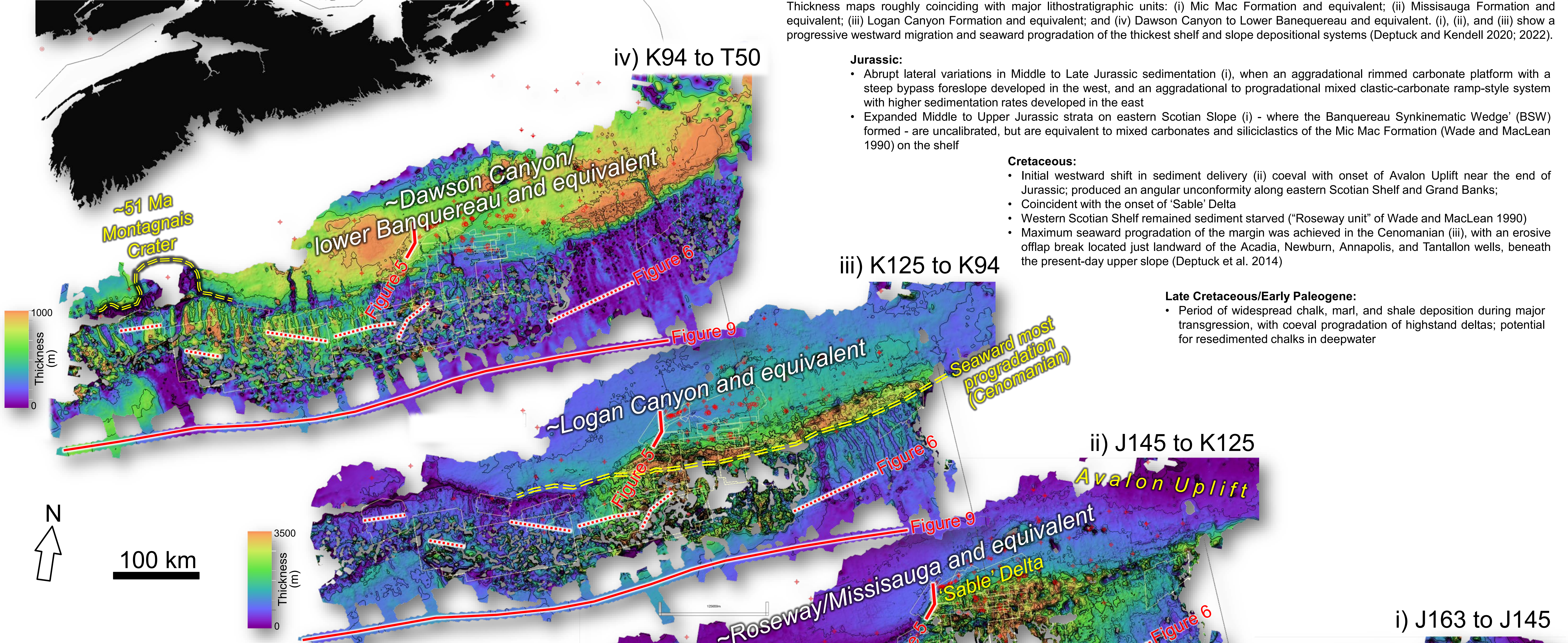

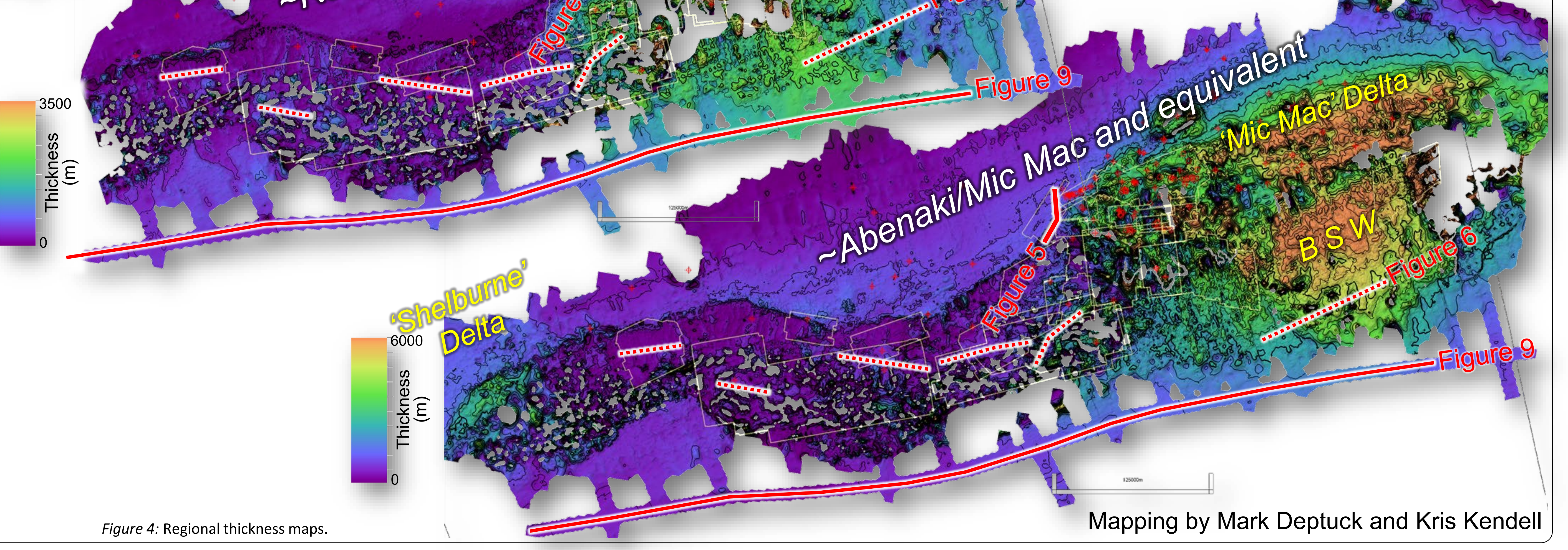

Figure 4: Regional thickness maps.

Thickness maps roughly coinciding with major lithostratigraphic units: (i) Mic Mac Formation and equivalent; (ii) Missisauga Formation and equivalent; (iii) Logan Canyon Formation and equivalent; and (iv) Dawson Canyon to Lower Banequereau and equivalent. (i), (ii), and (iii) show a progressive westward migration and seaward progradation of the thickest shelf and slope depositional systems (Deptuck and Kendell 2020; 2022).

Jurassic:

- Abrupt lateral variations in Middle to Late Jurassic sedimentation (i), when an aggradational rimmed carbonate platform with a steep bypass foreslope developed in the west, and an aggradational to progradational mixed clastic-carbonate ramp-style system with higher sedimentation rates developed in the east
- Expanded Middle to Upper Jurassic strata on eastern Scotian Slope (i) - where the Banquereau Synkinematic Wedge' (BSW) formed - are uncalibrated, but are equivalent to mixed carbonates and siliciclastics of the Mic Mac Formation (Wade and MacLean 1990) on the shelf

Cretaceous:

- Initial westward shift in sediment delivery (ii) coeval with onset of Avalon Uplift near the end of Jurassic; produced an angular unconformity along eastern Scotian Shelf and Grand Banks;
- Coincident with the onset of 'Sable' Delta
- Western Scotian Shelf remained sediment starved ("Roseway unit" of Wade and MacLean 1990)
- Maximum seaward progradation of the margin was achieved in the Cenomanian (iii), with an erosive offlap break located just landward of the Acadia, Newburn, Annapolis, and Tantallon wells, beneath the present-day upper slope (Deptuck et al. 2014)

Late Cretaceous/Early Paleogene:

- Period of widespread chalk, marl, and shale deposition during major transgression, with coeval progradation of highstand deltas; potential for resedimented chalks in deepwater

Inset:

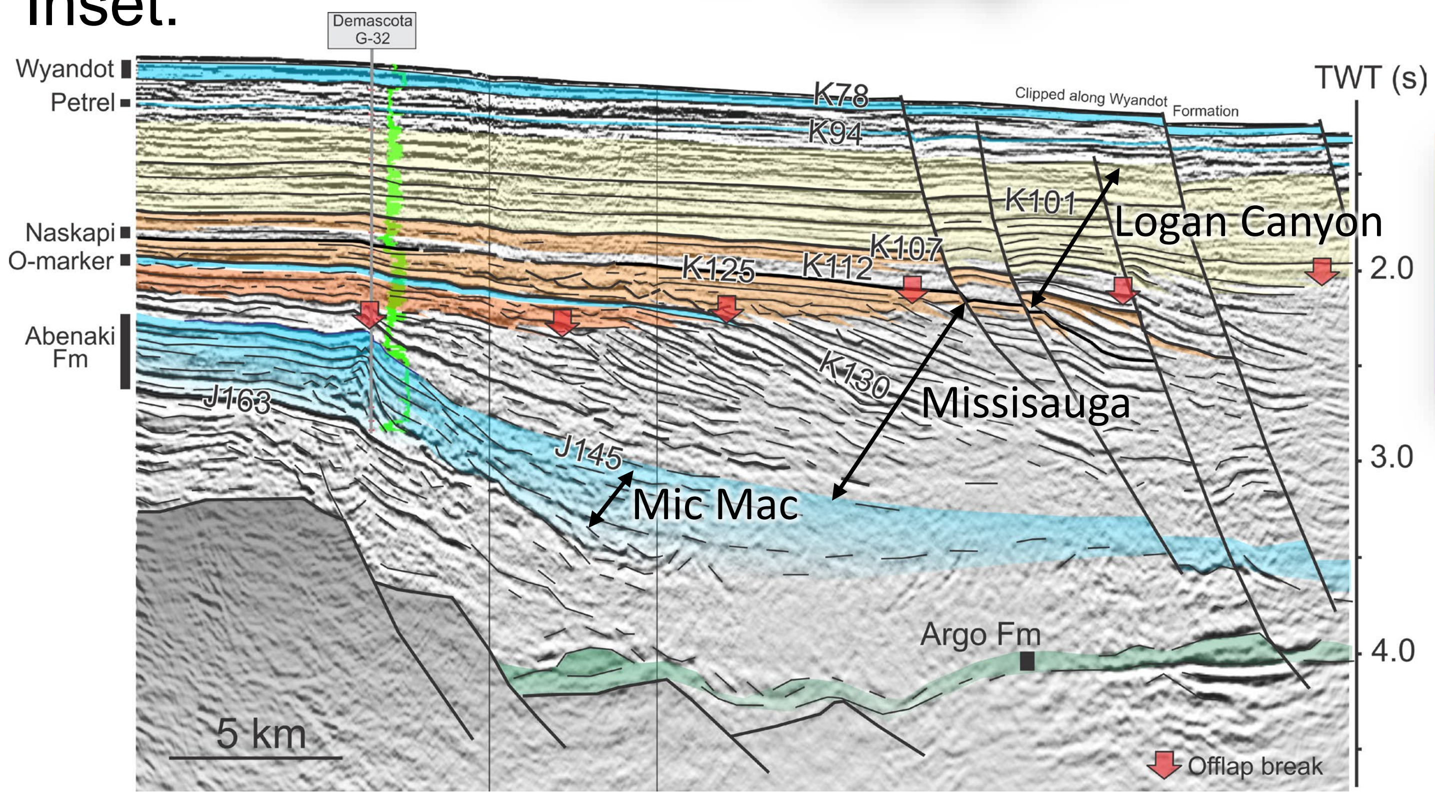

Figure 5: Composite seismic section parallel to the direction of Cretaceous sediment transport in the Sable Delta. Note the southward advance of the constructional offlap-break (red arrows) though several transgressive-regressive cycles (Modified from Deptuck 2008).

Mapping by Mark Deptuck and Kris Kendell

Abrupt lateral variations in Middle Jurassic to Paleogene sediment thickness on the shelf and slope

New Regional Seismic Interpretation

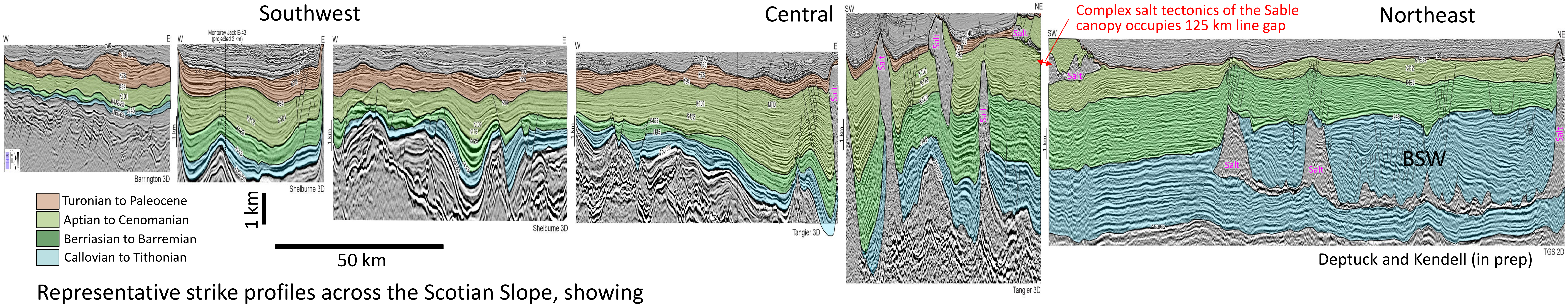

Deptuck and Kendell (in prep)

Representative strike profiles across the Scotian Slope, showing significant lateral variations in sediment thickness

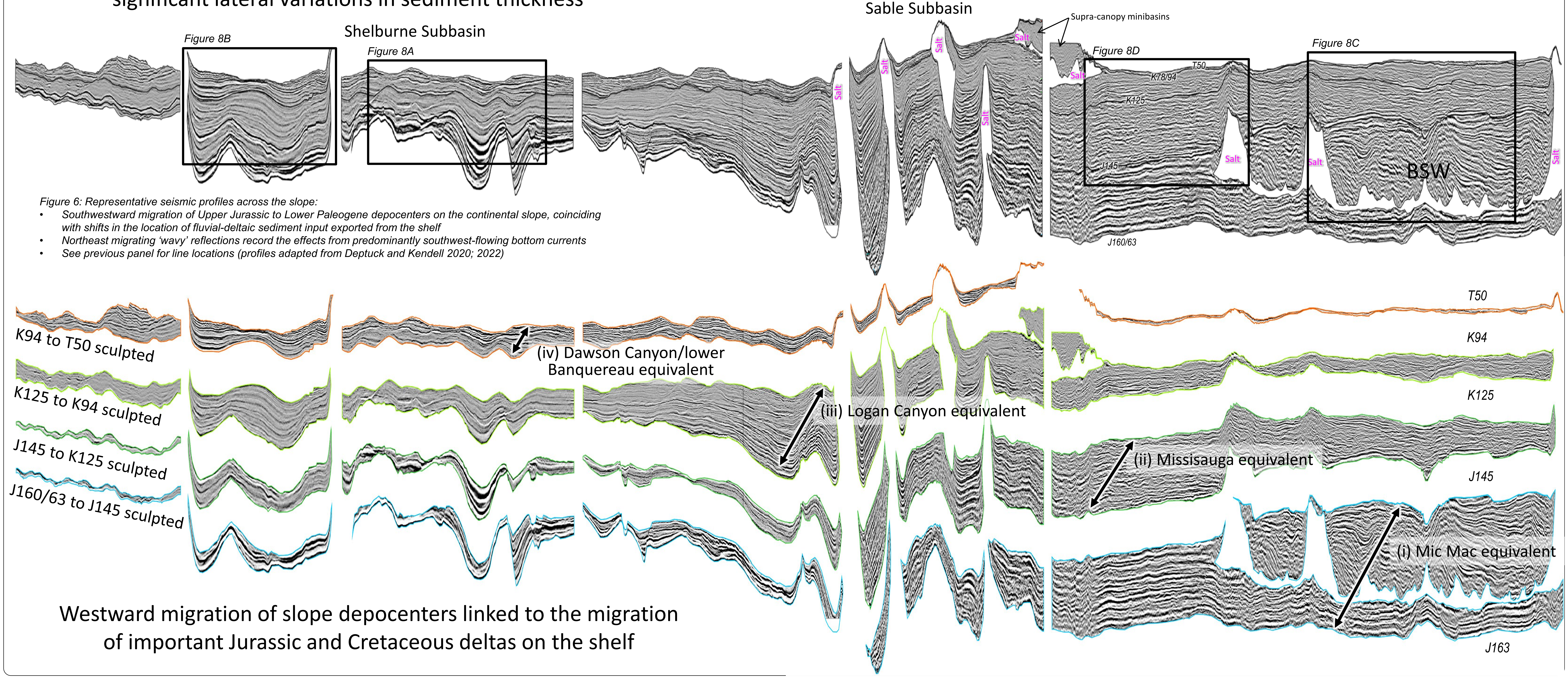

Figure 6: Representative seismic profiles across the slope:

- *Southwestward migration of Upper Jurassic to Lower Paleogene depocenters on the continental slope, coinciding with shifts in the location of fluvial-deltaic sediment input exported from the shelf*
- *Northeast migrating 'wavy' reflections record the effects from predominantly southwest-flowing bottom currents*
- *See previous panel for line locations (profiles adapted from Deptuck and Kendell 2020; 2022)*

Westward migration of slope depocenters linked to the migration of important Jurassic and Cretaceous deltas on the shelf

Abrupt Lateral Variations in Middle Jurassic to Paleogene Sediment Thickness on the Slope

Strong Lateral Variations in Sediment Thickness and Seismic Facies

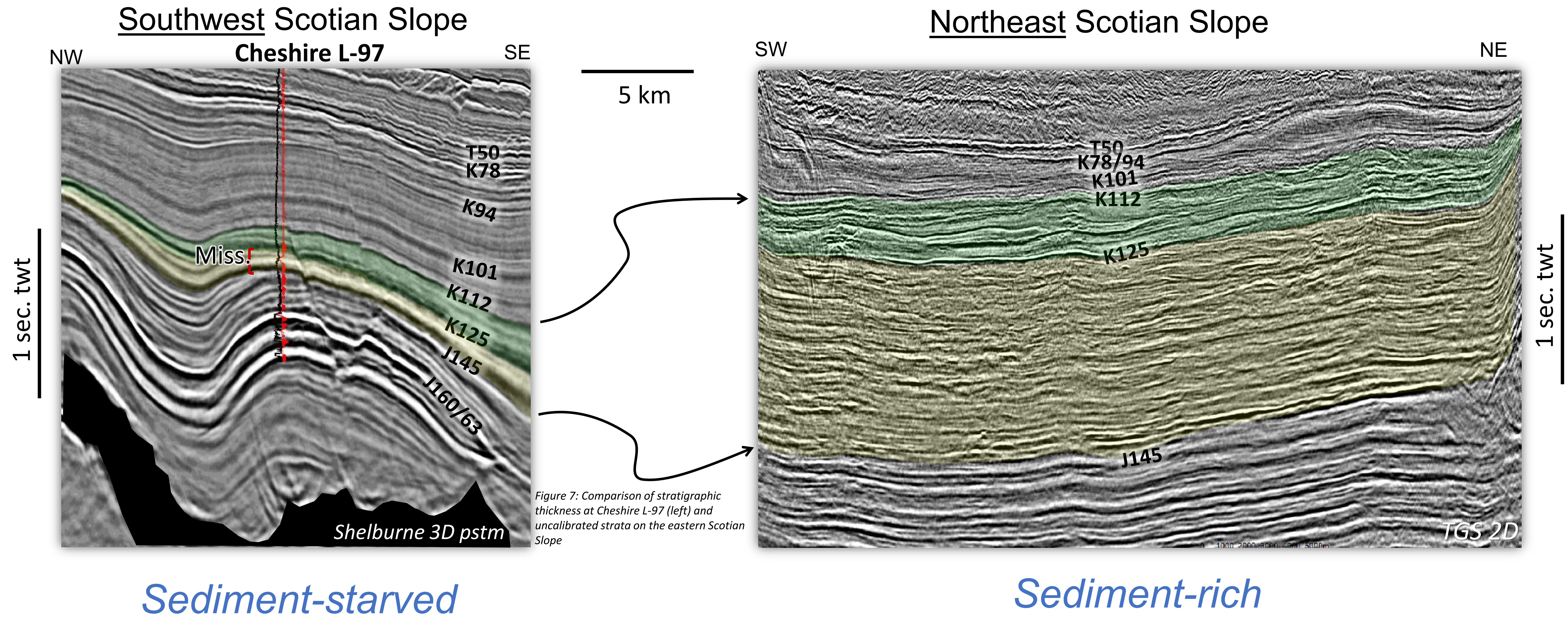

Figure 7: Comparison of stratigraphic thickness at Cheshire L-97 (left) and uncalibrated strata on the eastern Scotian Slope

Implications for reservoir distribution (from Deptuck and Kendell 2020)
The scarcity of reservoirs and lack of hydrocarbons in the Cheshire and Monterey Jack wells in the Shelburne Subbasin (western Scotian Slope), sharply contrast the Newburn, Aspy, and Annapolis wells in the distal Sable Subbasin (central Scotian Slope) that encountered both turbidite reservoirs and hydrocarbons (gas and condensate). There are clear patterns in the distribution and style of mid-Jurassic to Cretaceous slope sedimentation, reservoir expectations, as well as linkage to shelf depositional systems across the study area. Prolific development of fluvial-deltaic systems on the shelf (e.g. Sable Subbasin), clearly favours reservoir development on the slope, supported by the sharp along-strike contrasts in both seismic facies and sediment thickness on the slope. There is also widespread evidence for bottom current reworking and synchronous interactions as sediment was exported from the shelf and down the slope. See the following panel for a comparison between seismic facies produced on sediment-starved versus sediment-rich slope segments, with sustained bottom-current reworking. Some of these spatial/temporal patterns are highlighted below and described in more detail on related panels.

Southwest:	**Central to Northeast:**
• J163 to K112 - sediment-starved Mid-Jurassic to Lower Cretaceous slope succession (condensed Abenaki to Missisauga-equivalent strata)	• J163 to K112 - voluminous Mid-Jurassic to Lower Cretaceous sediment supply (reflecting Mic Mac/Sable fluvial-deltaic input) and equivalent accumulation on the slope
• Sediment transport perpendicular to carbonate bank; strongly influenced by vertical salt stocks on the lower slope	• North-south sediment transport (parallel to Mic Mac and Sable Delta progradation direction), strongly influenced by seaward-leaning salt feeders and salt canopies
• J145 to K112 surfaces converge above the low-accommodation upper slope, producing an erosive, amalgamated or condensed slope bypass assemblage; 8 to 10 periods of widespread channel incision with little or no channel aggradation until the distal parts of the salt basin	• J145 to K112 expanded section, with clear aggradation of turbidite channel-belts intermixed with lobe sheet sands or aprons; cores from the Tantallon well (northeastern upper slope) encountered hundreds of stacked fine-grained turbidites consistent with deposits from a channel overbank setting
• Increased K101 to T50 aggradation above the slope, probably reflecting increased sediment export as clastic shelf depositional systems migrated/prograded westward, but also potentially reflecting the increased transport of fines by southwest-flowing bottom currents	• Decreased K112 to T50 aggradation above the slope northeastern slope (in particular), potentially reflecting winnowing of fines by southwest-flowing bottom currents
• Strong evidence for post-K125 SW-flowing bottom currents sweeping upper slope and abyssal plain; clear eastward migration of successive slope channels/corridors and "sediment wave like" intercanyon highs (hybrid contourite-turbidite systems); giant hybrid turbidite/contourite channels seaward of salt basin	• Strong evidence for post-K130 bottom currents sweeping upper slope to abyssal plain (area seaward of salt basin); bottom current effects partly masked by much high sedimentation rates and more complex salt-related deformation, but clear unilateral migration of aggradational hybrid channel-levee systems, with indications of reworked lobe deposits
• Salt tectonics - mainly salt diapirs/walls, with episodic salt movement triggered by canyon incisions that unroof stalled/buried salt bodies ("diapir liberation" - some canyon reaches occupied by salt)	• Salt tectonics driven by N-S sedimentation from Sable Delta (diapirs with common salt overhangs, salt tongues, amalgamated canopies, and roho systems); large Jurassic salt-based detachment further east (Banquereau Synkinematic Wedge – BSW)
• K94 to T50 - widespread erosive surfaces separated by periods of chalk, marl, and calcareous mudstone aggradation; increased potential for resedimented chalk reservoirs	• K94 to T50 – erosionally condensed; merger of K78 with K94, potentially reflecting enhanced abrasion from bottom current

Sediment-Starved vs. Sediment-Rich Slope Segments

Strong Lateral Variations in Sediment Thickness and Seismic Facies

Bottom current reworking on sediment-starved slope….

Southwest Scotian Slope

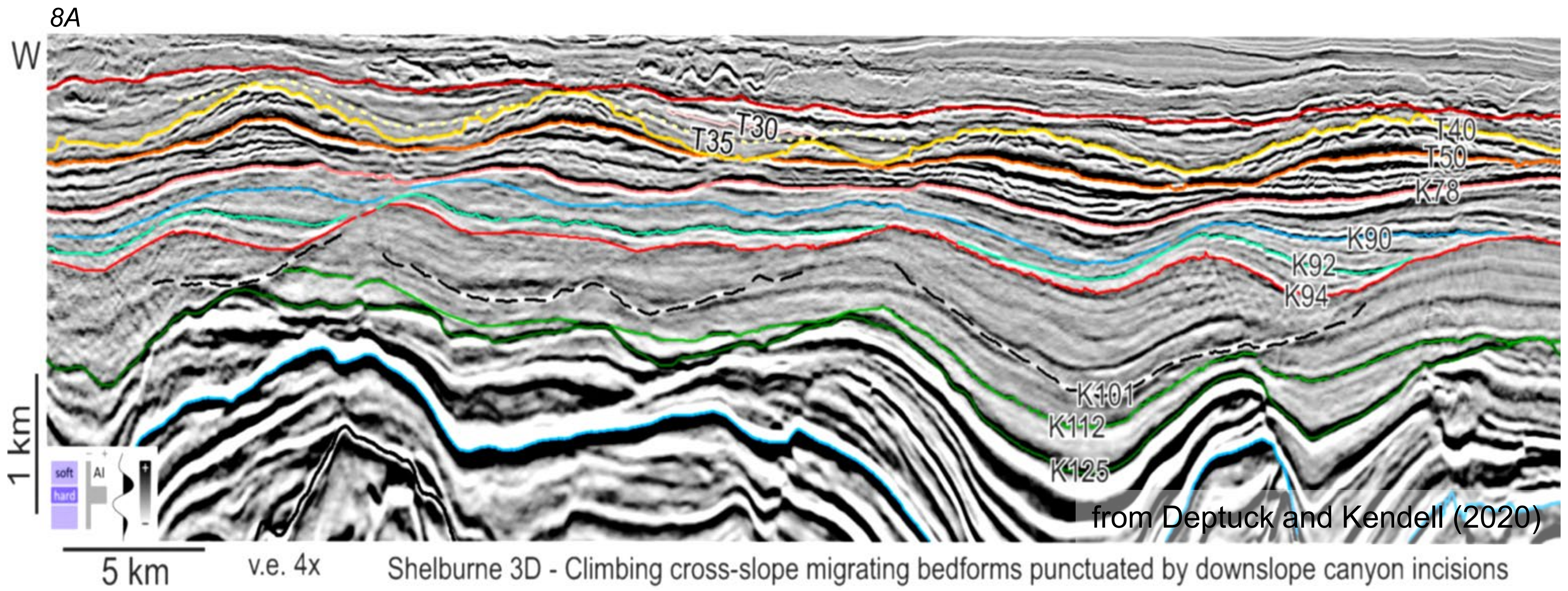

Shelburne 3D - Climbing cross-slope migrating bedforms punctuated by downslope canyon incisions

'Unidirectional migration' is a key characteristic of bottom-current influenced deepwater systems

Profile across **Monterey Jack E-43**

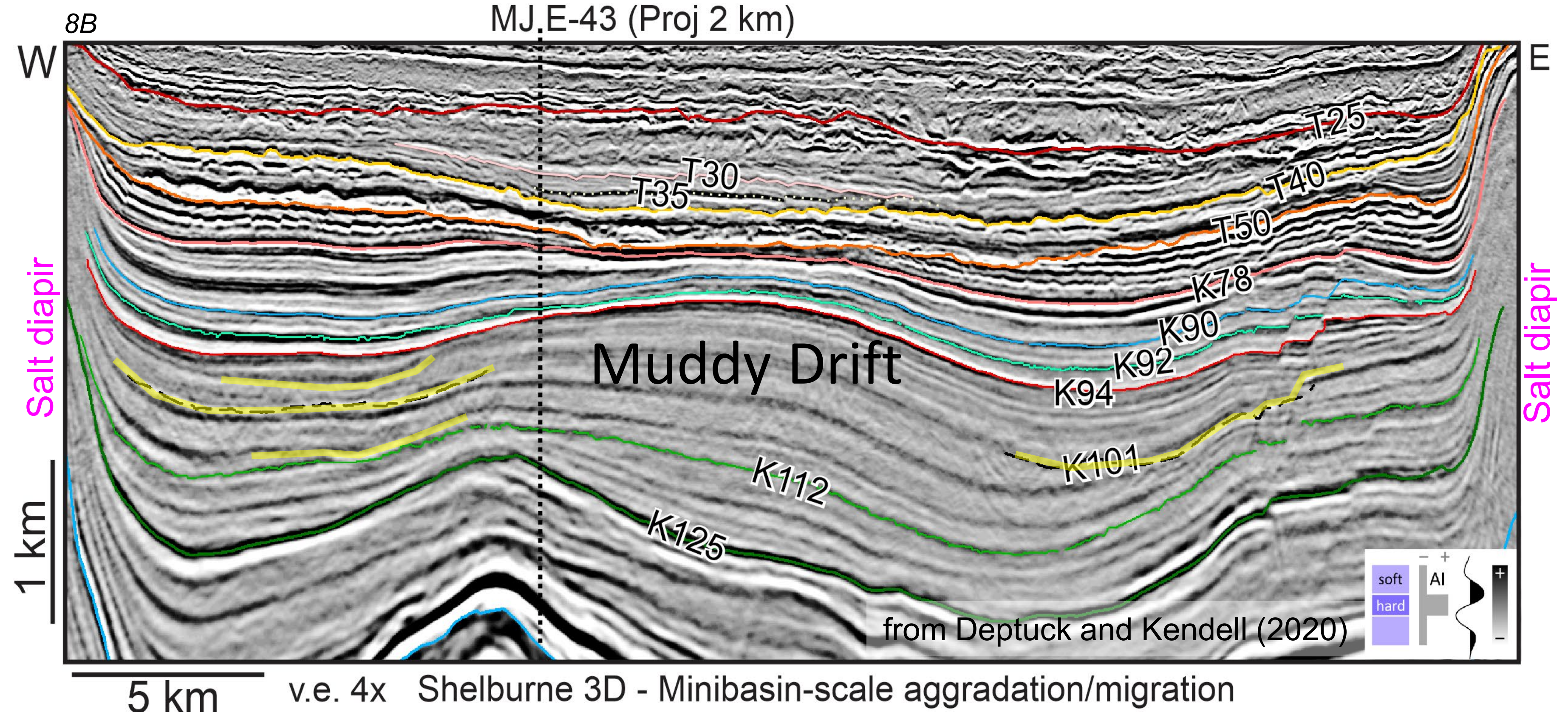

Shelburne 3D - Minibasin-scale aggradation/migration

Figure 8 : Comparison of seismic facies along the western Scotian Slope and uncalibrated strata on the eastern Scotian Slope – both affected by southwest-flowing bottom currents. The latter show much more complicated seismic facies, corresponding to Lower Cretaceous submarine fans

Drift avoidance – Thick at the center of minibasin is mud-prone; better sand potential along diapir margins; amp extractions show potential sands along channel axes confined between salt diapirs and drift crests (e.g. yellow scours between K112 and K94)

Sediment-starved

Bottom current reworking on sediment-rich slope….

Northeast Scotian Slope

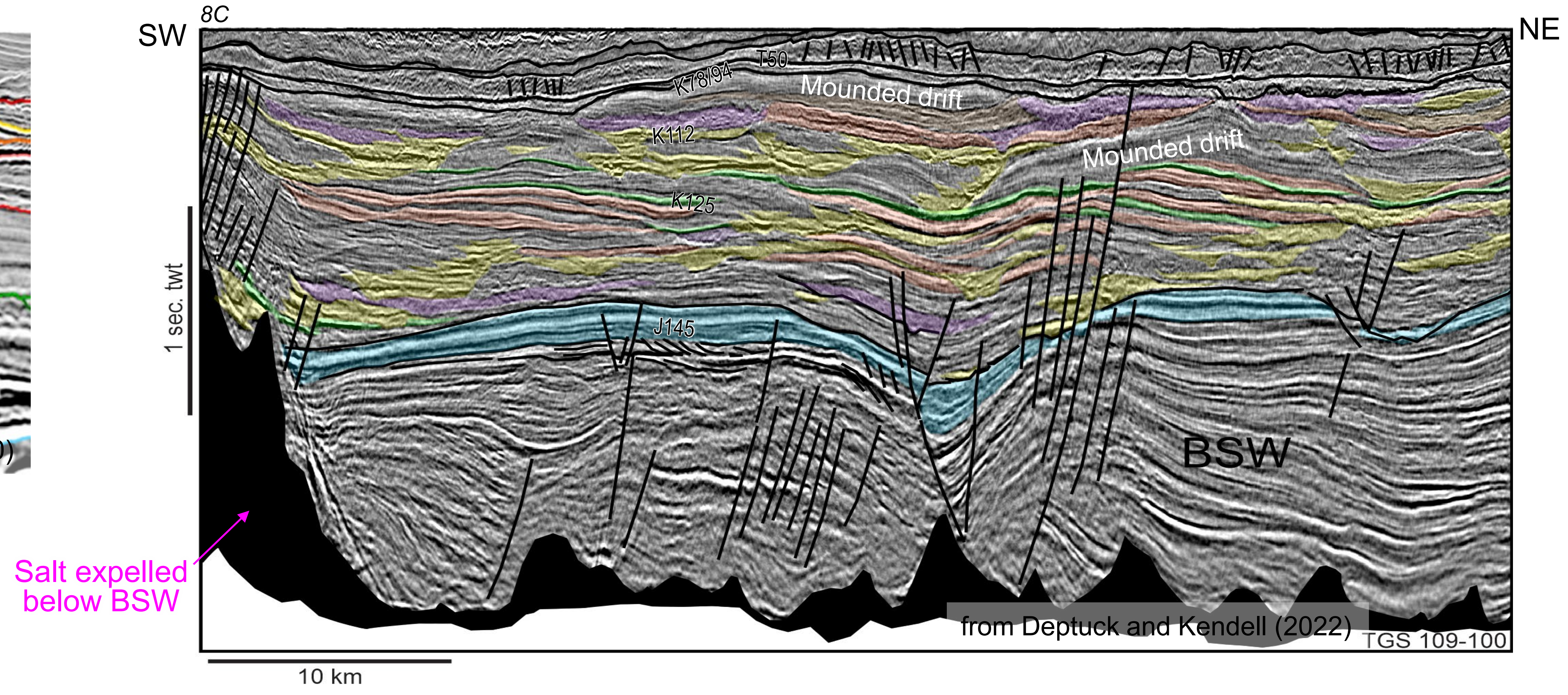

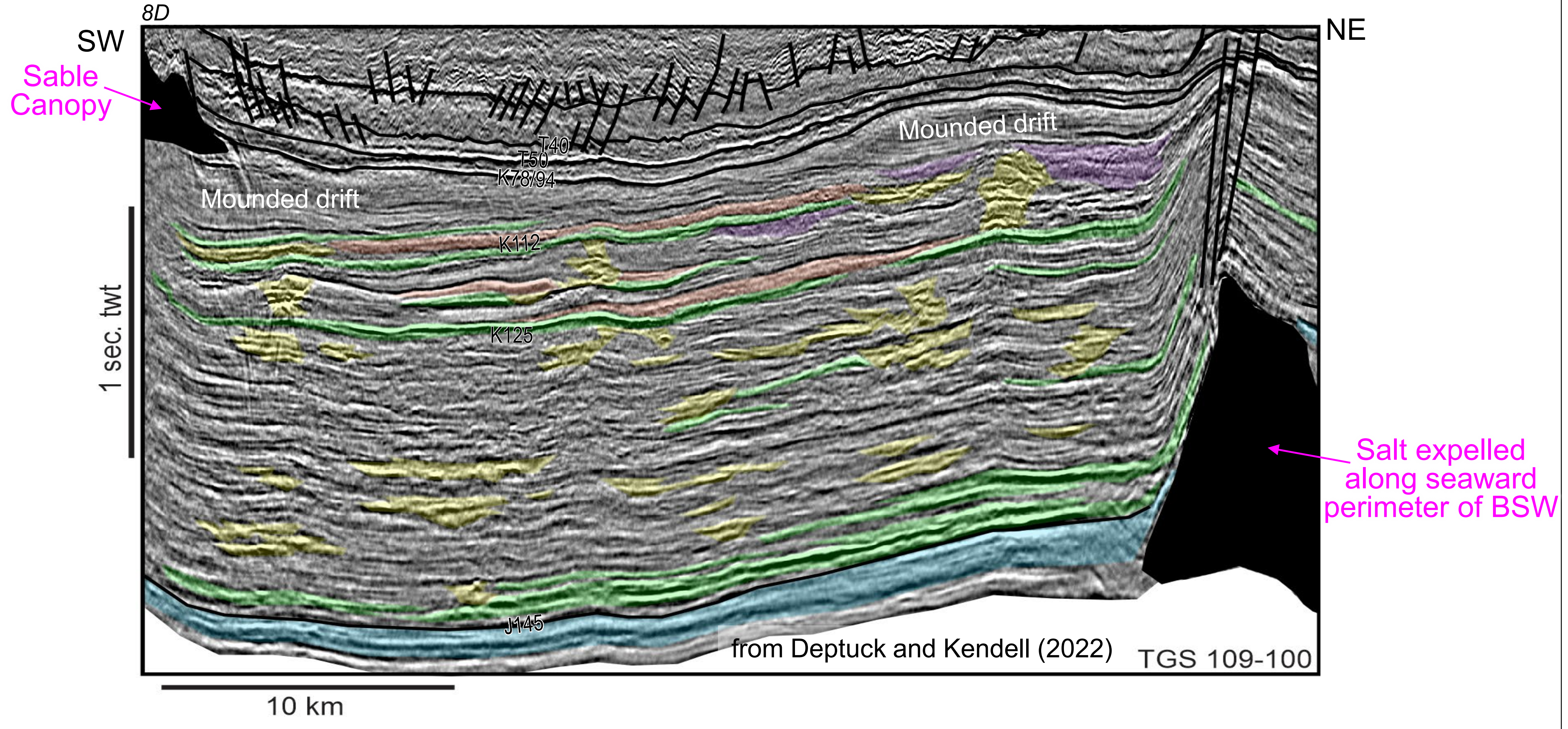

- 🟪 Mass transport deposit
- 🟥 Reworked lobe or levee facies?
- 🟨 Channel belt deposits
- 🟩 HARP or lobe sands
- 🟦 Latest Jurassic strata (eroded carbonates?)

Sediment-rich

Sediment-Starved vs. Sediment-Rich Slope Segments

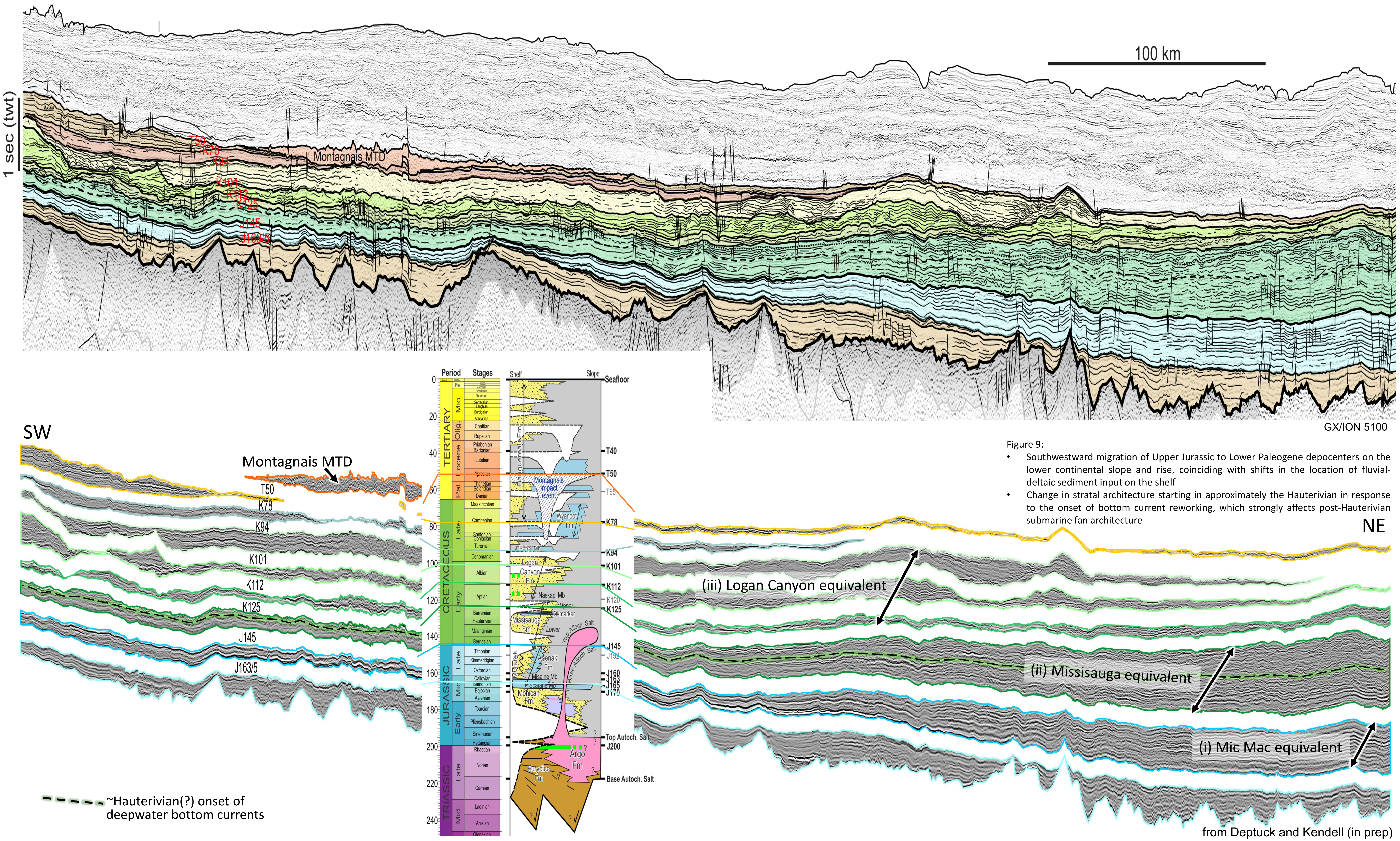

Figure 9:

- Southwestward migration of Upper Jurassic to Lower Paleogene depocenters on the lower continental slope and rise, coinciding with shifts in the location of fluvial-deltaic sediment input on the shelf
- Change in stratal architecture starting in approximately the Hauterivian in response to the onset of bottom current reworking, which strongly affects post-Hauterivian submarine fan architecture

from Deptuck and Kendell (in prep)

Framework Seismic Stratigraphy Seaward of Salt Basin

CHAPTER 2.2
HYDROCARBON OCCURRENCES – EVIDENCE FOR CHARGE MIGRATION

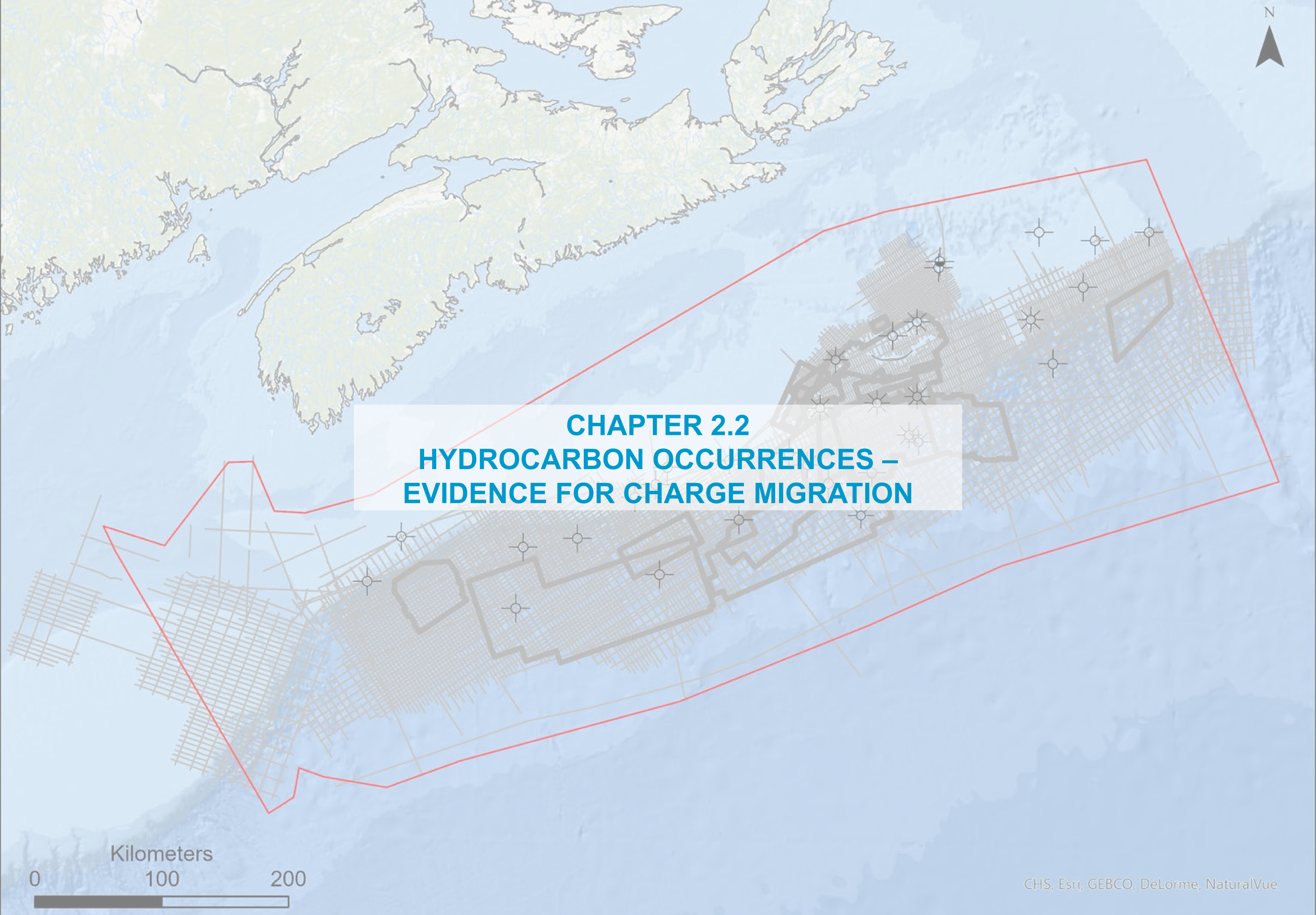

CHS, Esri, GEBCO, DeLorme, NaturalVue

Hydrocarbon Occurrences – Evidence for Charge Migration

Introduction

The 2011 Play Fairway Analysis (PFA) integrated numerous technical geoscience projects along the Scotian Margin with new integration and analysis work by Beicip Franlab. This modeled the potential for a regional Lower Jurassic oil prone (Type II) source rock that extends beyond the Sable sub-basin and underlies the whole margin (Beicip Franlab, 2011).

In the twelve years since, the Nova Scotia Department of Natural Resources and Renewables, in partnership with the Offshore Energy Research Association (OERA) and Beicip Franlab, have completed numerous uplifts to this original research in localized areas along the Scotian Margin including the Central Scotian Slope, the South West Scotian Margin, and the Laurentian Sub-Basin. In addition, several other projects relating to seismic reprocessing, paleogeography, and source rock have been completed. Section 2.2 aims to synthesize the last decade of source rock research along the Scotian Margin and the uplift in our understanding of the inferred Lower Jurassic Source Rock.

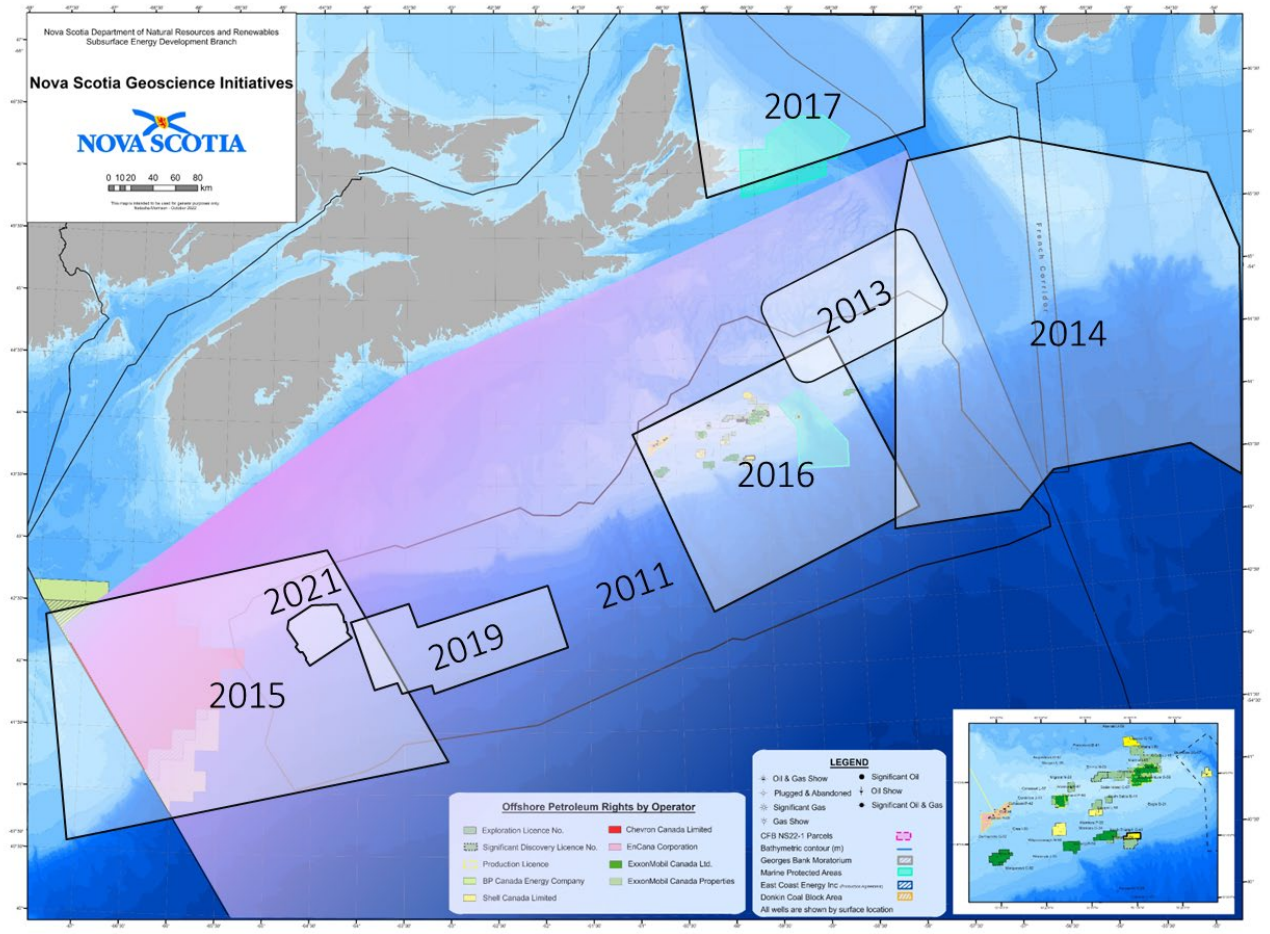

Figure 10: Outlines of project study areas since the 2011 Play Fairway Analysis. The pink color indicates other, margin wide paleogeographic, source rock, and seismic analysis work, completed in addition to the subsequent PFA's.

Historical Source Rock Understanding

The majority of the hydrocarbons discovered on the Scotian Shelf are gas often associated with light oils/condensates. These have a distinct terrigenous signature of a deltaic source rock with Type III-II organic matter, indicative of Nova Scotia's proven Tithonian aged Source Rock (e.g. Powel, 1982; Beicip et al., 2011; Fowler, 2020). Other source rocks on the margin have also been considered. The 2011 PFA provided a strong stratigraphic architecture that related source rocks to age instead of lithostratigraphy. In addition to the Tithonian, it considered 4 additional possible source rocks, including the Aptian, Valanginian, Callovian and Pliensbachian (Early Jurassic) (Beicip et al., 2011).

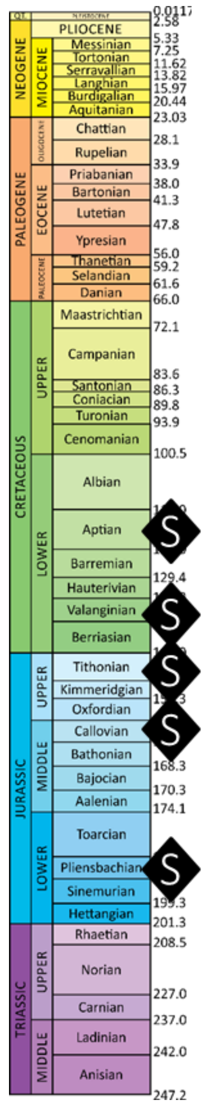

Source Rock	Approx. Age	Initial TOC	Kerogen type Initial HI	Description
APTIAN	122 Ma	2 % (constant)	III (continental) HI = 235 mgHC/gTOC	Potential source rock in the Naskapi shale (and equivalent), identified in some wells. Variable effective thickness between 0 – 100 m.
VALANGINIAN	136 Ma	1 % (constant)	III (continental) HI = 235 mgHC/gTOC	Very poor and scattered source rock (coal fragments in deltaic environment, through the Mississauga formation) Variable effective thickness between 0 – 200 m.
TITHONIAN	148 Ma	3 % (constant)	II-III mix HI = 424 mgHC/gTOC	Best defined SR, widely proven. Variable effective thickness between 0 – 50 m.
CALLOVIAN	160 Ma	2 % (constant)	II-III mix HI = 424 mgHC/gTOC	Potential source rock in the Misaine shale (and equivalent), uncertain extend and richness due to the lack of data. Variable effective thickness between 0 – 20 m.
PLIENSBACHIAN (L. M. Jurassic)	196 Ma	5 % (constant)	II (marine) HI = 600 mgHC/gTOC	Suspected, not proven. Potentially present above salt basins only. Assumed average thickness 20 m.

Figure 11: Five source rocks and their corresponding parameters modeled *in the 2011 Play Fairway Analysis (Beicip et al.,2011).*

Both Cretaceous and the Callovian source rocks were modeled to have limited hydrocarbon potential, representing, at most, a minor contribution to the discovered hydrocarbons. The 2019 Conjugate Margin Reconstruction (Beicip et al., 2019), also considered a possible Cenomanian-Turonian source rock based on evidence from the Moroccan Margin, however there was no evidence to prove its existence offshore Nova Scotia (Fowler, 2019). The proven Tithonian and hypothesized Lower Jurassic (Pliensbachian) source rock were modeled to have strong hydrocarbon potential. A full evolution of source rock parameters from the numerous PFA projects can be seen in Figure 12

As described by Fowler et al. in 2016, the Tithonian Verrill Canyon is the only interval with substantial evidence and confidence of existence. The Type III-II, deltaic source rock exhibits common terrestrial sourced characteristics including high pristane/phytane ratios, C29 steranes greater than C27 steranes and rearranged steranes greater than regular steranes (Fowler et al. 2016, Fowler, 2020).

On the other hand, there is no direct evidence of a Pliensbachian source rock on the Scotian Margin. Despite wells being drilled through to the Triassic or Basement on the shelf, no wells contain biostratigraphic evidence of Lower Jurassic sediments. A few wells, such as Mohedia P-15, have a biostratigraphic *indeterminate* section below the Middle Jurassic. Recent work hypothesizes that this section may be Lower Jurassic sabkha facies which are hard to date (McRea et al. in prep). The South Griffin J-13 well was noted to contain reworked Lower Jurassic Nannofossils in the Upper Jurassic sediment and to date this is the only evidence of marine conditions during the Lower Jurassic (Weston et al., 2012, Bishop, 2022). Finally, there is some evidence of a Lower Jurassic source in the Grand Banks and offshore Morocco.

Evidence of a Lower Jurassic Source Rock

Over the last two decades, many studies have been commissioned specifically to help de-risk the presence and effectiveness of a Lower Jurassic Source Rock. Despite there being no direct evidence for the occurrence of Lower Jurassic Marine sediments offshore Nova Scotia, these studies show credible indirect evidence in support of its existence. These studies followed four main pillars of investigation, each asking specific source related questions. These four pillars consisted of Analogues, Direct Evidence, Indirect Evidence and Modeling. A synthesis of these studies was conducted to draw together all of the evidence and provide a critical review of Lower Jurassic hydrocarbon charge potential in offshore, Nova Scotia and compile scenarios for source rock presence (Bishop, 2022)*.

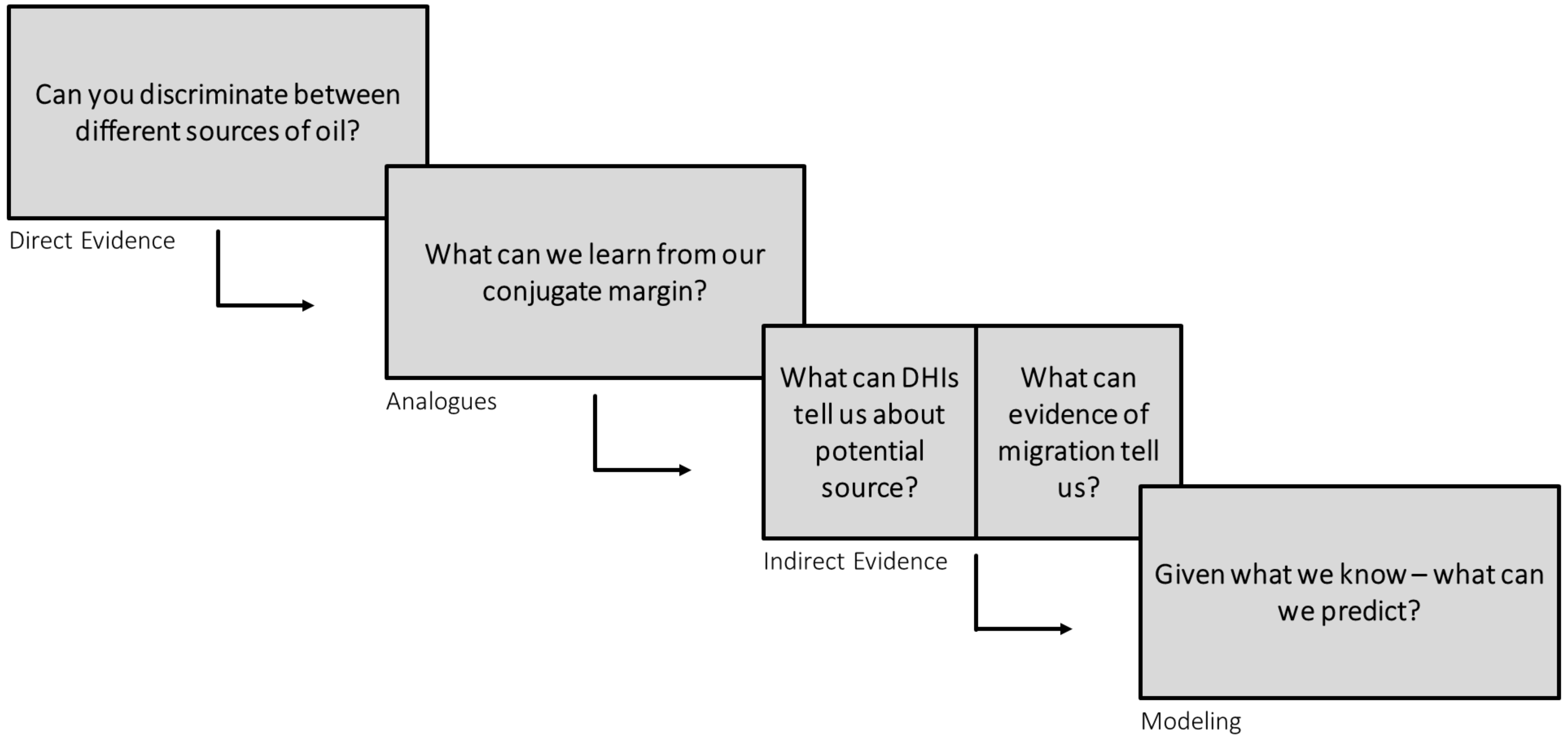

Can you discriminate between different sources of oil?

Direct Evidence

What can we learn from our conjugate margin?

Analogues

What can DHIs tell us about potential source?

What can evidence of migration tell us?

Indirect Evidence

Given what we know – what can we predict?

Modeling

* **Acknowledgement -** This work could not have been completed with out the geochemical analysis competed by Dr. Martin Fowler and APT International Inc. and research and synthesis completed by Dr. Andrew Bishop with Stratum Reservoir.

Dr. Andrew Bishop
OilTracers, Stratum Reservoir

Dr. Martin Fowler
APT International Inc.

	Source Rock	Age	Initial TOC	Kerogen Type	Thickness (m)	HI (mgHC/gTOC)	Focus
2011	Tithonian	148 Ma	3%	II/III (mix)	0-50	424	Basin wide study incorporating (1) previous studies (2) large existing geochemical database (+40 years of exploration) (3) review of all available and new TOC/Geochemical analysis, (4) characterization of oil families, and (5) new GC/GCMS analyses of oil, condensates and hydrocarbon fluid inclusions. Aptian and Vananginian sources also considered in this project.
	Callovian	160 Ma	2%	II/III (mix)	0-20	424	
	Pliensbachian (L.M. Jurassic)	196 Ma	5%	II (marine)	20	600	

	Source Rock	Age	Initial TOC	Kerogen Type	Thickness (m)	HI (mgHC/gTOC)	Focus
2014	Tithonian	148 Ma	5%	II/III (intermediate)	50	424	Focus on Laurentian Basin and surrounding area relying on (1) Review of existing TOC/Rock Eval (2) New TOC/Rock Eval (3) NS oil/cond Geochemistry. A Lower Jurassic source complex inferred by analogous source rocks in conjugate Portugal and Morocco.
	Misaine (Callovian)	166 Ma	3%	II/III (intermediate)	50	424	
	Pliensbachian	196 Ma	5%	II (Menil)	50	600	

	Source Rock	Age	Initial TOC	Kerogen Type	Thickness (m)	HI (mgHC/gTOC)	Focus
2015	Tithonian	150 Ma	3%	II/III (mix)	0-20	424	Focus on Southwest Scotian Margin. Only change in parameters was thickness of Tithonian, which is modeled to be thinner in this area.
	Callovian	163 Ma	2%	II/III (mix)	0-20	424	
	Lower Jurassic Complex	196 Ma	5%	II (marine)	20	600	

	Source Rock	Age	Initial TOC	Kerogen Type	Thickness (m)	HI (mgHC/gTOC)	Focus
2016	Tithonian	150 Ma	5%	II/III	20	424	Focus on Central Scotian Slope – tested three individual Lower Jurassic Sources (speculative parameters).
	Toarcian	182 Ma	2.5%	II	10	600	
	Pliensbachian	189 Ma	2.5%	II	10	600	
	Sinemurian	198 Ma	5%	IIS	10	600	

	Source Rock	Age	Initial TOC	Kerogen Type	Thickness (m)	HI (mgHC/gTOC)	Focus
2019	Tithonian	150-148 Ma	3%	II	50	500	Analogue approach relying on geochemical synthesis performed by Fowler, 2018 of Moroccan wells/data.
	Bathonian	168-166 Ma	3%	II	50	600	
	Pliensbachian	184-183 Ma	3%	II/III	50	450	

	Source Rock	Age	Initial TOC	Kerogen Type	Thickness (m)	HI (mgHC/gTOC)	Focus
2022	SR1	~199-184 Ma	1.5%	IV	100	150	Dr. Andy Bishop's independent view of NS Lower Jurassic source rock potential and parameterization (Summary of report found in Chapter 2.3). Defined 3 end members of a Sinemurian or Pliensbachian source.
	SR2	~199-184 Ma	3%	II/III	50	300	
	SR3	~199-184 Ma	4%	II	50	500	

	Source Rock	Age	Initial TOC	Kerogen Type	Thickness (m)	HI (mgHC/gTOC)	Focus
2023	Tithonian	150 Ma	0-5%	II/III	0-20	400	Synthesis of numerous studies regarding source rock on the Scotian Margin including (1) Dr. Andy Bishop's independent view of NS Lower Jurassic source rock potential and parameterization and regional review of Lias source rocks from Atlantic domain including Europe and globally, (2) Dr. Martin Fowler's research on the source of shelf oils indicating the presence of two distinct source rocks, and (3) various supporting paleogeographic and migration projects. Three scenarios of Lias source rocks tested (See Chapter 5 for details).
	Pliensbachian	196 Ma	3-4%	II	0-30	300-500	

Figure 12: Evolution of thought and rational of source rock parameters used from 2011 to today (Beicip et al.,2011,2014,2015,2016,2019,2023 and Bishop, 2022).

Hydrocarbon Occurrences – Evidence for Charge Migration

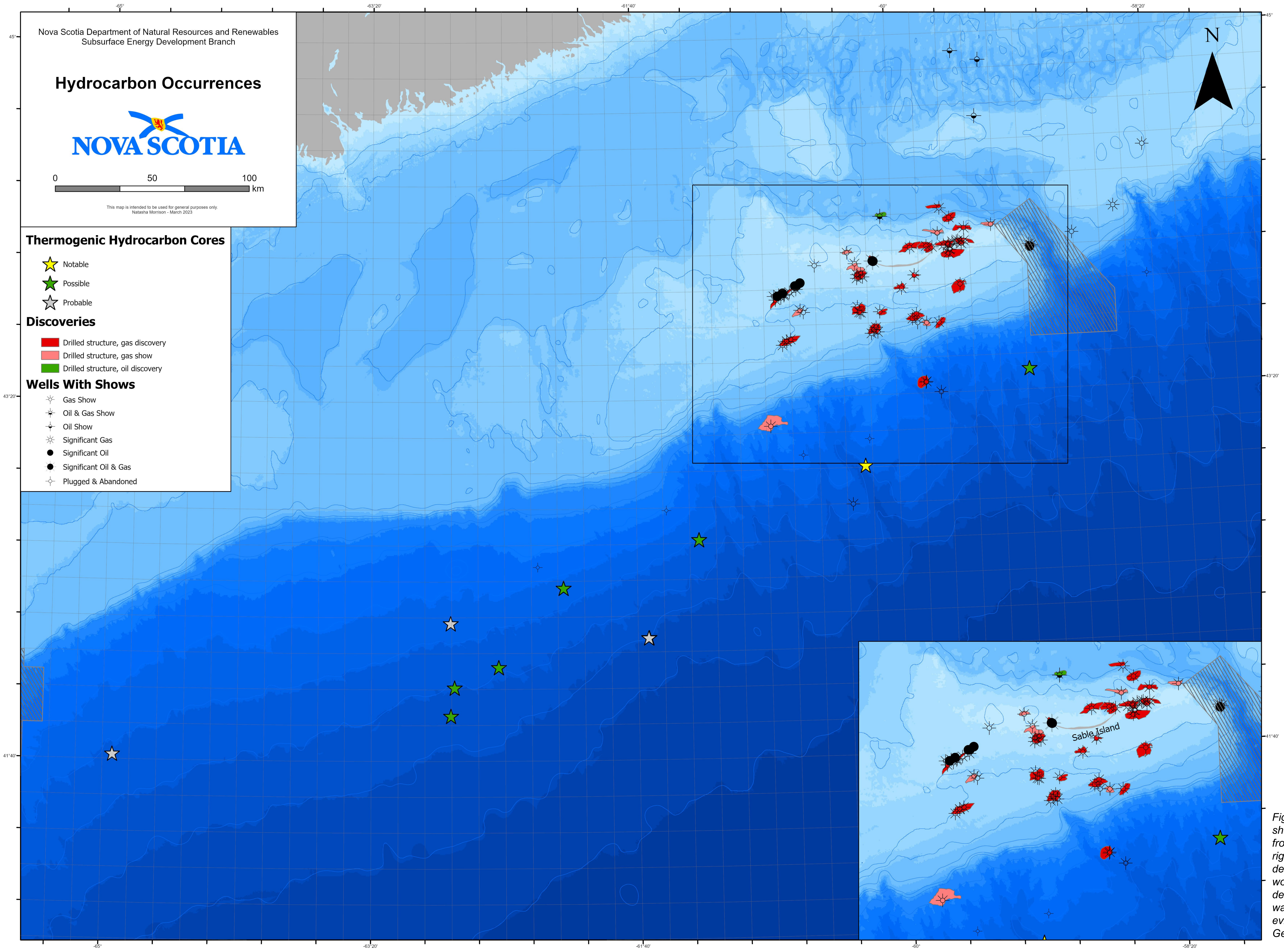

Figure 13: Distribution hydrocarbon discoveries and shows along the Scotian Margin. Discoveries modified from CNSOPB, 2012. The Sable Island area (bottom right inset) highlights the majority of exploration, development and production and clearly establishes working petroleum systems on the shelf. The Annapolis deepwater discovery proves working play in deep water, with the sea bed coring programs provides evidence for thermogenic source in the Central Slope to Georges Bank area.

Hydrocarbon Occurrences – Evidence for Charge Migration

ANALOGUES

To help better understand the geology of the Scotian Margin, the direct conjugate margin of Morocco, as well as other basins throughout the North Atlantic were studied.

Nova Scotia and Northern Morocco Conjugate Margins

In 2019, in collaboration with ONHYM and Beicip, a 2D reconstruction and petroleum systems study was completed across 4 regional transects spanning both margins, providing new insights regarding source rocks present in Morocco that may inform the petroleum potential of offshore Nova Scotia. In addition to the seismic reconstruction, petroleum systems modeling was also undertaken to better characterize the generation, migration and entrapment of hydrocarbons along both margins. Each transect was approximately 200 km apart and represented the variety of structures encountered along the margins (Beicip et al, 2019).

A key outcome of this study was to reassess the oil potential of source rocks in the Morocco margin to further the understanding of source rock and oil generation potential in Nova Scotia. Source rocks modeled included those present or hypothesized on both sides, including Ypresian, Turonian, Aptian, Tithonian, Bathonian, and Pliensbachian.

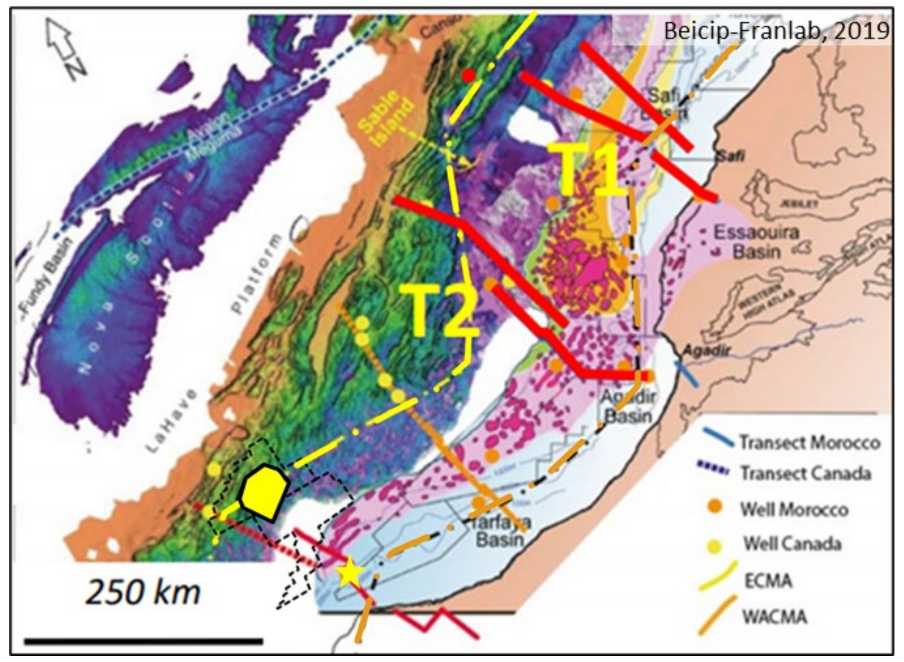

Figure 14: Position of conjugate transects. Plate reconstruction at 190 Ma (Deptuck and Altheim, 2018; Tari and Jabour, 2008).

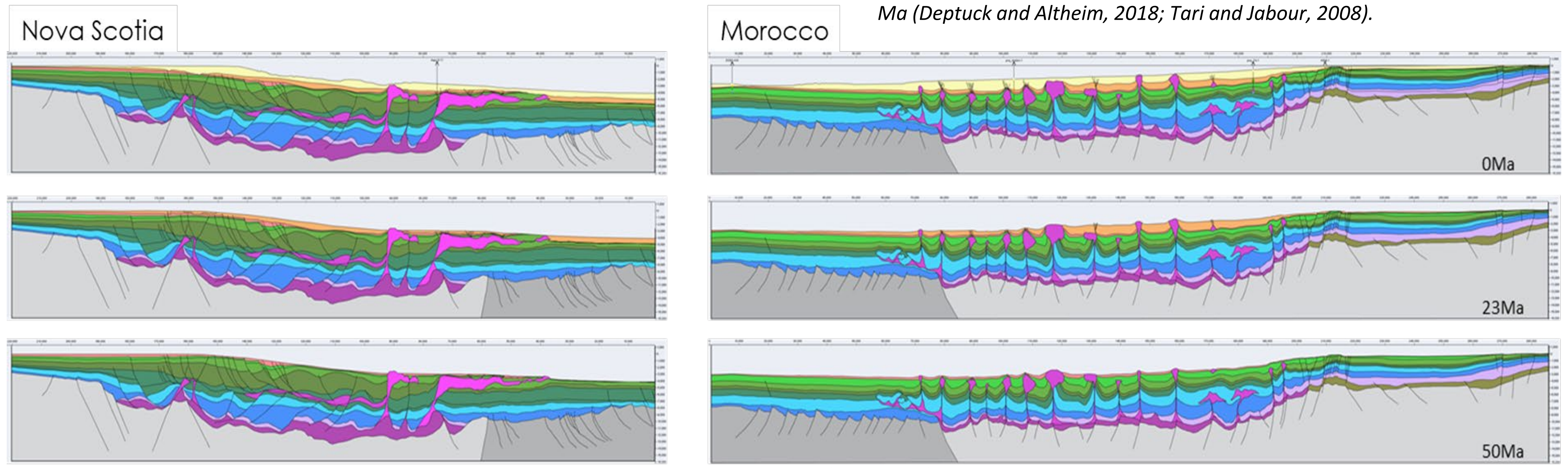

Figure 15: Examples of the conjugate margin reconstruction of Transect 2 from 0 to 50 Ma (NRR, 2020).

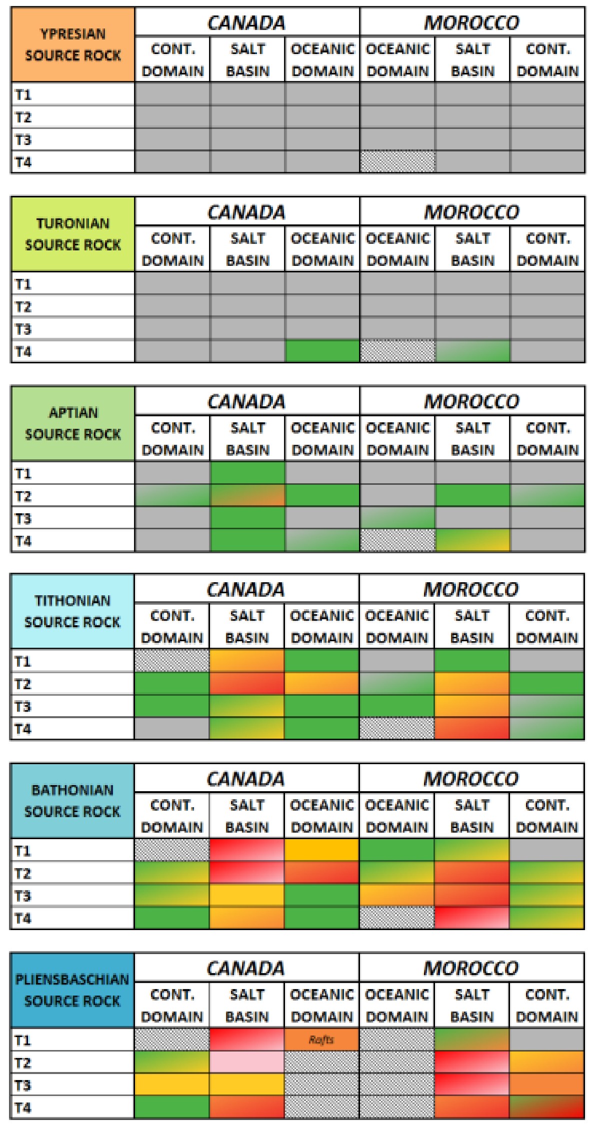

Key Conclusions

Key findings regarding Jurassic source rock were:

Tithonian SR
- Proven to be the main source in producing fields on Scotian Shelf
  - Inferred to be present in some deep water areas
- Low potential as a hydrocarbon source in Morocco.

Pliensbachian SR
- Not yet proven offshore on either margin (i.e. no wells have penetrated a Lower Jurassic source)
- Considerable indirect evidence supports its existence
  - Onshore Morocco: outcrops and wells
  - Offshore Morocco: several hydrocarbon shows in the Cape Juby area
  - Offshore Morocco (evidence in DSDP 547b - Toarcian)
  - Offshore Nova Scotia: numerous seeps identified in the deep Shelburne Sub-basin, etc.

If present, an Early Jurassic source rock would most likely exist in isolated deep mini-basins throughout the salt basin domain

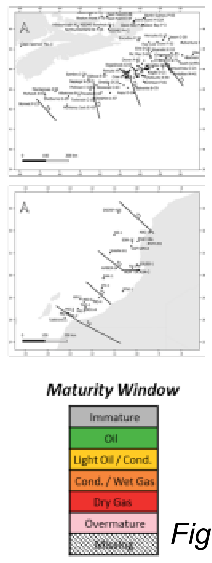

Figure 16: Source rock maturity on both conjugates based on results of 2D petroleum system models (Beicip et al., 2020).

North Atlantic Liassic Petroleum Systems Synthesis

In the absence of definitive, and direct evidence for a Lower Jurassic petroleum system offshore Nova Scotia, information was collected on source rock analogs around the greater North Atlantic region. Published in 2020, Dr. Andrew Bishop completed a project synthesizing the North Atlantic Liassic Petroleum Systems. Its objective was to compile information on organic rich sediments, as well as any associated known hydrocarbon occurrences, of Lias age in key Mesozoic basins. Consideration was also given to known Lias age petroleum systems to assess if there are any geochemical characteristics which are diagnostic for hydrocarbons of this age (Bishop, 2020).

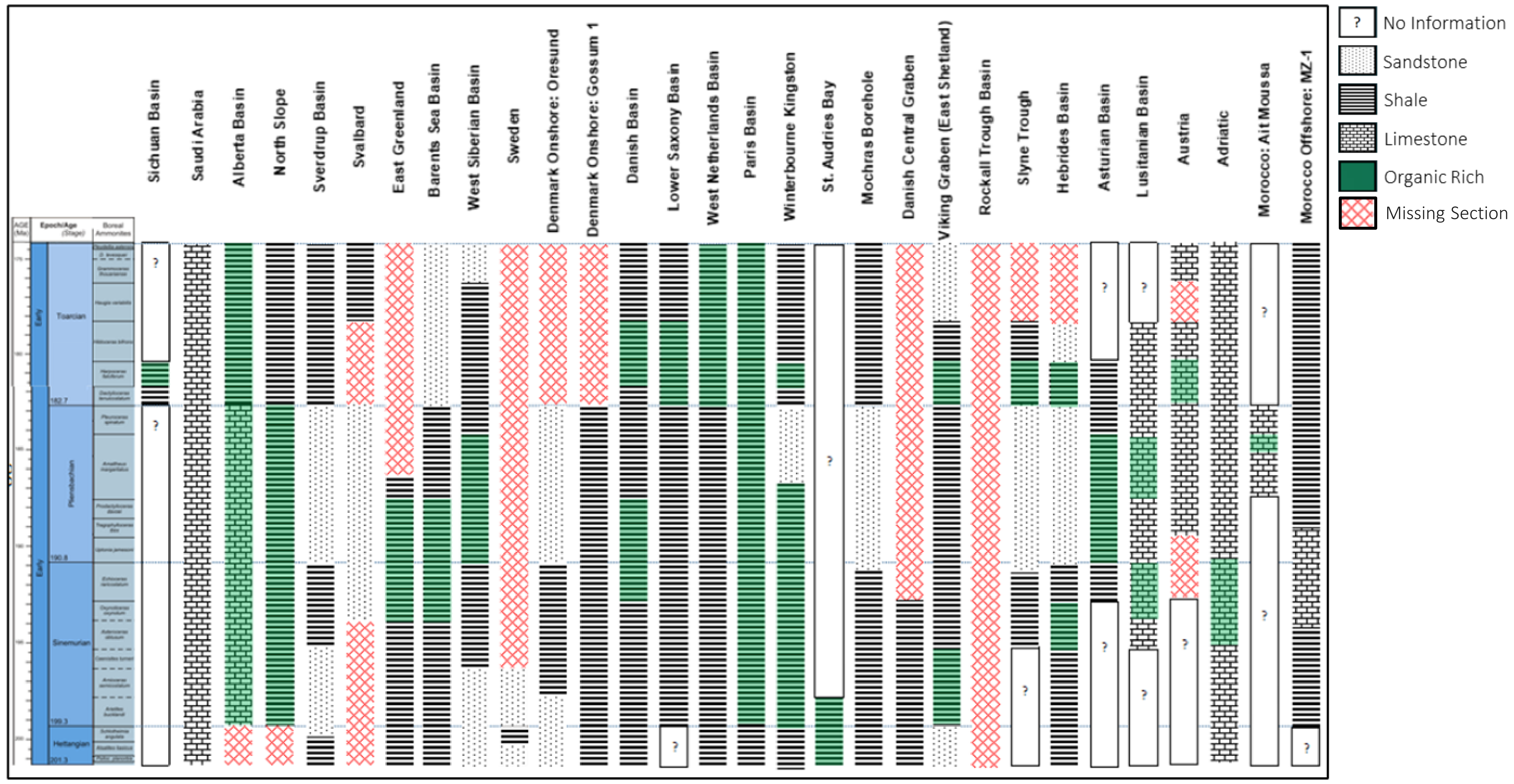

Figure 17: Synthesis of major Lias sections summarized in this study. Zones of organic enrichment highlighted in green. Lithologies for shale, sandstone and limestone shaded with standard symbologies (Bishop, 2020).

Key Conclusions

Lias source rocks are widespread globally, including around the North Atlantic. Each Lias stage is associated with source deposition, which varies from basin to basin. The main factors associated with source ***absence*** in the studied basins were proximal settings, uplift and erosion. Finally, oils generated from Lias source rocks appear to be consistently light isotopically with a carbon isotopic composition of ~ 30 ‰ (Bishop, 2020).

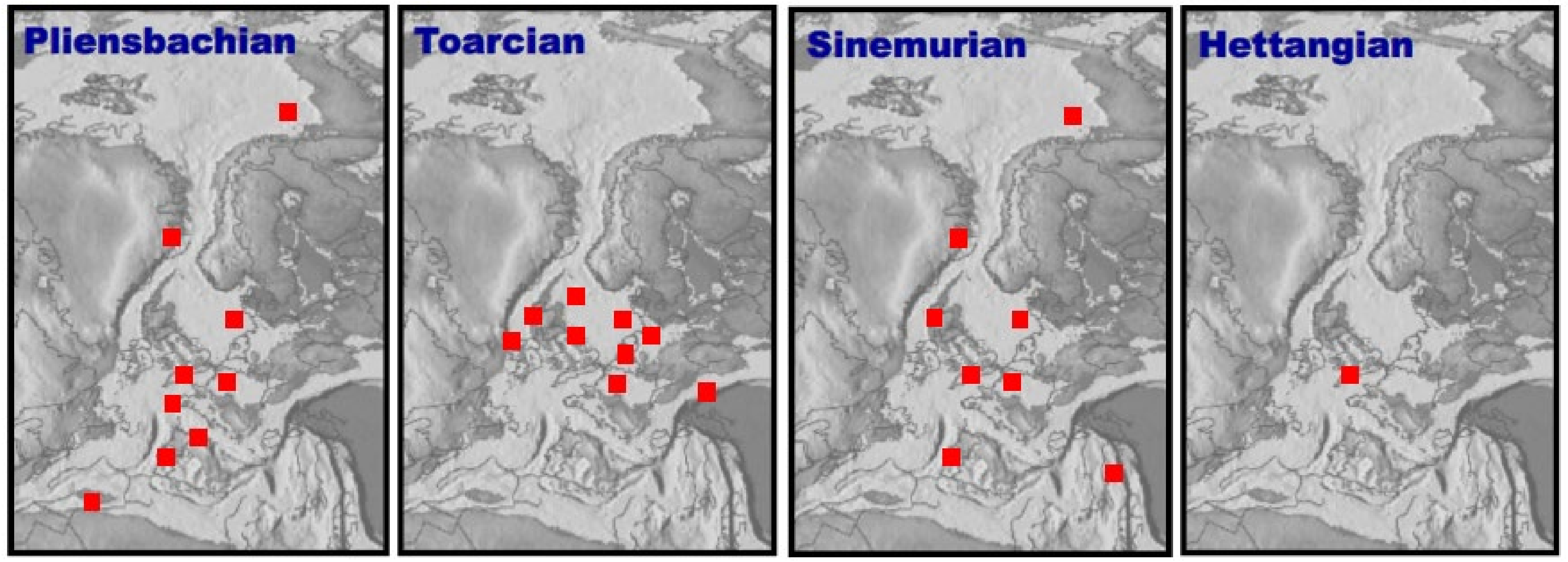

Figure 18: Distribution of significant organic rich sequences across the greater North Atlantic region, broken out by epoch. Locations per Figure . Lias (195 Ma) paleomap from Scotese (2014) (Bishop, 2020).

Given the Moroccan and greater North Atlantic analogues – there is **clear** evidence of a lower Jurassic SR in onshore Morocco and we can demonstrate through modeling that it may be present in NS as well.

Hydrocarbon Occurrences – Evidence for Charge Migration

SCOTIAN SHELF OIL GEOCHEMISTRY

To further develop the case of multiple source rocks on the Scotian Margin, Dr. Martin Fowler at ATP International undertook a project to look at the oils discovered on the Scotian Shelf. The objective of this being to review evidence for there being multiple source rocks for hydrocarbons, concentrating on evidence from liquid hydrocarbons rather than source rock data. Sampling and analysis focused on 13 stained Lower Cretaceous to Upper Jurassic intervals in 5 key wells indicated in the map on the right; Erie D-26, Mic Mac D-89, Mic Mac J-77, Missisauga H-54, and Wyandot E-53.

Whole Oil GCMS

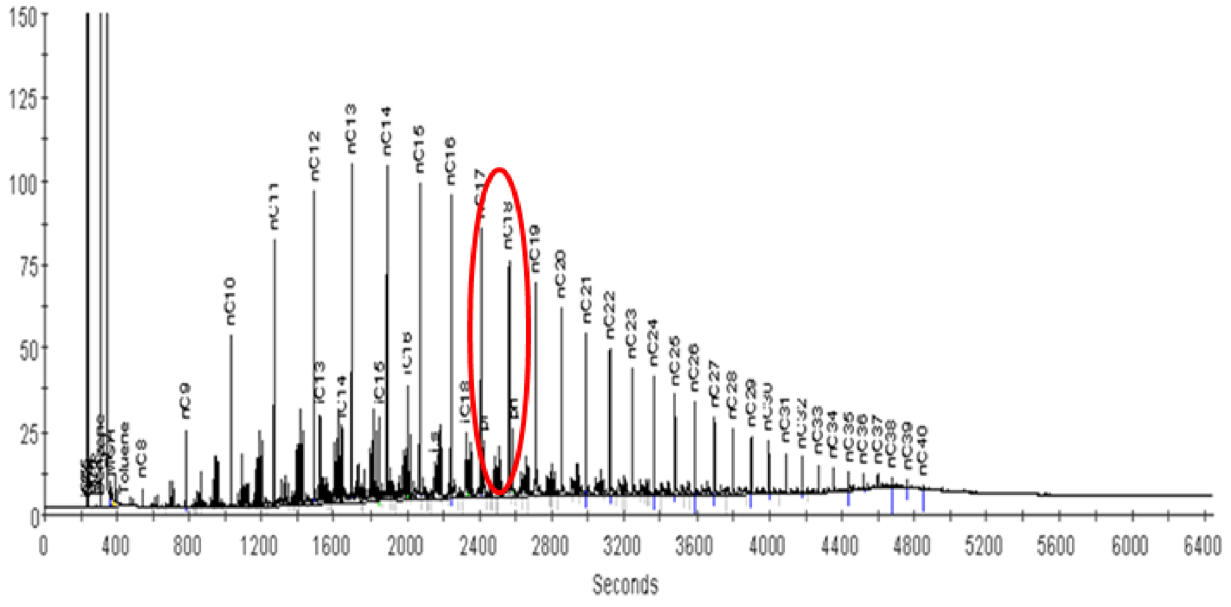

Figure 19: Mic Mac J-77 whole oil GCMS showing a low pristane/phytane value (Fowler, 2020).

Saturate GCMS m/z 191

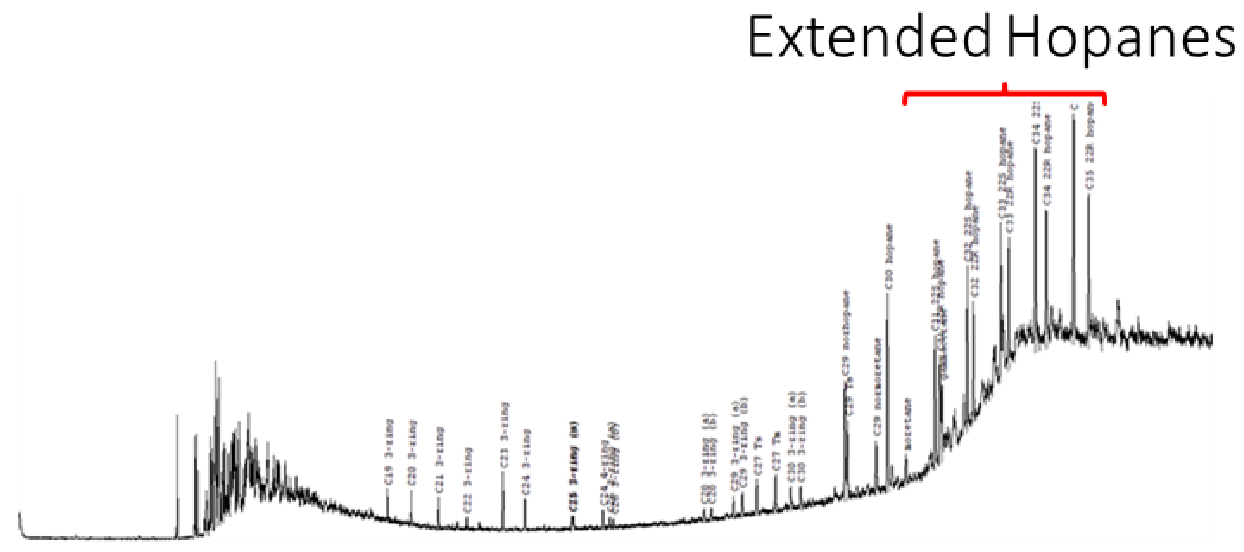

Figure 20: Mic Mac J-77 saturate GCMS (m/z 191) showing the extended hopane biomarkers (Fowler, 2020).

Saturate GCMS m/z 217

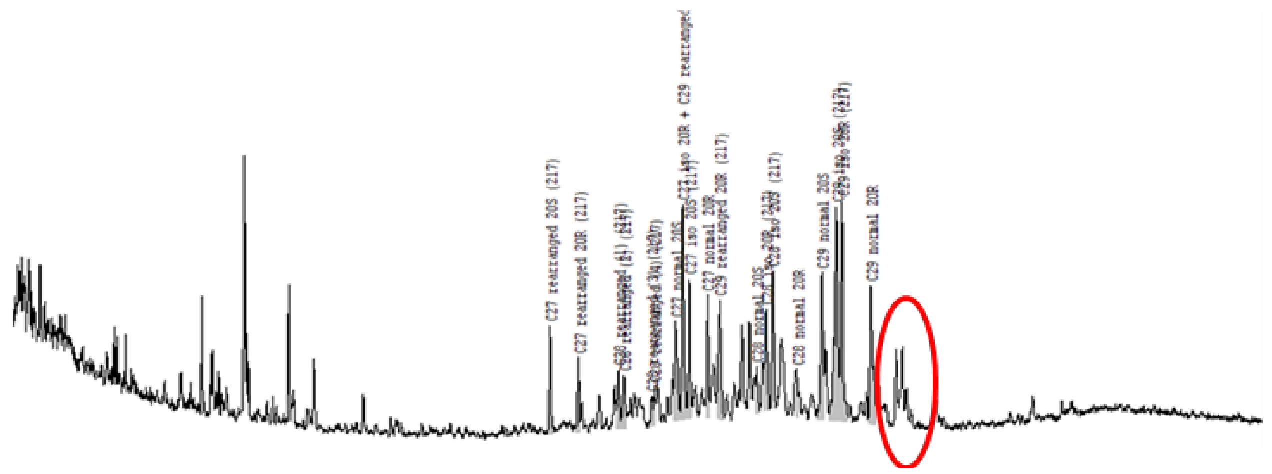

Figure 21: Mic Mac J-77 saturate GCMS (m/z 217) showing low levels of C30 sterane biomarkers (Fowler, 2020).

Mic Mac J-77

Reservoired oil in the Mic Mac J-77 well was discovered in the Missisauga Formation, with abundant staining also noted in the Logan Canyon and Mic Mac Formations (Kendell et al. 2013). Whole Oil Gas Chromatography Mass Spectrometry (GCMS) indicated an oil gravity of 37.8° with the hydrocarbon distribution representing a typical light oil composition, consistent with the relatively light oil gravity. This analysis also showed the oil had pristane/phytane value of 0.89 and a slight even-odd n-alkane caron predominance greater than C20 (Figure 19) (Fowler, 2020; Bishop, 2020). ***This is indicative of saline to hypersaline conditions associated with evaporite and carbonate deposition***.

The Saturate GCMS indicated a moderately mature sample with some intervals containing variably mature biodegraded oil. Despite this, all samples still shared the same distinctive anoxic marine carbonate signature. Most samples analyzed had elevated extended tricyclics, with bisnorhopane, a compound often associated with marine anoxia, present in several lower maturity samples. Fowler indicated that this implies that there ***were multiple phases of charge to the current day accumulation*** (Fowler, 2020; Bishop, 2022).

Hopane and sterane signatures showed the sample was moderately mature. The extended hopane distribution remained consistent with the hypothesized marine, anoxic source (Figure 20). The sterane distribution had moderately depressed diasterane content relative to the non-rearranged steranes, which given the level of maturity of these samples, remains also consistent with a carbonate signature. Finally, low levels of the C30 steranes also point toward a marine character (Figure 21) (Fowler, 2020; Bishop, 2022).

Erie D-26, Mic Mac D-89, Missisauga H-54 and Wyandot E-53:

The molecular geochemistry data for the rock extracts from these four wells exhibited varying degrees of biodegradation and, consistent with the oil sample from Mic Mac J-77, discernable anoxic marine characteristics. Furthermore, Rock-Eval/TOC analysis of the Tithonian source rock at Mic Mac H-86 suggests that this interval in this area of the basin is dominated by Type III terrestrial derived organic matter, suggesting that it is unlikely to be the source of the Mic Mac J-77 oil. This finding is based on both organic matter type and maturity grounds (Fowler, 2020).

The oils evaluated were split into two families:

Type A: likely a marl; marine source rock deposited under more restricted, and more carbonate influenced conditions than type B.

Type B: marine clastic source rock.

Despite having two different signatures, the differences observes are not large. Both can be found in the same well, are not restricted to a particular formation and have approximately the same maturity. Most importantly, both are **very different from Scotian Shelf light oils/condensates with Tithonian source rock** (e.g. produced hydrocarbons from the Sable Offshore Energy Project) (Fowler, 2020).

Lower Jurassic age marine source is favored for the staining hydrocarbons in the Mic Mac J-77 area.

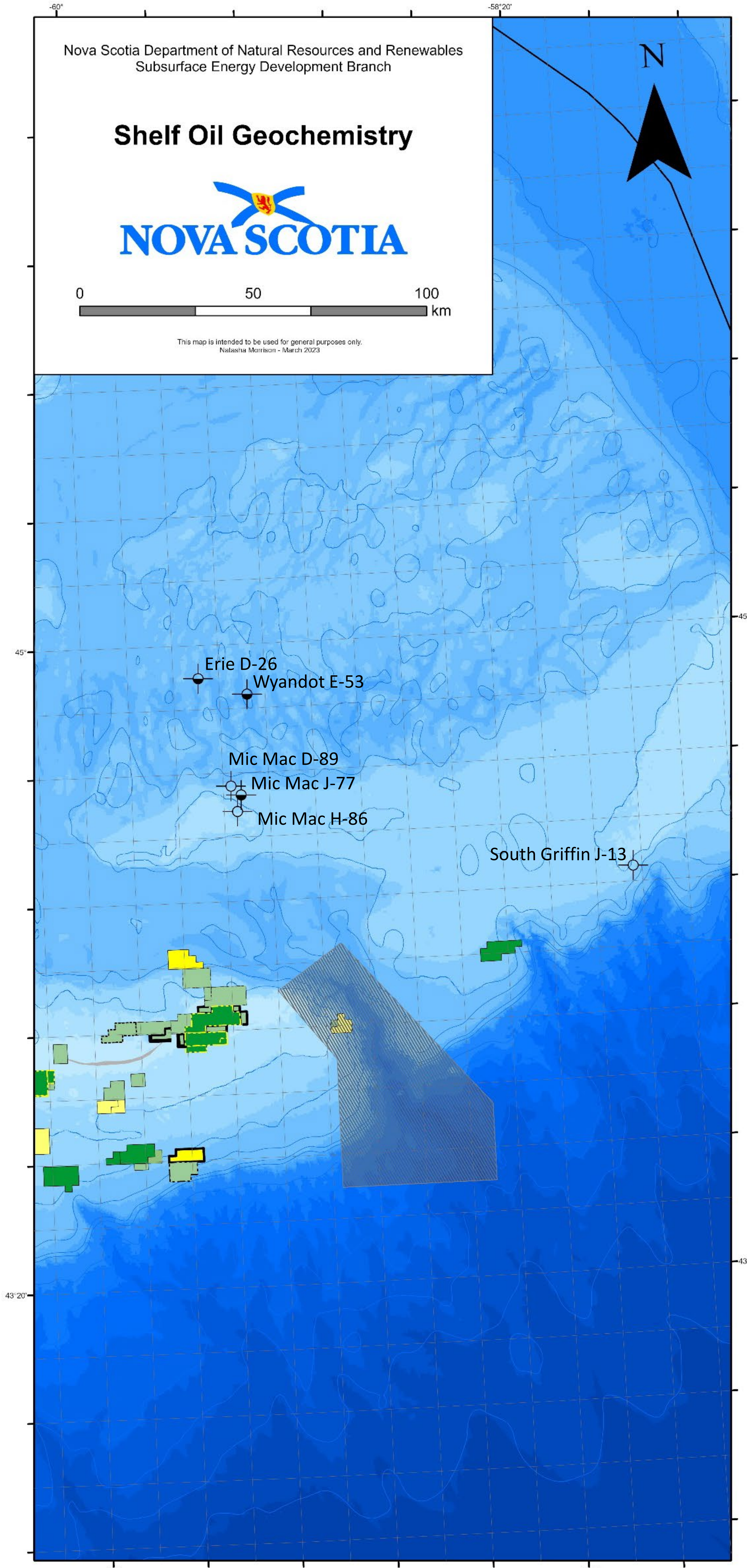

Figure 22: Map of offshore Nova Scotia showing the five key wells within the source Rock Oil Geochemistry study and the South Griffin J-13.

Hydrocarbon Occurrences – Evidence for Charge Migration

BARRINGTON 3D REPROCESSIN, ROCK PHYSICS, AND AVO ANALYSIS

Beginning in 2020, the Department of Natural Resources and Renewables began a project with WesternGeco (Schlumberger) to reprocess the legacy Barrington narrow-azimuth, 3D survey. The Barrington 3D survey was originally acquired by WesternGeco for PanCanadian (now Ovintiv) in 2001. It covers approximately 1,800 km^2 of the shelf to slope transition, in water depths ranging from 530 – 2,200 m (Figure 23). New reprocessing and analysis described here included modern techniques such as adaptive deghosting, full tilted transverse isotropy Kirchhoff pre-stack depth migration and litho-elastic inversion. There are no wells within the survey area, therefore the rock physics analysis and inversion was completed using deterministic and stochastic rock physics models using data from adjacent wells Cheshire L-97, Monterey Jack E-43, Bonnet P-23, and Aspy D-11 (Dasgupta et al., 2021).

The project was designed to test the potential prospectivity of a slope margin and feeder system geometry play, known as Cayuga (e.g. Deptuck, 2015), which was clear in the amplitude mapping of the legacy dataset. From the identification of numerous potential DHI's, including flat spots & amplitudes, this prospect consists of multiple levels of amplitude anomalies associated with turbidite and slope margin feeder channels, formed during the Cretaceous (Cayuga Deep) and Lower Tertiary (Cayuga Shallow) (Figure 24).

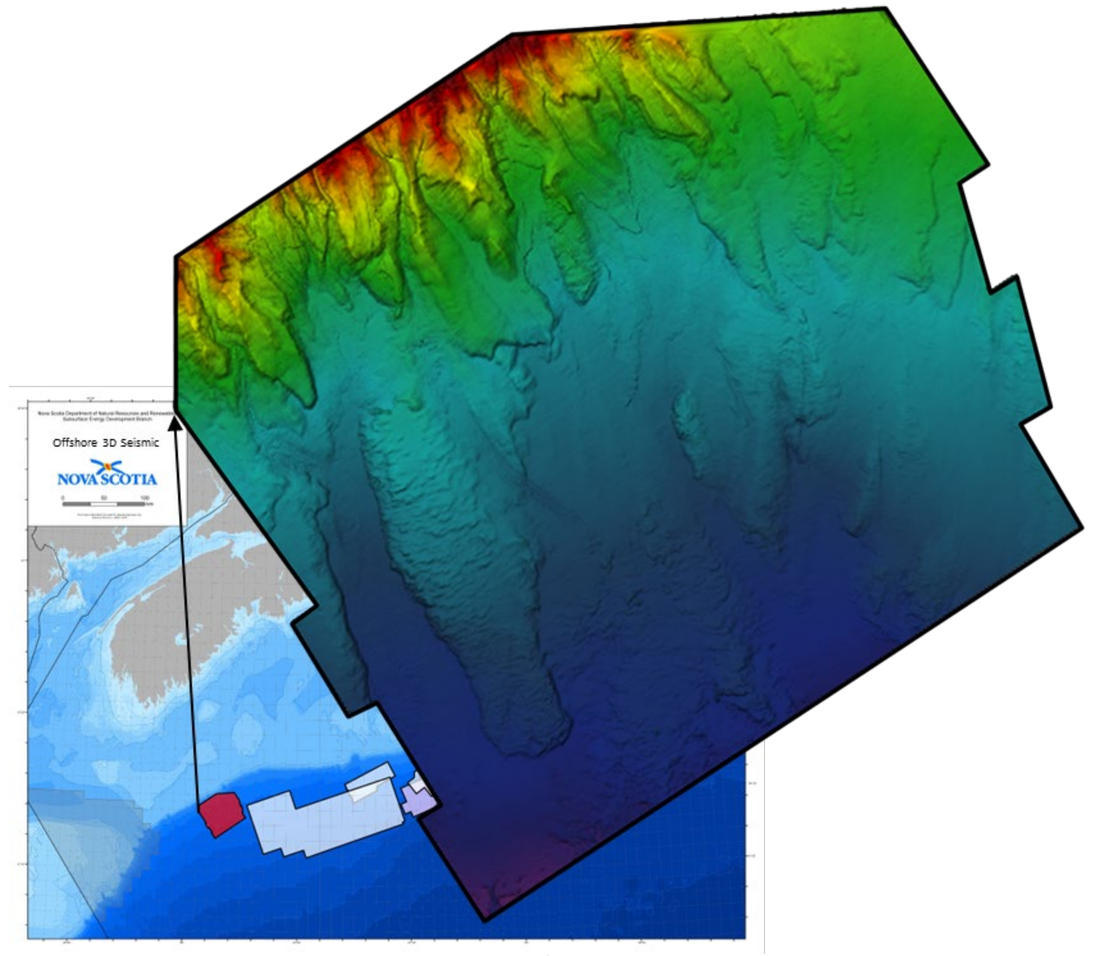

Figure 23: Map indication the location of the Barrington 3D survey with an overlay of the seafloor surface (MacAdam et al. 2023).

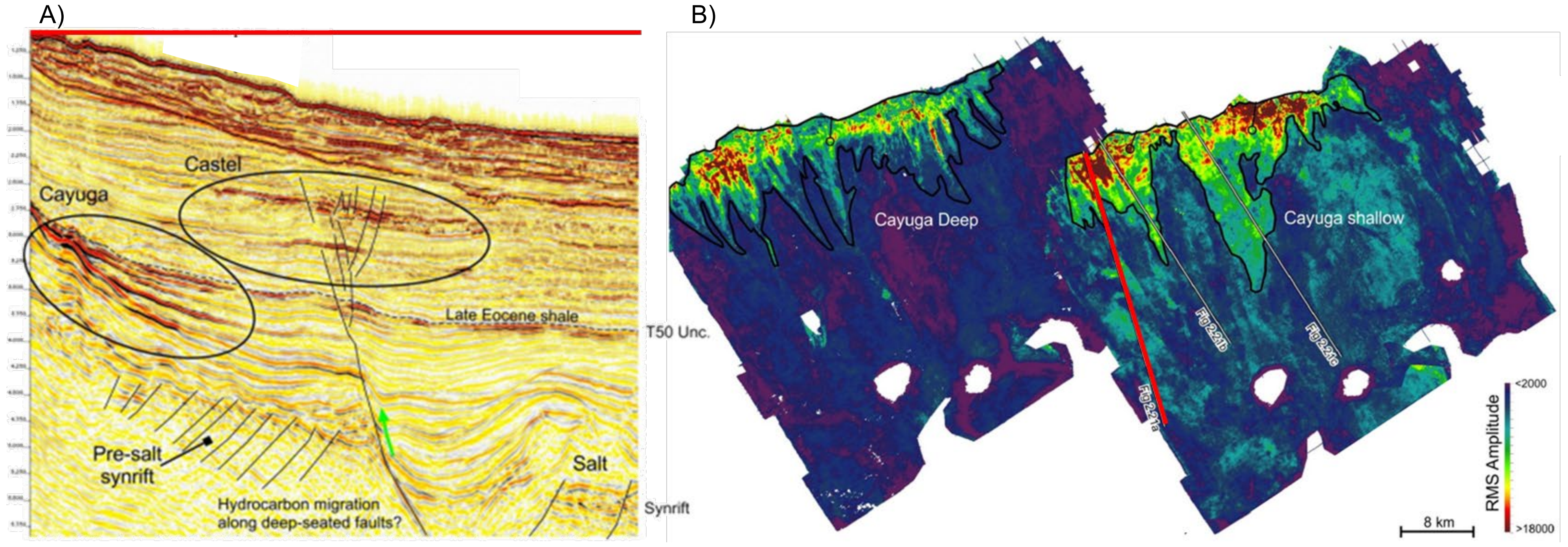

Figure 24: A) Seismic line displaying the Cayuga amplitude anomalies. B) RMS extractions of the T50 and K94 horizons outlining the Cayuga Shallow and Cayuga deep anomalies (Modified from Deptuck et al. 2015).

The 3D reprocessing was conducted to assess the de-risking impact on the exploration prospectivity using processing advances developed in the past 20 years since Barrington was acquired and to enhance the overall quality of the 3D data. It was also expected that the underlying Jurassic section could be better resolved in order to gain an understanding of source rock characterization, specifically an early Jurassic source rock, and to map areas of potential source intervals present that could vertically charge the overlying amplitudes.

2020/21 KPSDM reprocessing of Barrington 3D has revealed:

- Middle Jurassic carbonate reef anomaly (Figure 25)
- Late Jurassic flat spots (Figure 25)
- Cretaceous Turbidites amplitude anomalies (Figure 24)

Further rock physics, AVO and Inversion analysis revealed:

- Conformance with structure (Figure 26)
- Gathers dimming with offset (Figure 27)
- Downdip amplitude dimming and terminations (Figure 24)

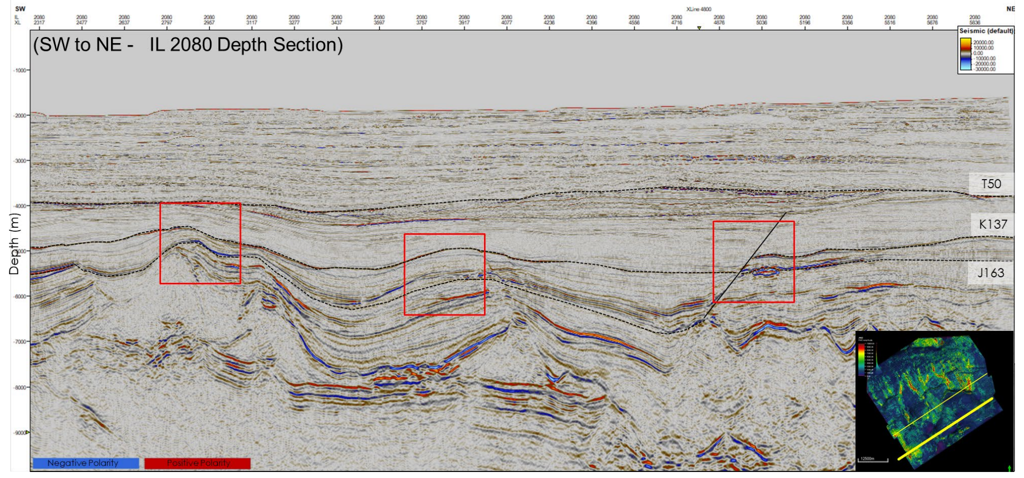

Figure 25: IL 2080 from the reprocessed survey highlighting 3 potential new leads (MacAdam et al. 2023).

Key Findings

In identifying evidence for support of an Early Jurassic source rock, the most convincing finding was a flat spot within a reef morphology at J163 level (Figure 26). This feature exhibited clean internal seismic character and an interesting phase reversal at its edges, potentially indicating a hydrocarbon contact. The plan view in Figure 23B indicated the anomaly is lensoidal in shape which would be consistent geometrically with other deep-water carbonate discoveries such as the Aptian Ranger discovery in Guyana. Interpretation suggests this reef formed during, or before, the Callovian and was deposited at a time of shallow water depths with a nearby well, Monterey Jack providing corroborating evidence for limestones, carbonates and marls at this time. This feature is located on the carbonate foreslope, basinward of the Abenaki carbonate bank. RMS extracts of horizons through the Oxfordian and Callovian seen in Deptuck (2020) clearly show the slope morphology and reef margin positions with lower slope isolated features during this time.

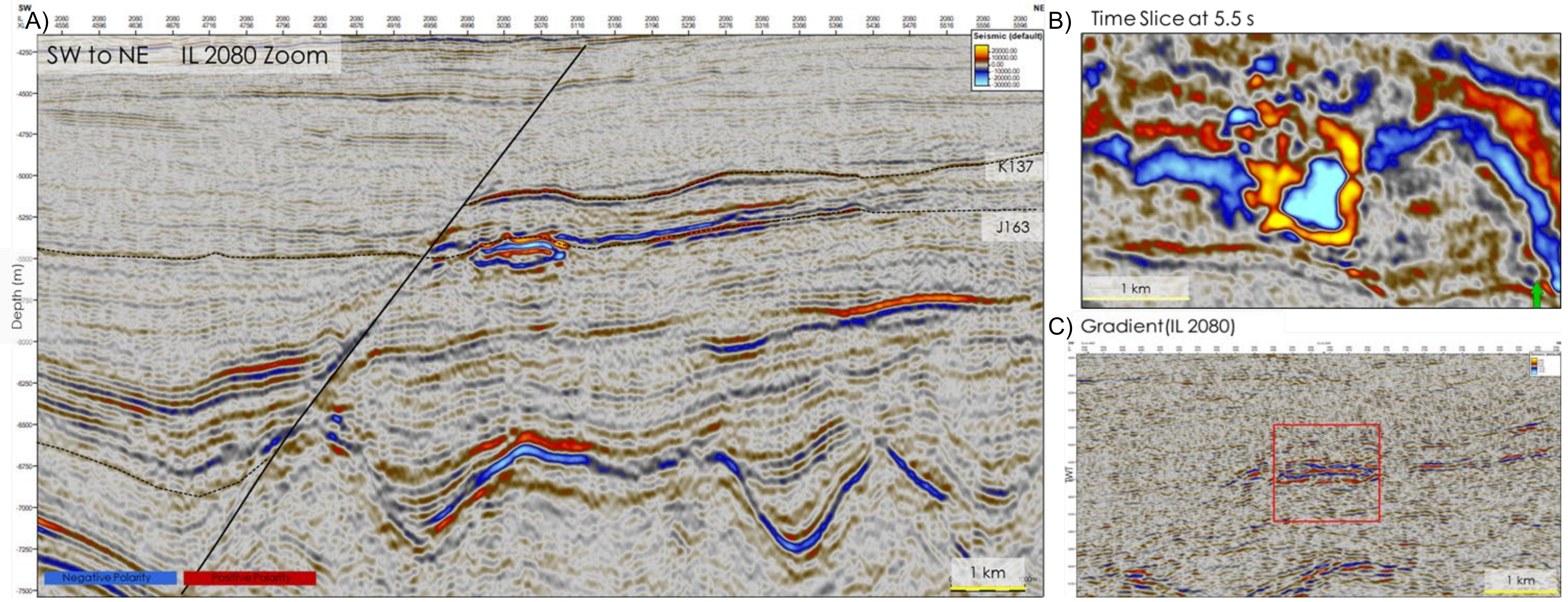

Figure 26: A) Jurassic Type IV AVO Anomaly from IL 2080 of the reprocessed survey B) Time slice at 5.5 S showing reef morphology C) Positive gradient values within feature (MacAdam, 2021).

This feature exhibited a Type 4 AVO anomaly with a strong negative intercept and a positive gradient, as seen above. The inverted elastic parameters show high P-impedance rock (below) overlaying a very compliant zone with anomalously low Vp/Vs ratio. This is consistent with rock physics model values of a carbonate overlying a charged gas sand (or an analogous carbonate overlying a more porous carbonate). Gathers exhibited a strong trough, overlying a peak, with both gathers dimming with offset. While this feature would likely not be of commercial size, at ~1.5 km^2 and 100 m thickness, it does provide clear and encouraging support for a working thermogenic Lower Jurassic charge system.

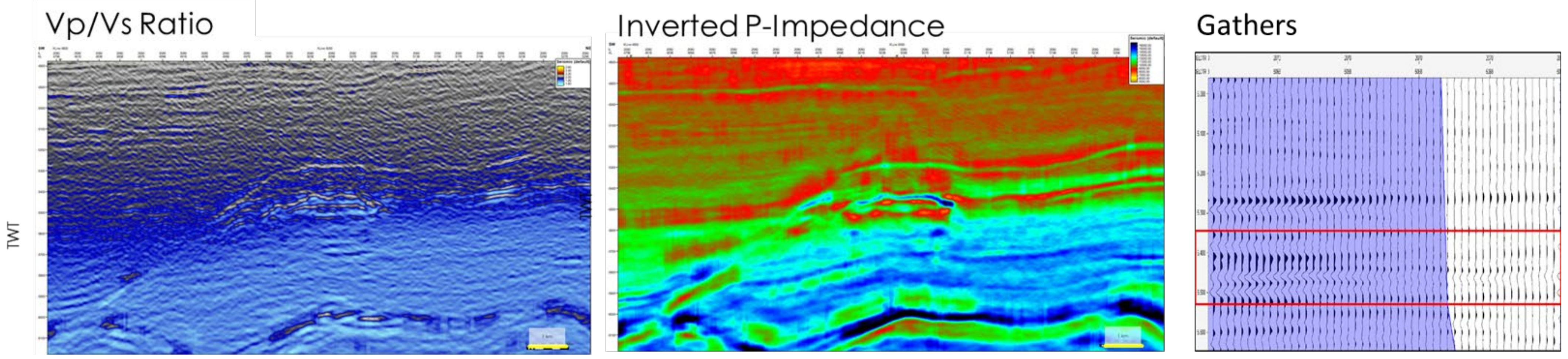

Figure 27: VP/VS Ratio, Inverted P-Impedance, and examples of gathers from the Jurassic Reefal Anomaly (MacAdam, 2021).

Looking at the new Tithonian HC Expulsion map (Figure 28), it is evident the Tithonian has not expelled any hydrocarbons in this location, thus not able to provide charge. Combined with the interpretation suggesting this reef formed during or before the J163 Callovian, this evidence provides support for charge from the postulated EJ source rock.

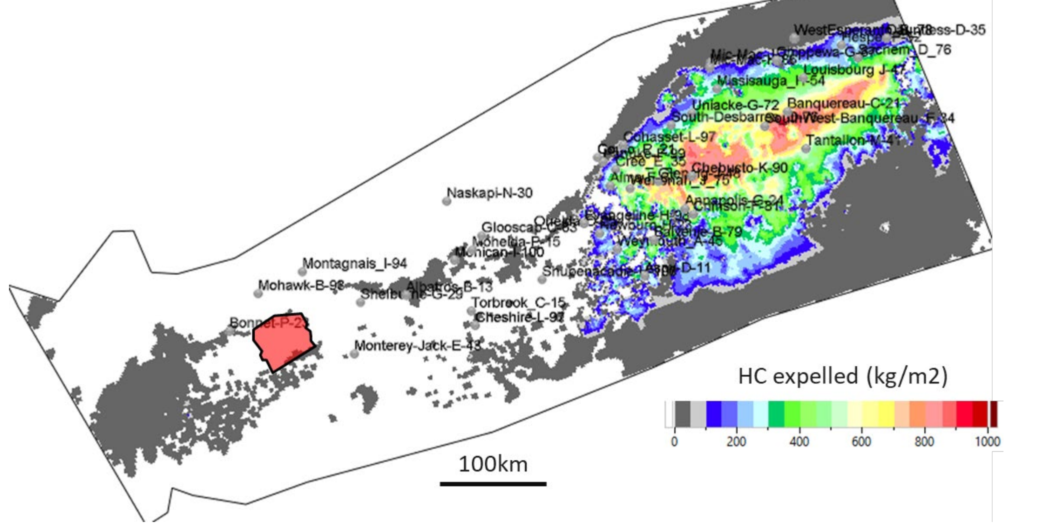

Figure 28: Tithonian hydrocarbon expulsion map showing this source rock has not expelled any hydrocarbons in the area of the anomaly.

Hydrocarbon Occurrences – Evidence for Charge Migration

INTEGRATED EVIDENCE FOR HYDROCARBON MIGRATION

This project aimed to de-risk source rock by working to understand distribution of both surface and deep hydrocarbon indicators. This was approached through two distinct means, the first of which being looking at seabed indications. This included methods such as piston coring, geochemistry, microbial genomics, and the use of both AUV and ROV. Additionally, subsurface indications, including Seismic DHIs, migration indicators, amplitude anomalies were also observed. Once integrated, these indicators provided a wealth of evidence for the presence of thermogenic hydrocarbons, decreasing the risk in overall source rock presence.

Seabed Piston Coring

Nova Scotia has been researching, surveying, and piston coring potential offshore hydrocarbon seeps along the deep-water Scotian Slope since 2015. This work has produced evidence that indicates the presence of thermogenic hydrocarbon in the deepwater offshore Nova Scotia, thus implying there is a working thermogenic petroleum system. A summary of the cruises is as follows:

2015 - captured 29 locations
- positive results for hydrocarbon in two samples

2016 - captured 50 locations
- positive results for hydrocarbon in ten samples
- good evidence differentiating gas and oil

2018 - captured 10 locations at 3 sites
- Reconfirmed 2016 positive results at Site 41

2020 - AUV work to define seabed sites

2021 - ROV work to sample in-situ hydrocarbon seeps

With the cores collected, the NRR partnered with different institutions including Saint Mary's University, the University of Calgary, and Genome Atlantic and Genome Alberta to undergo geochemistry and microbial genomics analysis, both of which showed indications of thermogenic oil, gas and light hydrocarbon. With access to the very high quality and resolution Shelburne and Tangier 3D seismic surveys, a screening was completed for features on the sea floor to identify potential seepage sites. Once identified, select features were confirmed and visualized with both the AUV and ROV surveys.

Over all conclusions indicate thermogenic hydrocarbons are present across the entire margin.

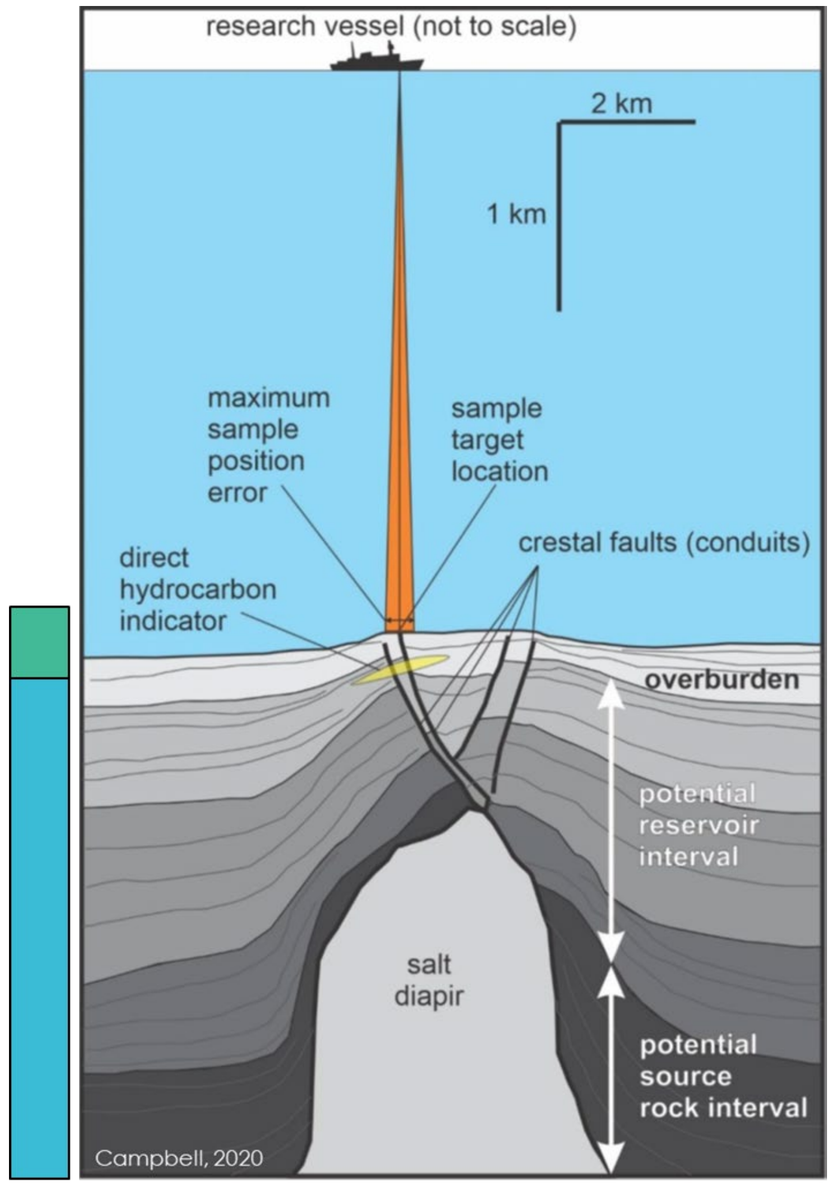

Figure 29: Diagram indicating an example of a piston coring target and potential error in coring location. Green bar represents depth of surface indication methods and blue the subsurface efforts (Campbell, 2020).

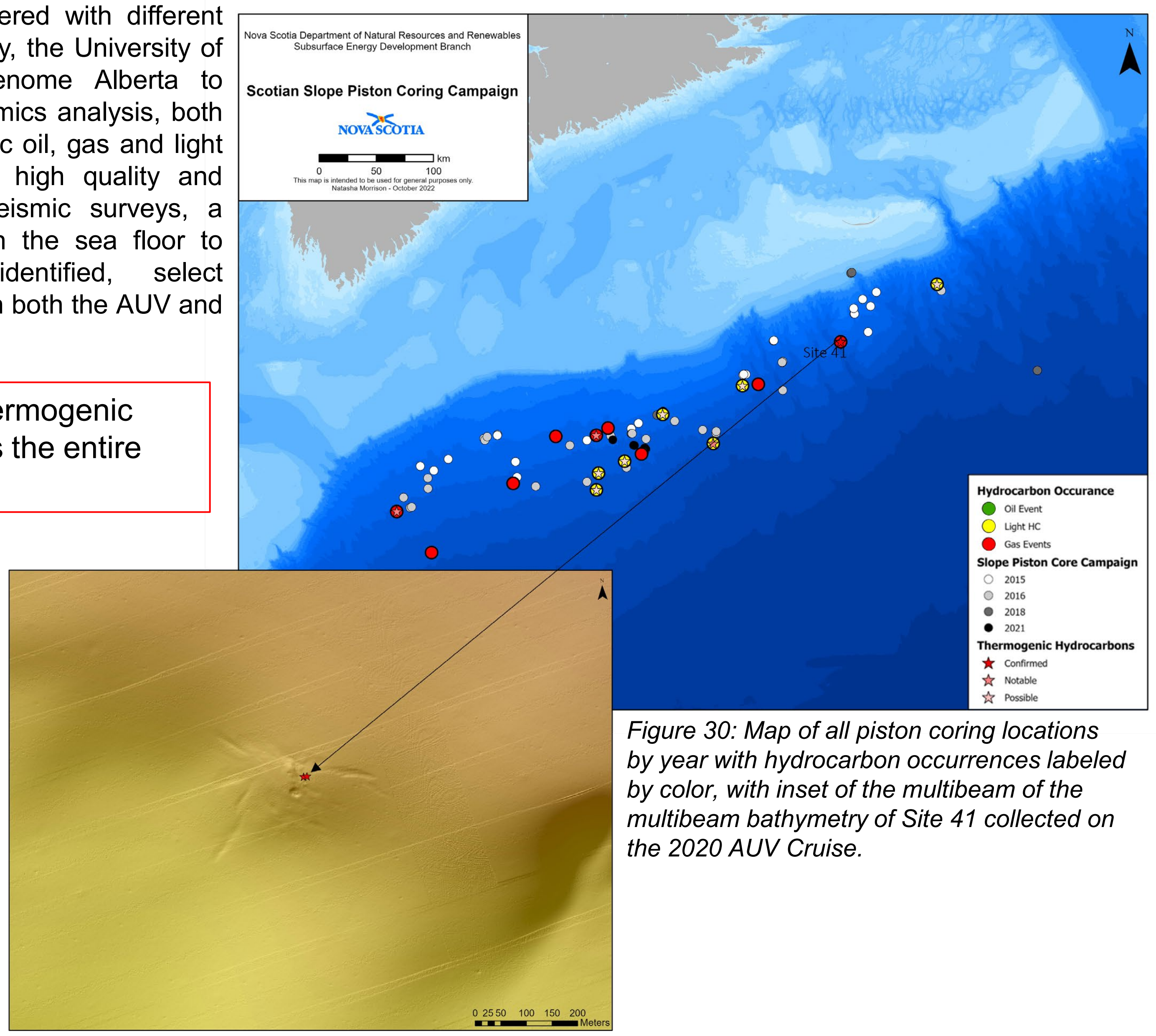

Figure 30: Map of all piston coring locations by year with hydrocarbon occurrences labeled by color, with inset of the multibeam of the multibeam bathymetry of Site 41 collected on the 2020 AUV Cruise.

Geochemical Results

Geochemical analysis was completed my Dr. Martin Fowler and his team at ATP International. Different types of analysis were completed to determine if the piston cores contained thermogenic hydrocarbons:

- Gas composition and isotopes of headspace gases
- Gas Chromatograms of sediment extracts
- Biomarker analysis of extracts to determine presence of thermogenic versus biological compounds

The most prospective core was Site 41 from the 2016 cruise which had very good evidence for liquid thermogenic hydrocarbons; providing confidence that it was located near a seep. This was confirmed by 2018 Site 7 which was cored close by (Fowler, 2018, Fowler and Webb, 2016). Several other sites show possible geochemical evidence for the presence of thermogenic hydrocarbons that could have migrated from the subsurface, such as extracted organic matter gas chromatographs with a high abundance of lighter hydrocarbons or gases with a thermogenic methane component.

A) Sediment Extracts - Biomarker (terpanes and hopanes) GC-MS data

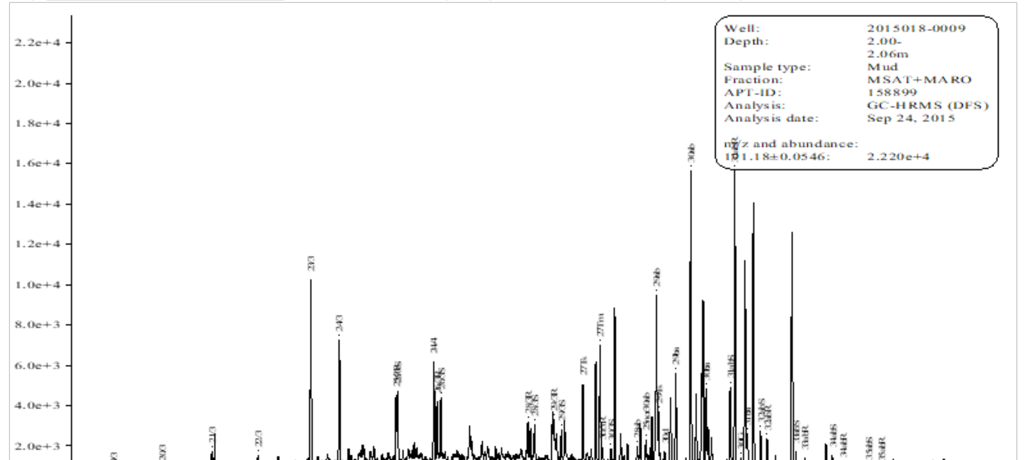

B) Gas Analysis - Whole extract GC

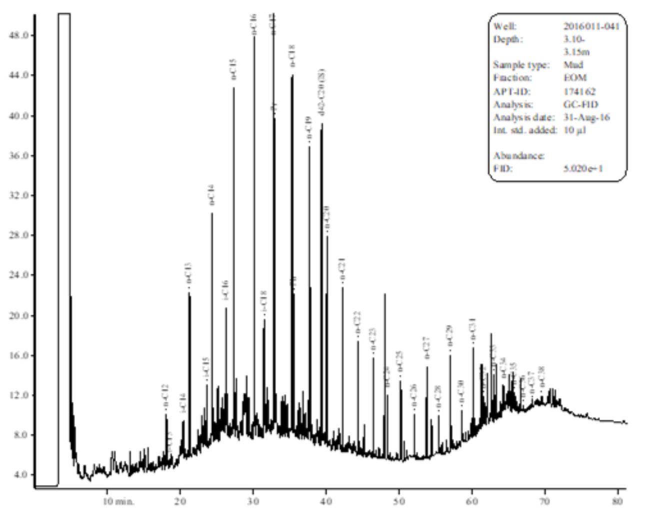

Figure 31: A) Example GCMS of sediment extracts from the 2015 cruise (Webb, 2015) B) Example whole extract GC gas analysis from the 2016 cruise (Fowler and Webb, 2016).

Gas Analysis – Bernard Diagram

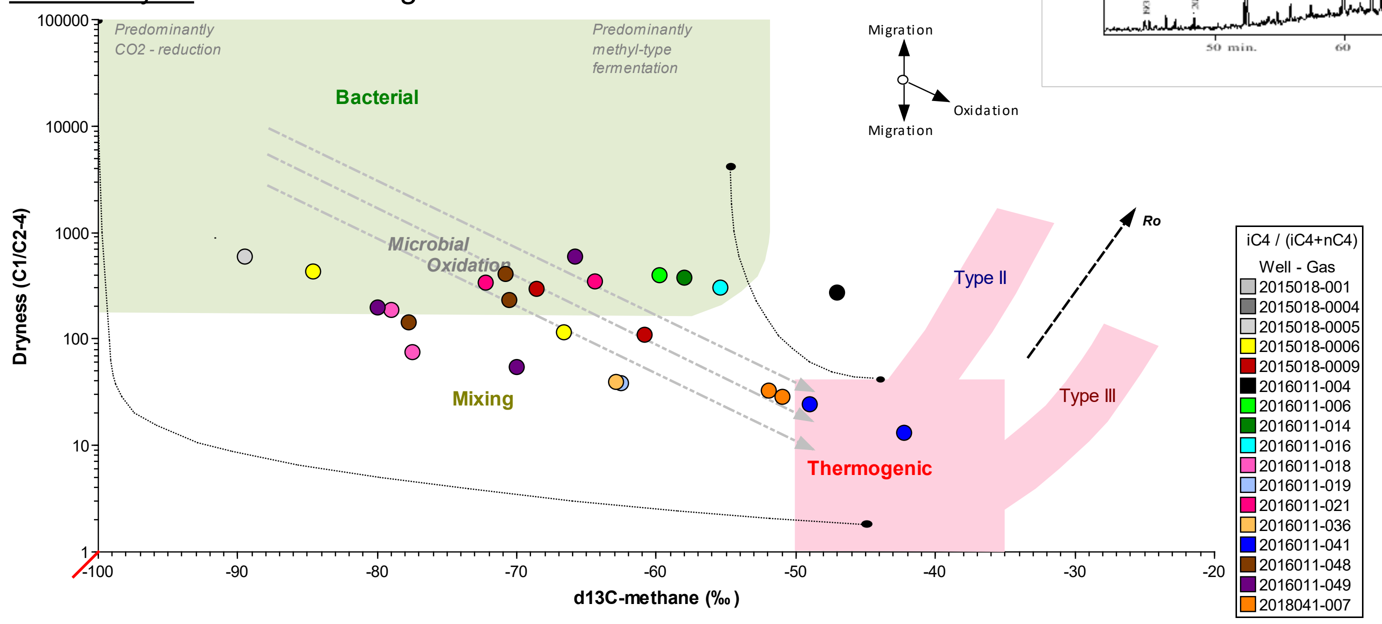

Figure 32: Bernard Diagram of δ13C methane versus gas dryness. Modified after Bernard et al. (1978); Whiticar, 1994) (Fowler, 2022).

Microbial Genomics

Dr. Casey Hubert and his team at the University of Calgary have been using microbial genomics to identify thermogenic hydrocarbons at the seep sites. Once example of such analysis is identifying thermophilic spore forming bacteria in seabed samples. These "thermospores" are genetically similar to bacteria that live in deep hot oil reservoirs. They are believed to be transported to the surface with thermogenic hydrocarbon seepage (Gittins et al. 2022).

Thermospore DNA signals in sediments cluster according to petroleum geochemistry. According to the figure below from Gittins et al. (2022), Site 16-41 and 18-7 both show strong hydrocarbon signals (Figure 34).

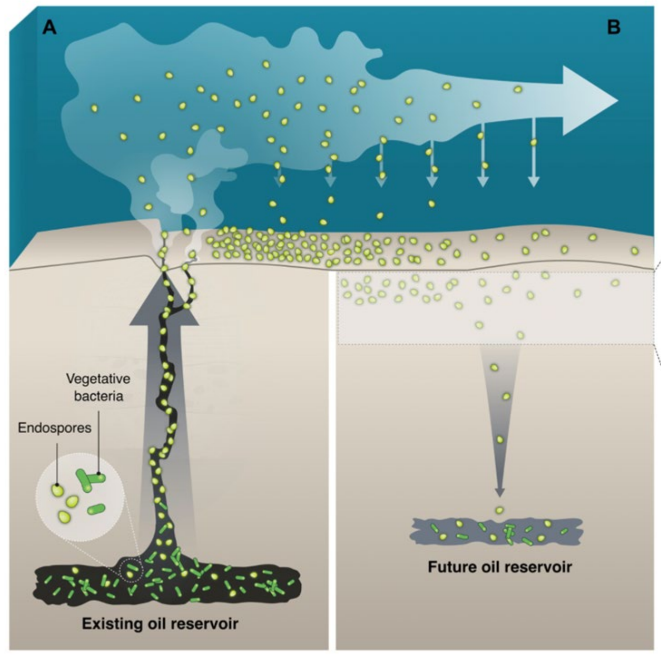

Figure 33: Diagram picturing the thermospore distribution process (Gittins et al. 2022)

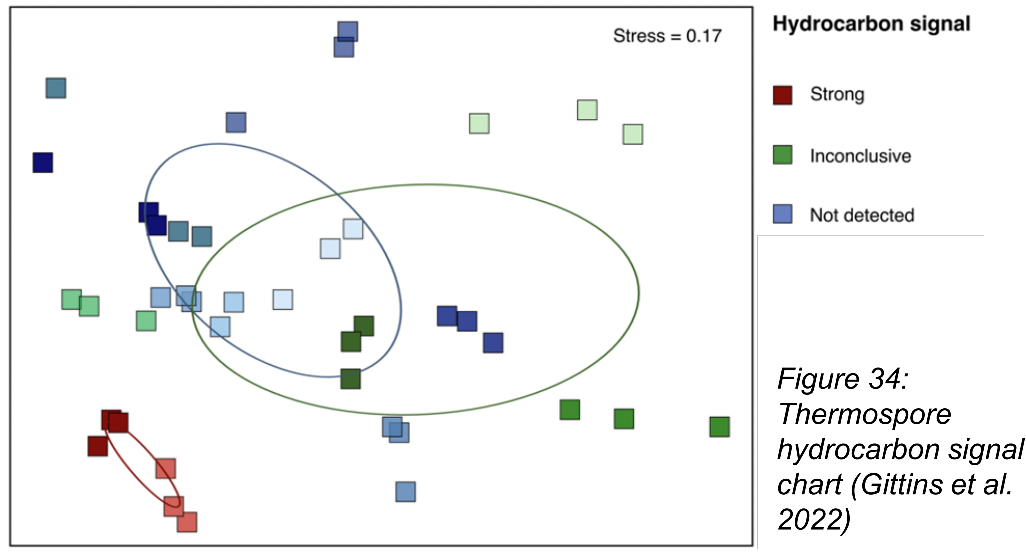

Figure 34: Thermospore hydrocarbon signal chart (Gittins et al. 2022)

Indirect Evidence – Hydrocarbon Migration

Hydrocarbon Occurrences – Evidence for Charge Migration

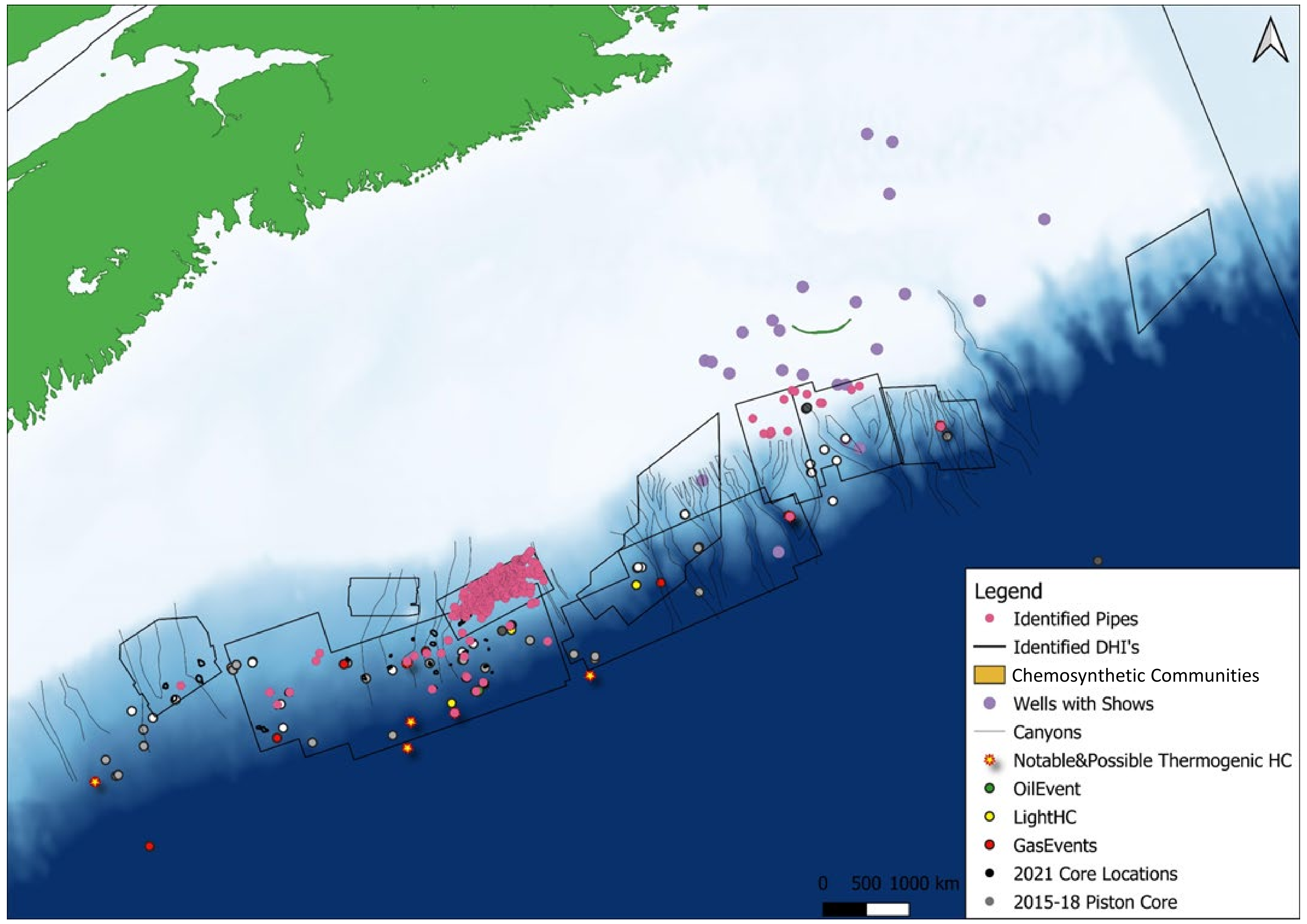

Figure 35: Map of 3D studies included in the project and key identified features (MacAdam, 2023).

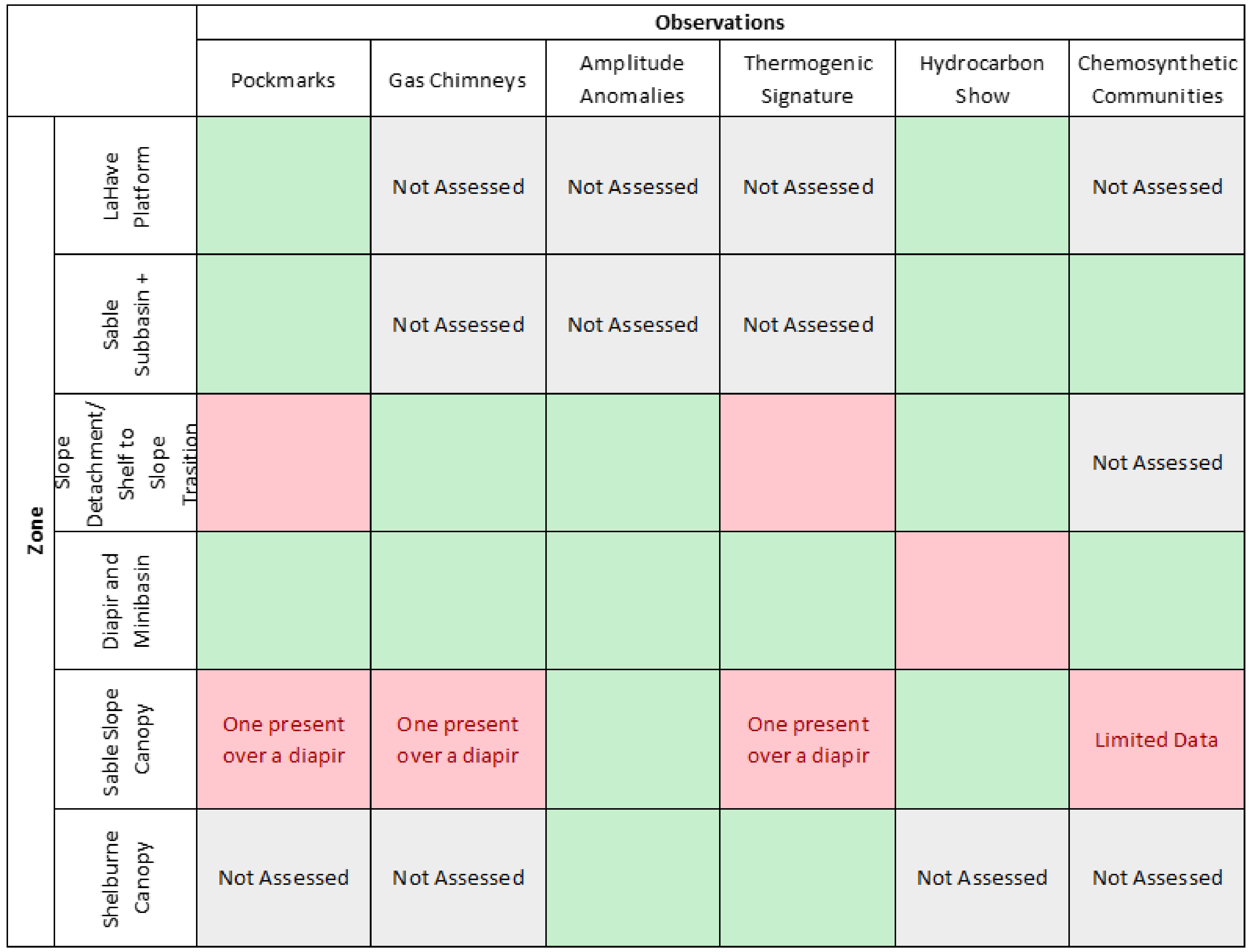

Zone	Observations: Pockmarks	Gas Chimneys	Amplitude Anomalies	Thermogenic Signature	Hydrocarbon Show	Chemosynthetic Communities
LaHave Platform	🟩	Not Assessed	Not Assessed	Not Assessed	🟩	Not Assessed
Sable Subbasin +	🟩	Not Assessed	Not Assessed	Not Assessed	🟩	🟩
Slope Detachment/ Shelf to Slope Trasition	🟥	🟩	🟩	🟥	🟩	Not Assessed
Diapir and Minibasin	🟩	🟩	🟩	🟩	🟥	🟩
Sable Slope Canopy	🟥 One present over a diapir	🟥 One present over a diapir	🟩	🟥 One present over a diapir	🟩	🟥 Limited Data
Shelburne Canopy	Not Assessed	Not Assessed	🟩	🟩	Not Assessed	Not Assessed

presence of evidence
no evidence
not assessed/data not present

Figure 37: Crossplot corelating evidence vs zone. Each block is labeled with one of three colors; green indicating the presence of evidence, red for no evidence, and grey for not assessed/data not present. (MacAdam, 2023).

Seismic Imaging of Migration Pathways

With the evidence gained from the piston coring program, and the background work that went into completing them, the project was then taken one step further to attempt to actively identify migration pathways for these hydrocarbons using the ten 3D deepwater seismic surveys available to the department (Figure 35). Features such as gas chimneys, shallow direct hydrocarbon indicators (DHIs), and pock marks were studied with the main objective being to aid in the derisking of petroleum systems along the Scotian margin by understanding the relationship between DHI's, piston coring data and geochemistry results.

The majority of the DHI's and pipes observed occur above salt diapirs in deepwater (Figure 36). Additionally, many have also been identified around Gas hydrate stability zones, including the well studied Bottom Simulating Reflector (BSR) present in the Torbrook survey (e.g. Cullen et al., 2008). In order to draw practical observations and conclusions, the margin was split into zones (Figure 37 and 38) to attempt to understand the extent and possible causation of the migration indicators. This allowed for a cross correlation of key evidence to be compiled. The key evidence included pockmarks, gas chimneys, amplitude anomalies, Thermogenic Signature, Hydrocarbon Shows in wells and seafloor chemosynthetic communities observed during the ROV cruise. Key observations drawn were the main migration pathways along the margin seem to be diapirism and subsequent faulting; while the main barrier is the impermeable salt canopy. The Eastern and Western anomalies, were predominantly clustered near the shelf or on the shelf to slope transition, to the north and east of the salt canopy. This could be an indication of hydrocarbons migration towards a more hydrostatic shelf. Regarding the seafloor indications of seepage the major control appeared to be seafloor and shallow lithology. This deep migration assemblage supports the presence of source rock on the Scotian Slope (MacAdam, 2022).

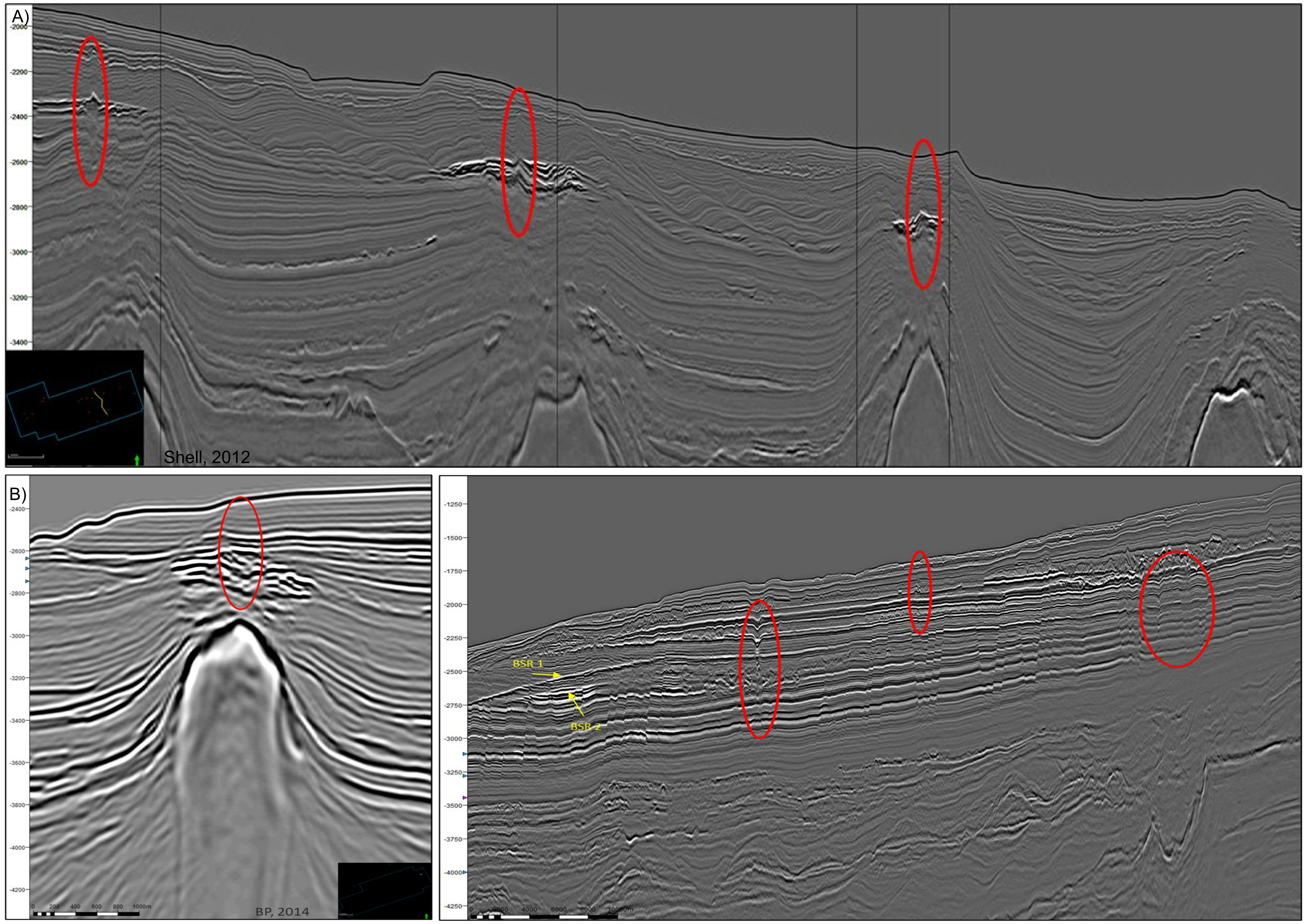

Figure 36: A) Examples of supra diapir DHIs and gas chimneys in the Shelburne 3D Survey. B) DHI and gas chimney associated with Site 14 from the Tangier 3D survey. C) BSR (as described by Cullen et al. 2008) and gas chimneys in the Torbrook 3D survey (MacAdam, 2023).

Hydrocarbon Occurrences – Evidence for Charge Migration

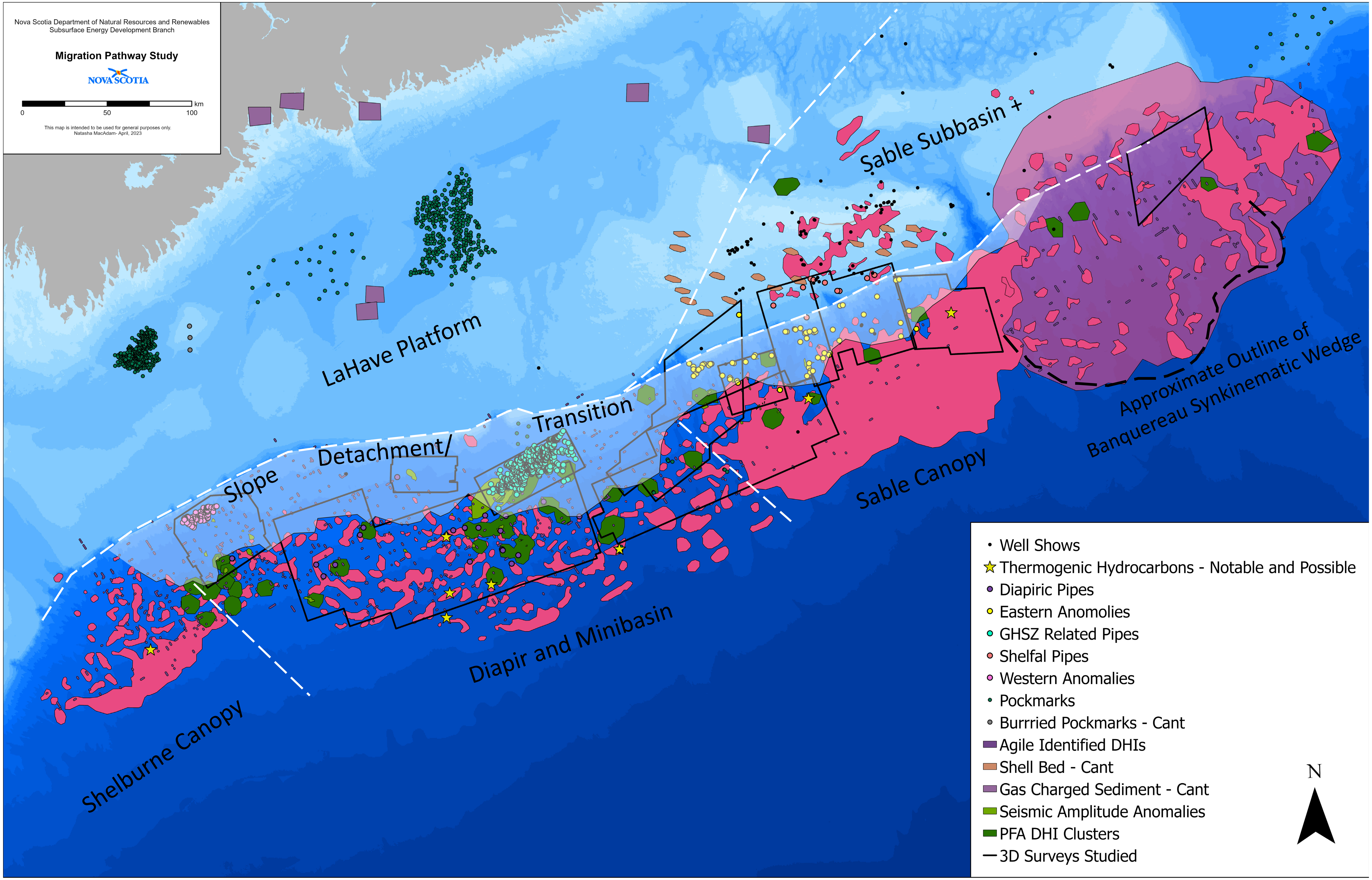

Figure 38: A) Map highlighting all mapped features with the broken up into zones to observe differences in evidence. Zones based loosely on those outlined in Deptuck and Kendall, 2012.

CHAPTER 2.3
JURASSIC SOURCE ROCKS – SYNTHESIS AND NEW MODELS

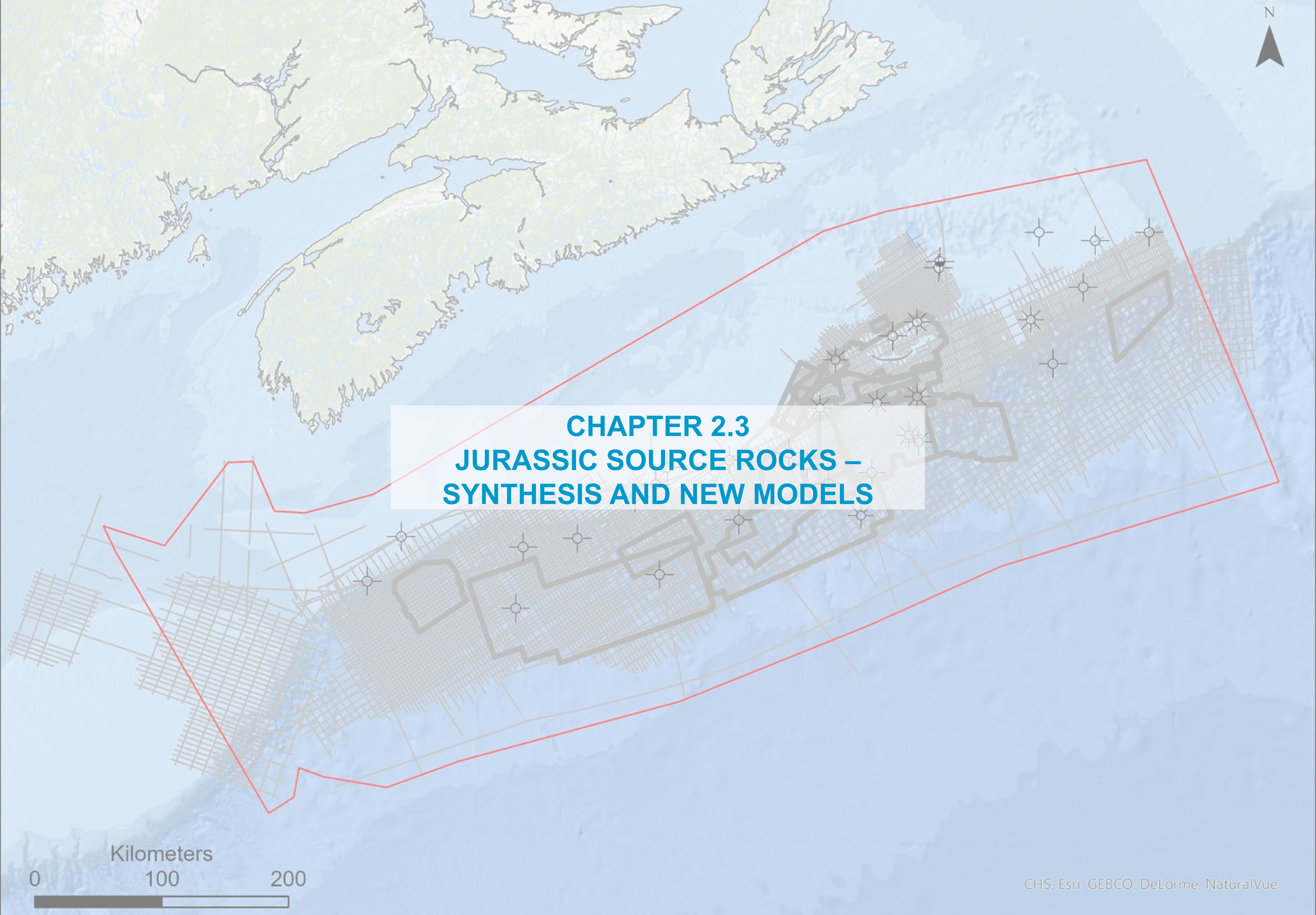

CHS, Esri, GEBCO, DeLorme, NaturalVue

Jurassic Source Rocks – Synthesis and New Models

Scotian Basin Integration Atlas 2023 – CANADA – June 2023

ORGANIC FACIES PREDICTION AND RISKING OF JURASSIC SOURCE ROCKS

Scougal et al., 2021

As part of a program with 12 projects completed to increase the understanding of Nova Scotian paleogeographic topics, Getech completed a source rock modeling project with the objective of predicting the distribution of Tithonian and Early Jurassic (Toarcian, Pliensbachian, Sinemurian, Hettangian) source rocks in offshore Nova Scotia. Modeling was completed based on:

- Biogeographic principles derived from modern environments
- paleoenvironmental interpretations derived from paleogeographic mapping
- Getech's proprietary organic facies prediction (OFP) modelling

A variety of data, including tectonic and structural morphology, were used to create the Gross Depositional Environment (GDE) which provided a spatial understanding of coastlines, bathymetry and depositional environments (Scougal et al. 2021). The Organic Facies Prediction Modeling (OFP) was first conducted with using the expansive European Tethys to more adequately ground truth predicted TOC and HI values. The boundary conditions consisted of Getech's palaeographical and bathymetric reconstitutions. This was followed by higher resolution modeling within the Hispanic Corridor area of interest. This used the modern analogue of the Black Sea to define the oceanographical conditions in Nova Scotia during the four time periods (Scougal et al. 2021).

The maps seen in Figure 30 were built by incorporating the gross depositional environment maps, with the organic content (TOC), richness (HIA) and oxygen levels and identify favorable to unfavorable conditions. It should be noted that the maps do not take accommodation space, potential thickness, preservation or maturity into account (Scougal et al. 2021).

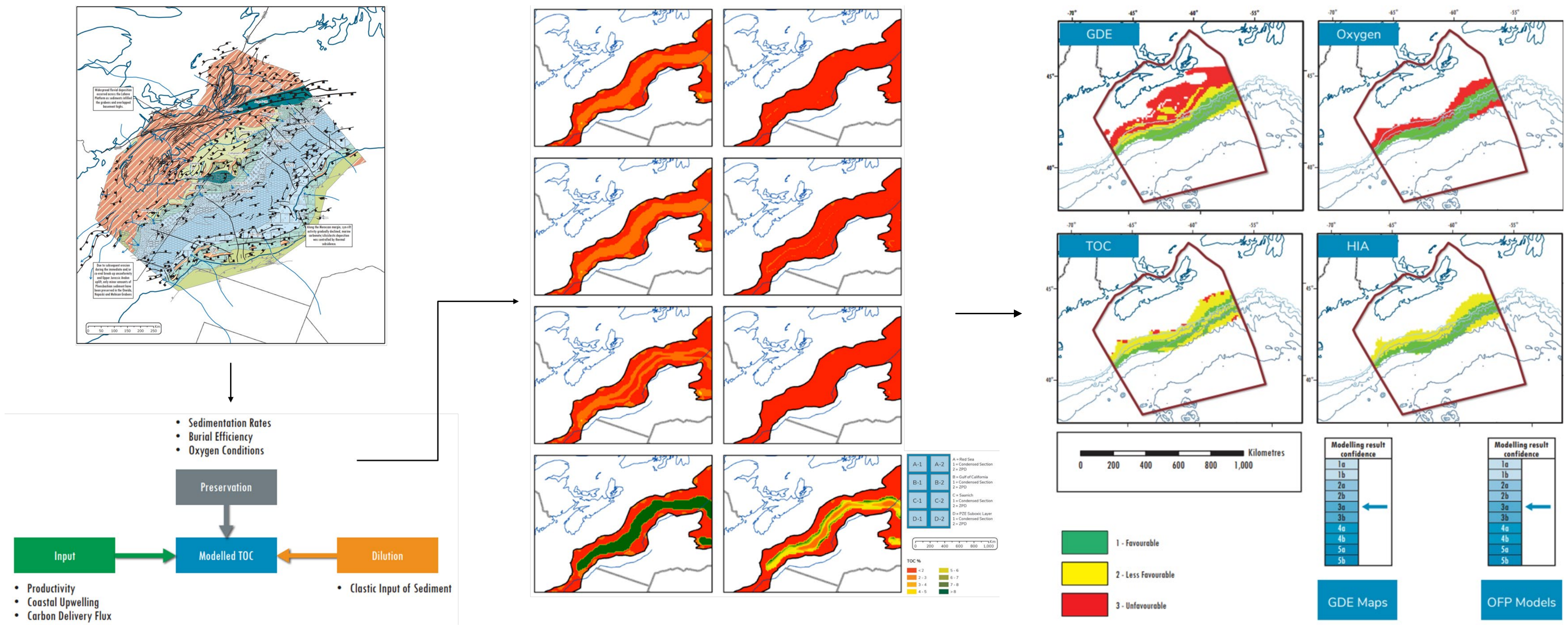

Figure 39: Getech's source rock prediction and risking method (Derived from Scougal et al., 2021).

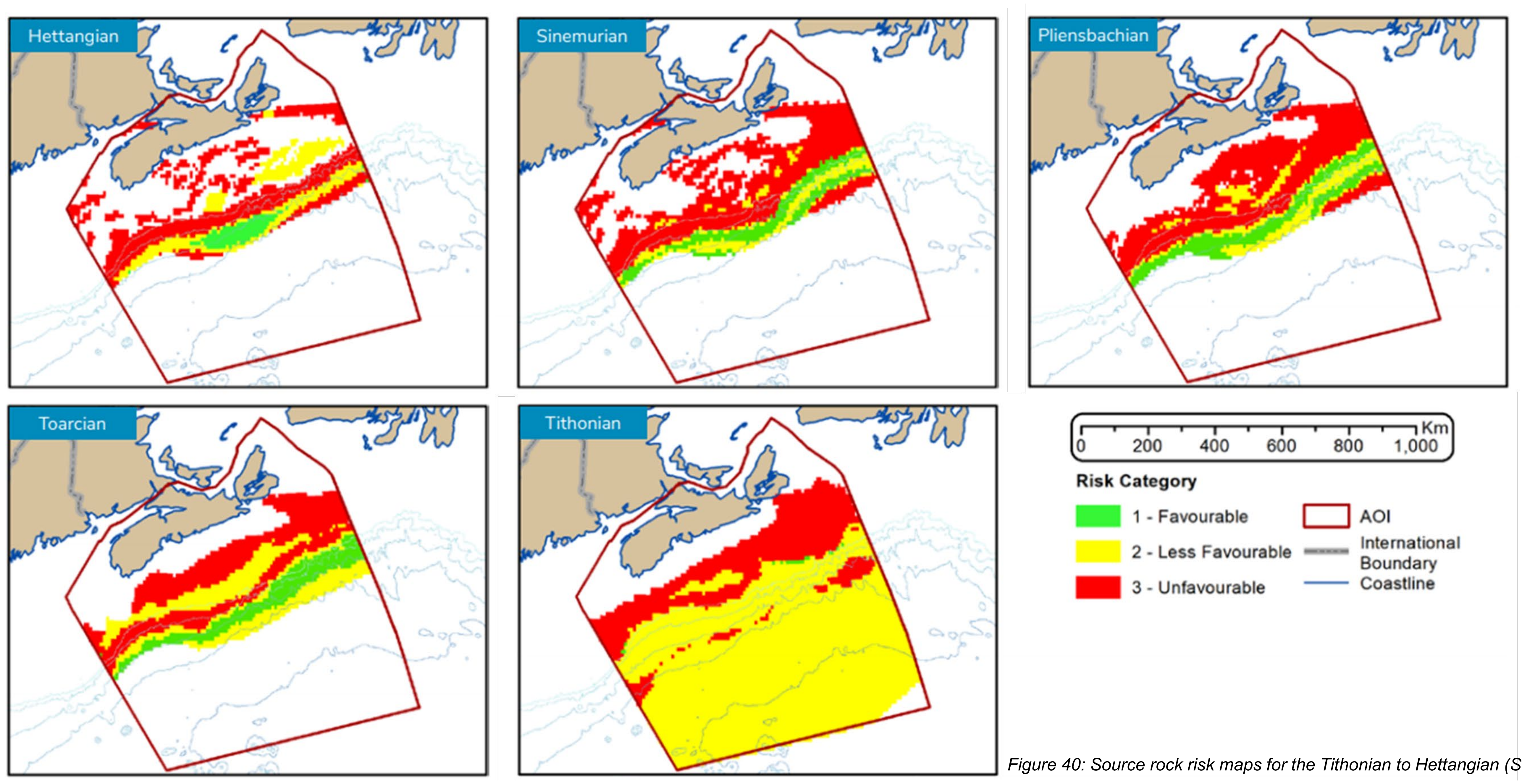

Figure 40: Source rock risk maps for the Tithonian to Hettangian (Scougal et al., 2021).

Results of this project indicated that, if present, all four Jurassic intervals studies showed favorable conditions for source rock development (Figure 40). This was due to the shallow low oxygen conditions, coupled with the high carbon delivery flux and sedimentations rates predicted. Margins of the marine basin show widespread favourable conditions for deposition of organic rich sediments (Scougal et al., 2021).

There are some uncertainties, as with any modeling. TOC modeling of the Pleinsbachian indicate highest TOCs are predicted for moderate depth, distal marine locations, outboard in the Tethys ocean. Bishop (2022) notes that this result is counterintuitive as these conditions are not thought to produce optimal source rocks. In addition, areas such as the Lusitanian Basin, which is known for its significant accumulations of organic rich sediment, do not stand out in these maps. Though a scientifically robust approach, there are several factors that cannot be reasonably predicted at this time (Bishop, 2022).

EQUIVOCAL EVIDENCE

Some early studies conducted as part of the play fairway analysis program, have since been shown to be equivocal and/or unreliable. The 2011 PFA included three sets of observations that have since been re-analysed and shown to be questionable. These are recorded here for completeness.

Local Source Stringers in Salt

Photomicrographs of fluid inclusions found in salt sections from Glooscap C-63 and Weymouth A-4 revealed thin organic rich stringers, assumed to be a remnant of algae/bacteria deposited in the evaporitic environment. These indications are likely to be the product of the maturation of these in-situ organic stringers. There is no evidence of shows in the sedimentary section above and thus, this evidence is unlikely to be relevant to Lower Jurassic source potential (Bishop, 2022).

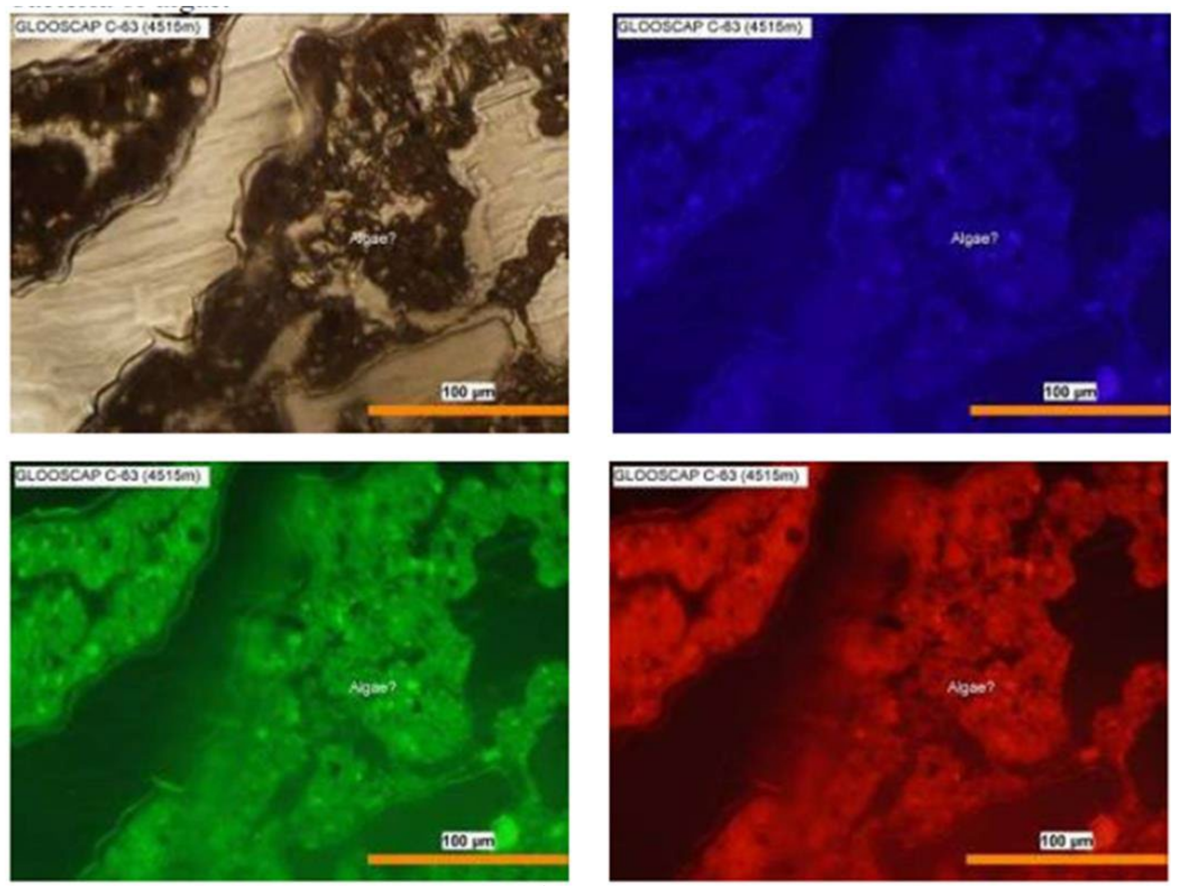

Figure 41: Thin section photomicrograph of organic rich laminae within an autochthonous salt sample from Glooscap C-43 (Kettanah, 2010).

Uniacke G-72

The 2011 PFA reported that the Uniacke G-72 well contained 'remobilized Liassic sediments', with Fowler et al. (2020) indicating that the well had penetrated the Lower Jurassic. Biostratigraphic analysis, however, indicated this well was actually completed in an interval dated Kimmeridgian-Oxfordian (RPS, 2010). The reworked signature at 4,585m was also dated to the Callovian-Bajocian indicating that Uniacke G-72 does not provide evidence for the Lower Jurassic (Bishop, 2022).

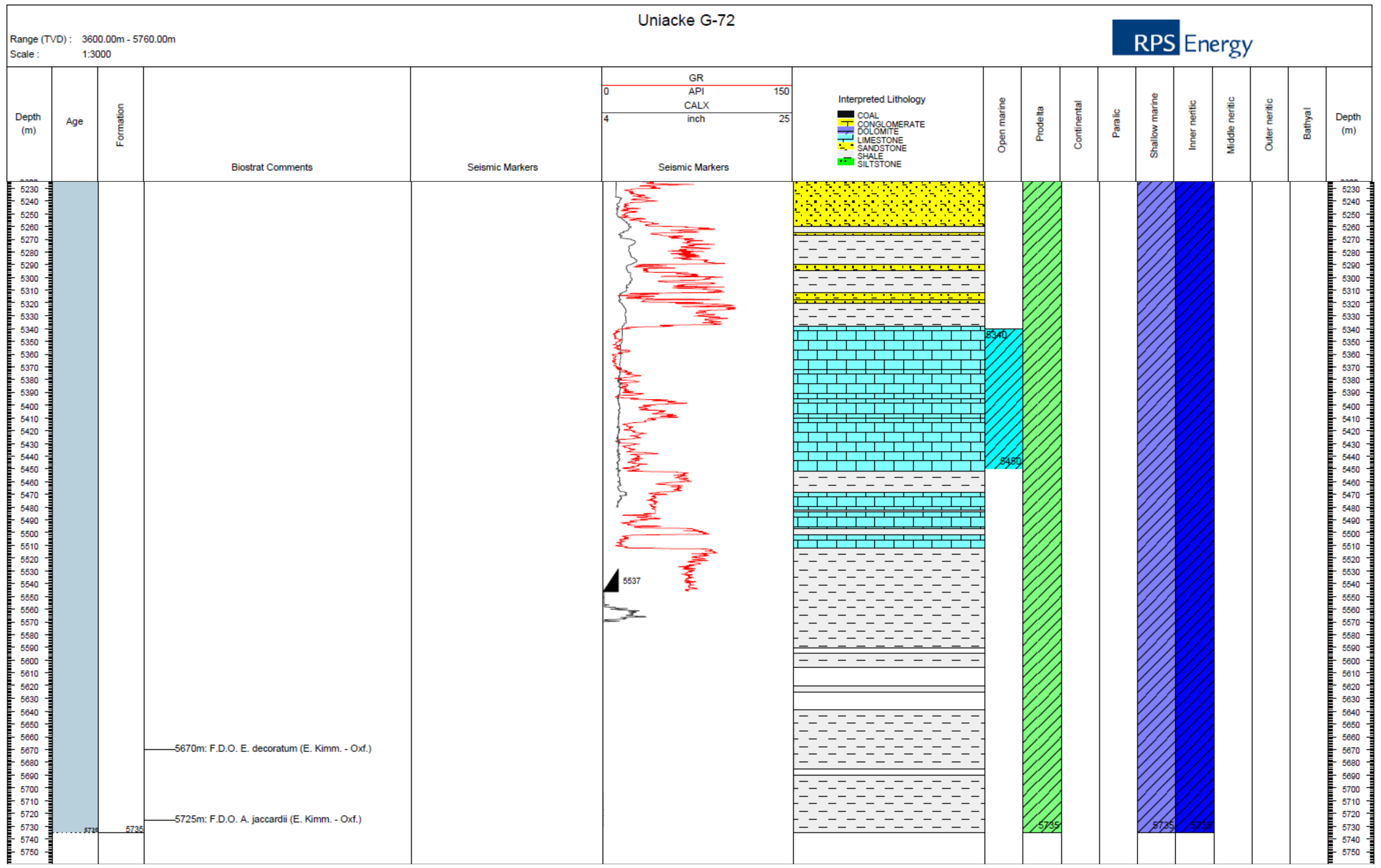

Figure 42: Biostratigraphic Summary Chart of the base of Uniacke G-72 (RPS, 2010).

Gammacerane

Geochemical analysis of the Venture B-13 occurrence of Gammacerane in the condensate of DST#6 (Beicip et al, 2011). Gammacerane is often interpreted as indicating a stratified, hypersaline environment (like the Early Jurassic in Nova Scotia). However, later review showed that the observations of gammacerane were almost certainly due to the result of contamination of lignosulfonate, a common mud-additive often used in offshore Nova Scotia.

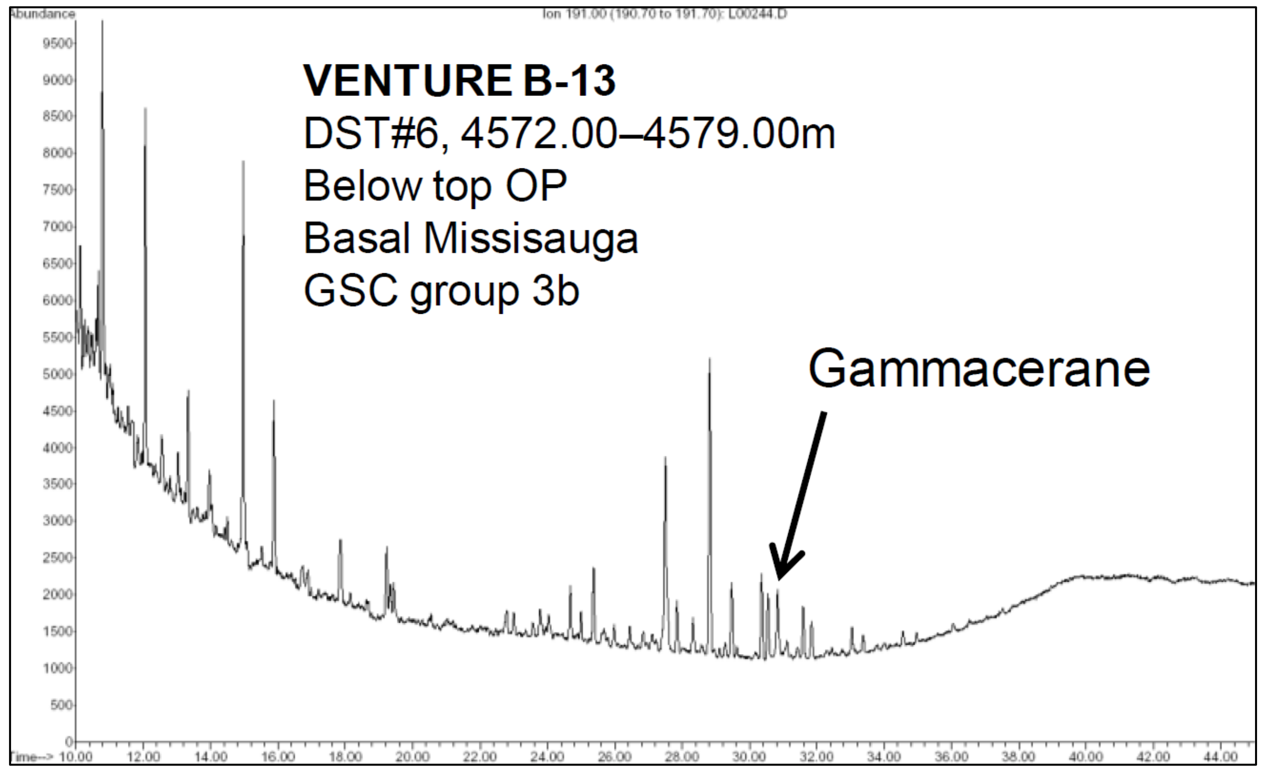

Figure 43: Hopane traces (m/z 191) of the Venture B-13 condensate a significant displaying a Gammacerane anomaly compared to the other oils and condensates in the area (Beicip et al., 2011).

Figure 44: Hopane traces (m/z 191) of a cutting sample from 4580m from the Venture B-13 well once again showing the Gammacerane anomaly (Beicip et al., 2011).

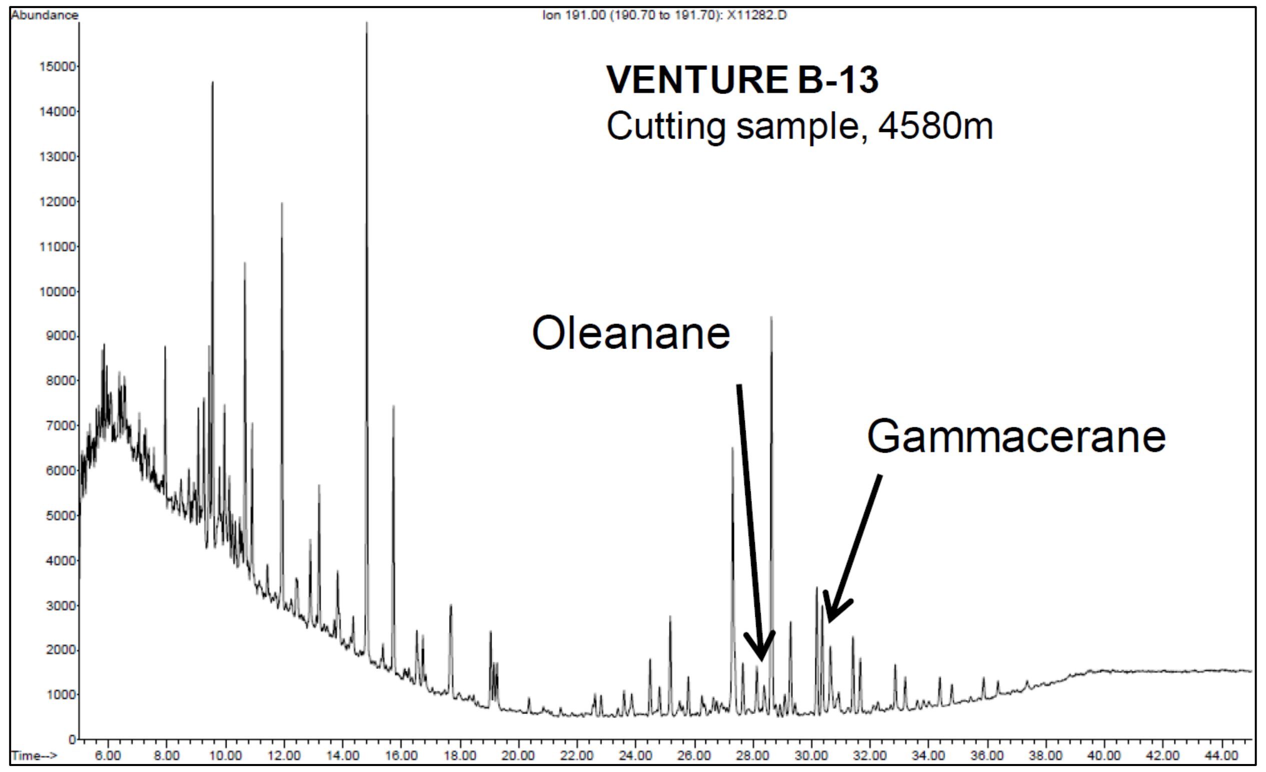

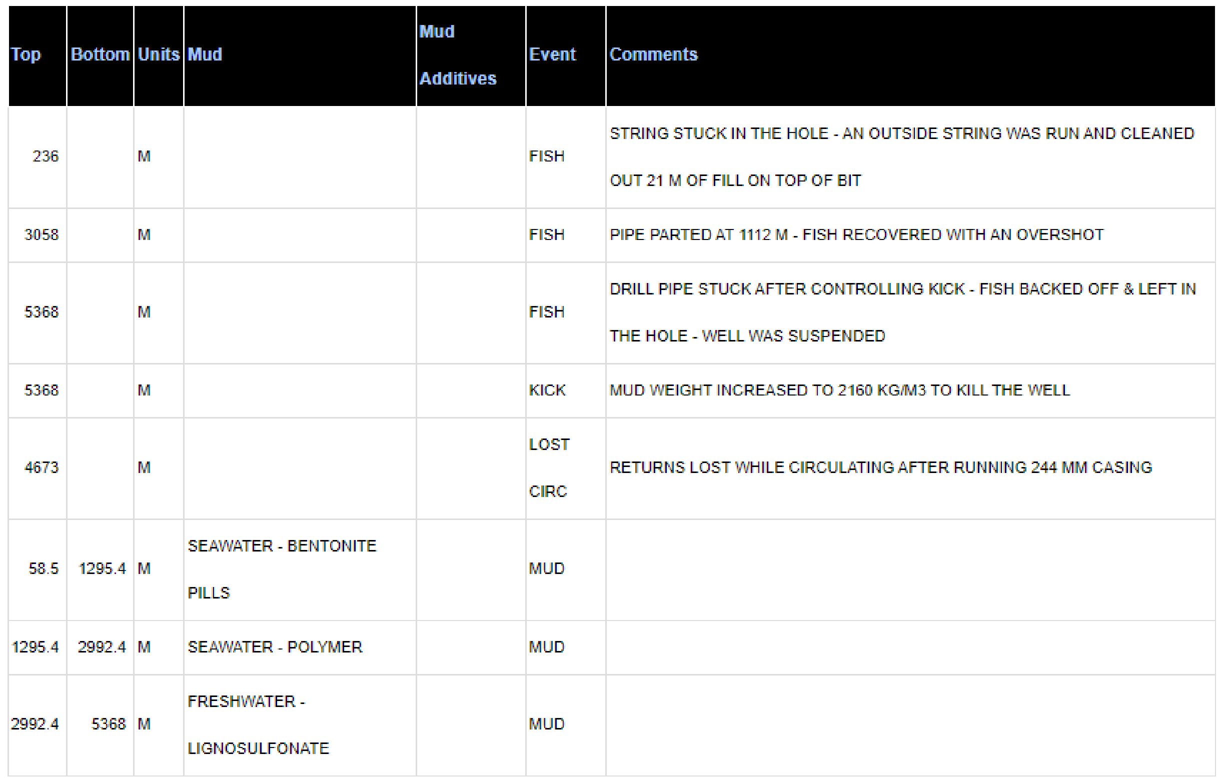

Top	Bottom	Units	Mud	Mud Additives	Event	Comments
236		M			FISH	STRING STUCK IN THE HOLE - AN OUTSIDE STRING WAS RUN AND CLEANED OUT 21 M OF FILL ON TOP OF BIT
3058		M			FISH	PIPE PARTED AT 1112 M - FISH RECOVERED WITH AN OVERSHOT
5368		M			FISH	DRILL PIPE STUCK AFTER CONTROLLING KICK - FISH BACKED OFF & LEFT IN THE HOLE - WELL WAS SUSPENDED
5368		M			KICK	MUD WEIGHT INCREASED TO 2160 KG/M3 TO KILL THE WELL
4673		M			LOST CIRC	RETURNS LOST WHILE CIRCULATING AFTER RUNNING 244 MM CASING
58.5	1295.4	M	SEAWATER - BENTONITE PILLS		MUD	
1295.4	2992.4	M	SEAWATER - POLYMER		MUD	
2992.4	5368	M	FRESHWATER - LIGNOSULFONATE		MUD	

Figure 45: Mud Types and Drilling Events of Venture B-13 from NRCan's Basin Database.

SYNTHESIS AND CRITIQUE OF LOWER JURASSIC HYDROCARBON CHARGE EVIDENCE

With 12 years of new geoscience research on the presence of a Lower Jurassic, Dr. Andy Bishop of Stratum Reservoir undertook a project to both validate and verify observations and inference related to Lower Jurassic hydrocarbon charge potential in offshore Nova Scotia. These panels represent excerpts from that report, with all previous work summarized in this chapter was included in this review. (Bishop, 2022). This was completed in four key steps:

- Incorporating all source rock related studies since 2011
- Ground truthing evidence
- Exploring factors influencing source rock deposition - critical boundary conditions for source rock development in this region
- Deriving source rock presence maps for the area of interest

Ground Truthing Lias Presence

There are multiple lines of evidence indicating Lower Jurassic marine sedimentation took place offshore Nova Scotia including:

(1) Reworked diagnostic Lower Jurassic nannofossils in South Griffin J-13. These are similar to the Lower Jurassic markers found in wells such as the Bittern M-62 well on the Grand Banks (Bishop, 2022).

(2) Ongoing biostratigraphic work indicating the 'indeterminate' aged sabkha sections in select shelf wells are tentatively Lower Jurassic sediments, suggesting deeper oceanic conditions would be expected down slope (Figure 46,48). Further validation of these observations and extrapolation to neighboring wells will help constrain the timing of earliest fully marine conditions (Bishop, 2022; Weston et al., 2012; MacRae, pers. comm.).

(3) Potential source rock indications or positive environments for source rock deposition are found in four wells outlined in Figure 46 and 47. On the Eastern North Atlantic Margin, MZ-1 biostratigraphy recorded an abundance of marine amorphous organic material between 6,050m and 6,115m (RPS, 2016). Though there is no geochemical evidence of source rock here (e.g. Fowler, 2019), this may represent a marginal facies related to effective source deposition further out in the basin. In addition, DSDP 547B shows geochemical signatures, though immature, indicative of sulfidic anoxic conditions in its Lower Jurassic section (Bishop, 2022). Figure 45 shows evidence of other indications of normal salinity marine environments in the post-salt Lower Jurassic beginning in the Late Sinemurian.

(4) On the Newfoundland Margin, the Heron H-73 well has an ~700 m section of Lower Jurassic sediments. While these sediments are indicative of relatively shallow water, there is likely to be a thick, equivalent basinal facies deposited outboard. The presence of elevated concentrations of extended tricyclic terpanes, a typical signature for the Lower Jurassic, provide an important calibration point of how a local Lower Jurassic geochemical signature may appear (Bishop, 2022). The presence of an anomalous and overmature section of organic rich sediments in Bittern M-62 (3,246.1 – 3,365.0 m), could also be representative of a marginal source facies with TOC values between 1 and 2% (Bishop, 2022).

Though no direct evidence of a Lower Jurassic source rock in offshore Nova Scotia exists, this indirect evidence coupled with hydrocarbon indicators in the form of recovered oil samples and stains from Mic Mac Area wells, seafloor hydrocarbon seep work, and direct hydrocarbon indicators in seismic also lend support to the hypothesis of the presence of a Lower Jurassic source rock on the Scotian Margin.

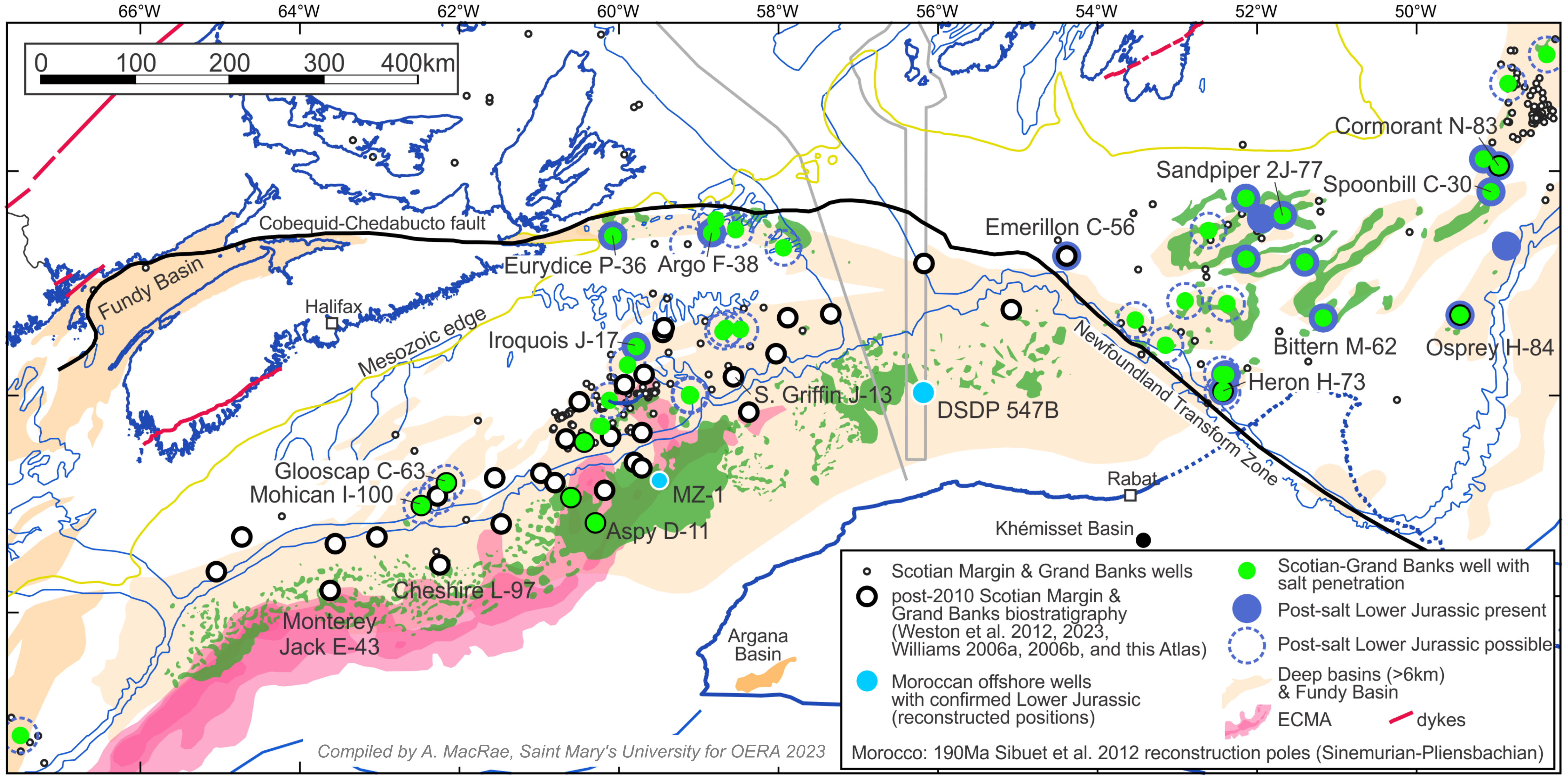

Figure 46: Distribution of wells with proven or tentative indications for the presence of post-salt Lower Jurassic sediments, southern Grand Banks and offshore Nova Scotia (Bishop, 2022; MacRae, pers. comm.). Ages used in this compilation are from recent biostratigraphic studies (Weston et al. (2012), in the OERA Laurentian Subbasin PFA (2014), and other OERA-sponsored PFA studies), Barss et al. (1979), Williams (2006a, 2006b), and summaries of industry reports in the Geological Survey of Canada's BASIN database. Approximate deeper basin outlines and Mesozoic edge are based on Williams and Grant (1998) and the Fundy Basin outline is based on Wade et al. (1996). Salt structure outlines are based on Deptuck and Kendell (2017) on the Scotian Margin and Balkwill and Legall (1989) on the southern Grand Banks.

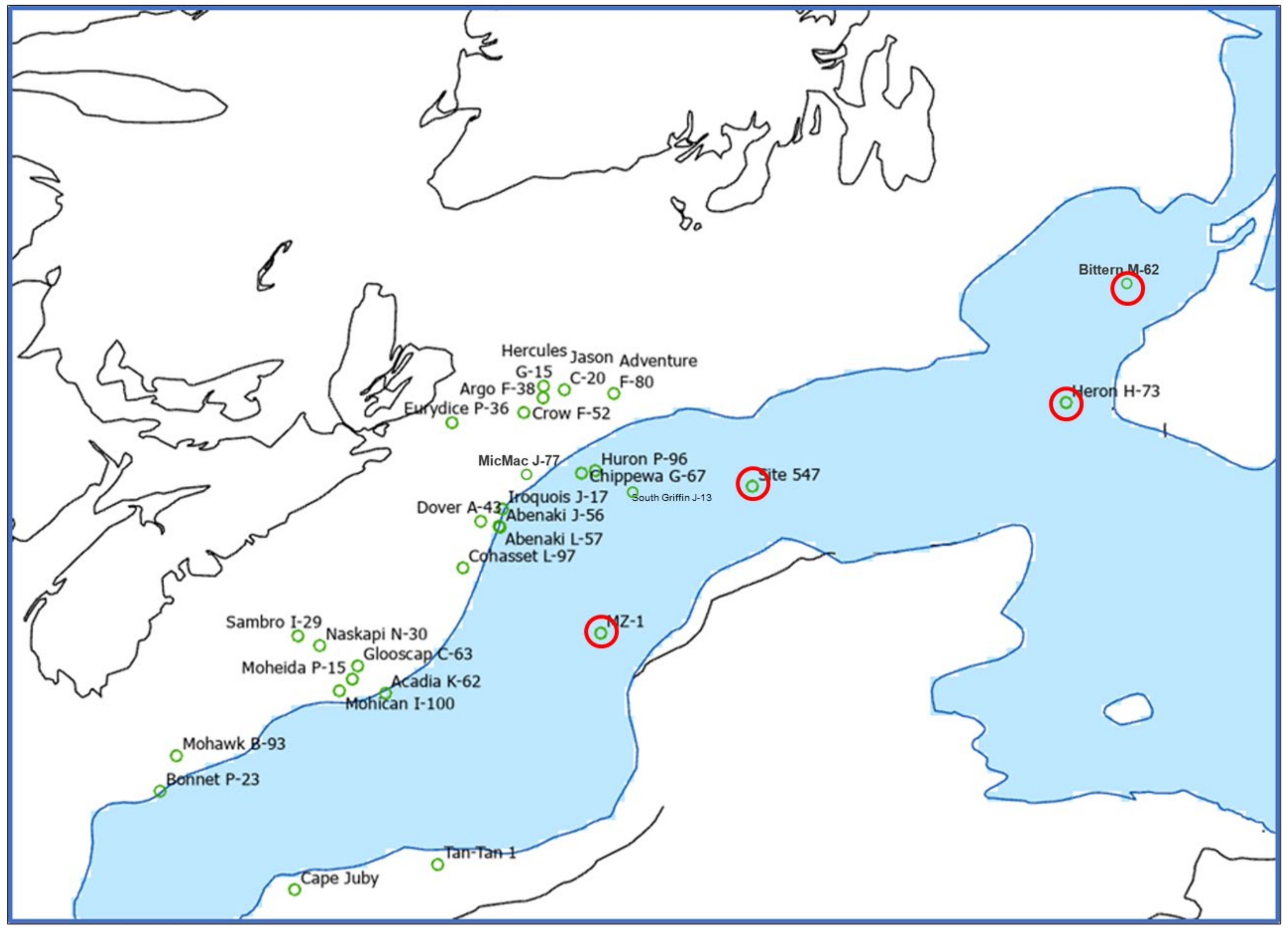

Figure 47: Wells relevant to the Bishop 2022 study with four wells highlighted with potential source rock indications. Two (MZ-1 and DSDP Site 547) are on the Moroccan conjugate margin and are shown in their approximate plate reconstructed positions.

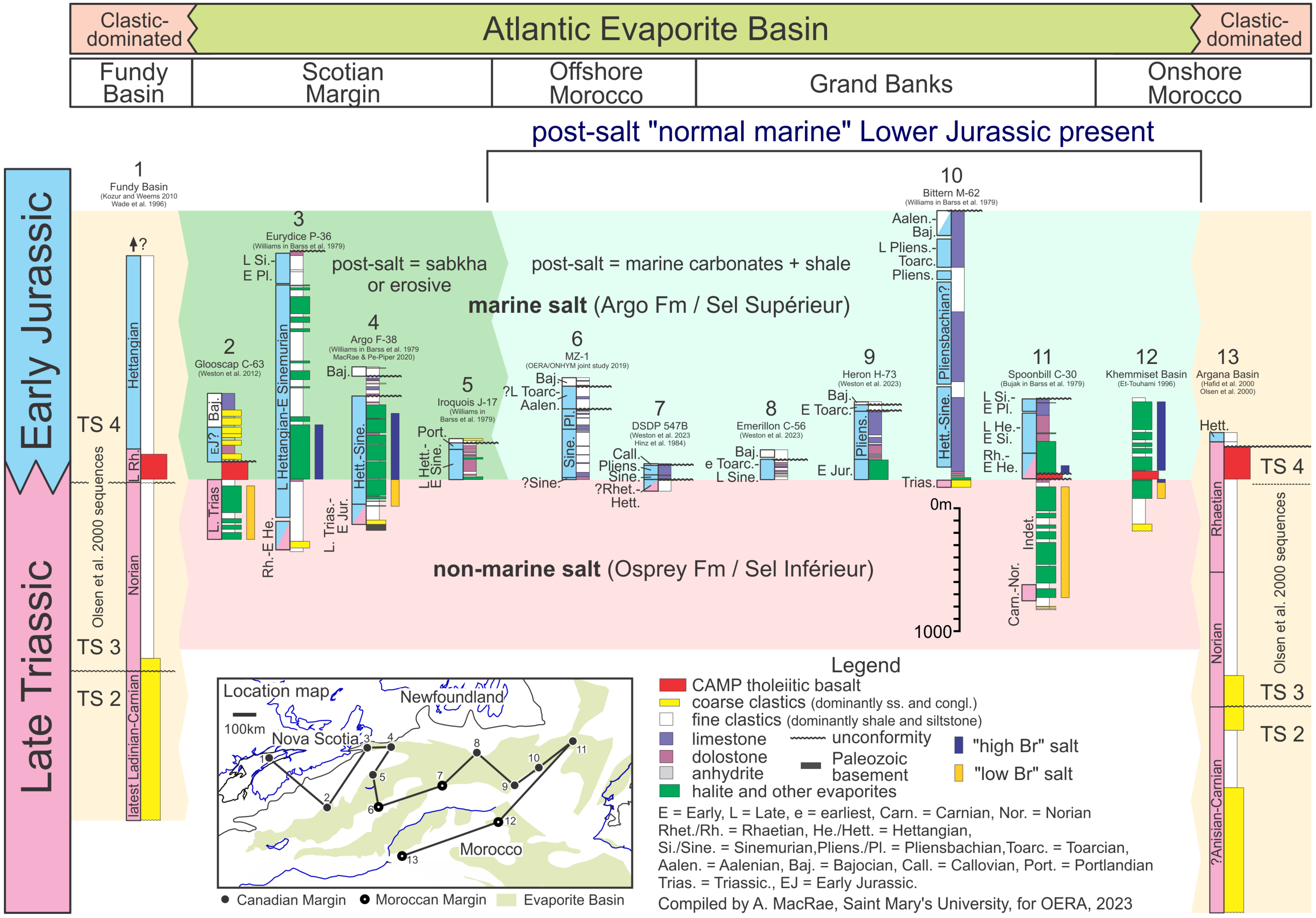

Compiled by A. MacRae, Saint Mary's University, for OERA, 2023

Figure 48: Upper Triassic-Lower Jurassic Central Atlantic Correlation

Figure 48 shows a stratigraphic correlation in the Upper Triassic-Lower Jurassic of the Scotian Margin, Grand Banks of Newfoundland, and the Moroccan Margin based on outcrop and offshore well sections. The simplified gross lithology and biostratigraphic age of the sections is indicated based on industry well history reports and the literature. Biostratigraphic information ranges from recent studies (this Atlas and Weston et al., 2012; 2023) to vintage (Barss et al. 1979), much of it summarized in the Geological Survey of Canada's BASIN database. Citations to biostratigraphy sources for individual sections are indicated on the plot.

Biostratigraphy in this interval is challenging due to the widespread presence of continental, sabkha, and evaporite environments that exclude normal marine salinity microfossil groups such as dinoflagellates, nannofossils, and foraminifera, leaving only lower-resolution terrestrial palynology (pollen and spores) as age indicators. This limitation is reflected in sometimes relatively imprecise age determinations (e.g., undivided or questioned "Early Jurassic"), a caveat that should be kept in mind when evaluating the correlations proposed here.

In general, more outboard outcrop locations such as the Bay of Fundy of the Scotian Margin or the Argana Basin of the Moroccan margin are non-marine clastic-dominated rift basins that are subdivided into tectonostratigraphic sequences (TS) by Olsen et al. (2000). More central basins have similar clastics interbedded with extensive (kms) evaporite deposition, mainly in the form of halite (salt). This "Atlantic Evaporite Basin" extends the entirety of the Central Atlantic (eastern North American and west African margins) and north onto the Grand Banks and Portuguese margins (Deptuck and Kendell, 2017; Leleu et al., 2016). The salt occurs in two geochemically distinct units:

1) a lower, low bromine concentration (<60ppm), continental salt deposited in Upper Triassic saline lakes, known as the Osprey Formation on the Grand Banks (Holser et al., 1988; McAlpine, 1990), and the Sel Inférieur on the Moroccan Margin (Et-Touhami, 1996; Hafid, 2000). This salt extends onto the Scotian Margin, though it is not as extensive (Deptuck and Altheim, 2018; MacRae et al., 2013; MacRae and Pe-Piper, 2020)

2) an upper, high bromine concentration (>60ppm), marine salt deposited in earliest Jurassic (Hettangian-?early Sinemurian) known as the Argo Formation (Wade and MacLean, 1990; McAlpine, 1990), and the Sel Supérieur on the Moroccan Margin (Et-Touhami, 1996; Hafid, 2000).

The transition between these two salt units on both Canadian and Moroccan margins is often associated with the occurrence of tholeiitic basalts of the Central Atlantic Magmatic Province (CAMP) (McAlpine, 1990; Hafid, 2000), the CAMP approximating the time of the Triassic-Jurassic boundary (Blackwell et al., [2013]), which is also used as a datum on the plot. This transition from continental to marine salt is likely linked to the culmination of CAMP magmatism and beginning of ocean spreading, which likely introduced marine waters into the narrow evaporite-dominated rift basin.

The commencement of normal marine salinity deposition in the "post-salt Lower Jurassic" is only clearly observed in wells on the Grand Banks and offshore and onshore Morocco, likely due to wells on the Scotian Margin being on the basin flanks within non-marine or sabkha facies, and Lower Jurassic strata being below well total depths in more basinal locations. The earliest indications of "normal marine" faunas and floras in the region occur in the late Sinemurian in wells such as MZ-1 and the DSDP 547B on the Moroccan margin (this Atlas and Weston et al., 2023) and Heron H-73 (Weston et al., 2023) and Bittern M-62 on the Grand Banks (Barss et al., 1979). The presence of a full suite of marine microfossils (dinoflagellates, nannofossils, and foraminifera) allows confident age determinations and recognition of Pliensbachian and Toarcian strata as well, though often abbreviated by unconformities.

In summary, there is conclusive evidence of the invasion of "normal marine" conditions into the Central Atlantic by late Sinemurian times, allowing the possibility for development of marine source rocks within the Lower Jurssic of the region depending on other oceanographic and basin configuration factors.

Controls for Deposition of Marine Source Rocks

In the absence of direct evidence of source rock presence, it is necessary to consider the conditions that would be favourable for such deposits. main controls on the accumulation of organic rich facies are productivity and preservation. Productivity is dependent on nutrient supply and is typically related to upwelling, with additional potential drive from semi-distal fluvial input. Preservation is primarily related to exposure to oxygen. Organic matter stands the best chance of being preserved in low oxygen water column conditions, i.e. anoxic deposition (Bishop, 2022). Bishop considered 5 boundary conditions for this review:

- Upwelling
- Restriction
- Accommodation space
- Bathymetry
- Negative water balance

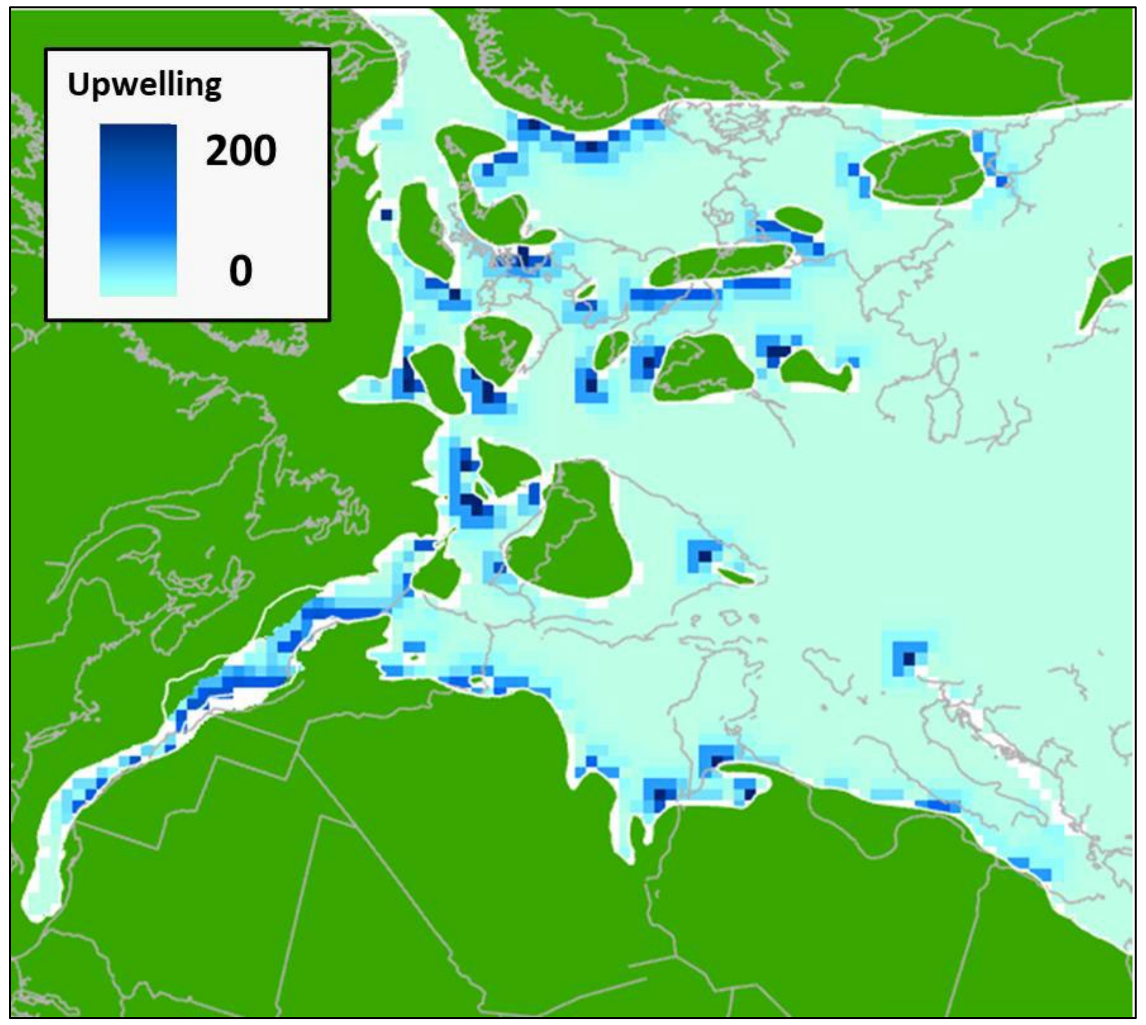

Figure 49: Calculated upwelling intensity for the central Atlantic during the Pliensbachian. Base paleogeography from Getech study (Scougal et al., 2021) (Bishop, 2022).

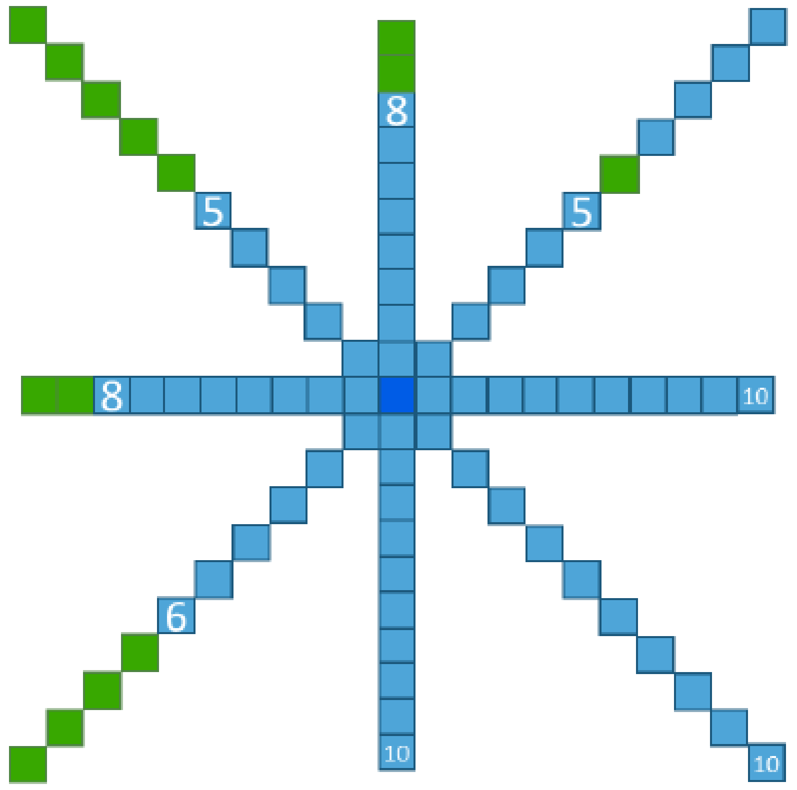

Figure 50: Geometrical approach for restriction calculation. Distance to the nearest land is calculated for the eight cardinal and ordinal directions, which are then summed to provide a measure of restriction. (Bishop, 2022).

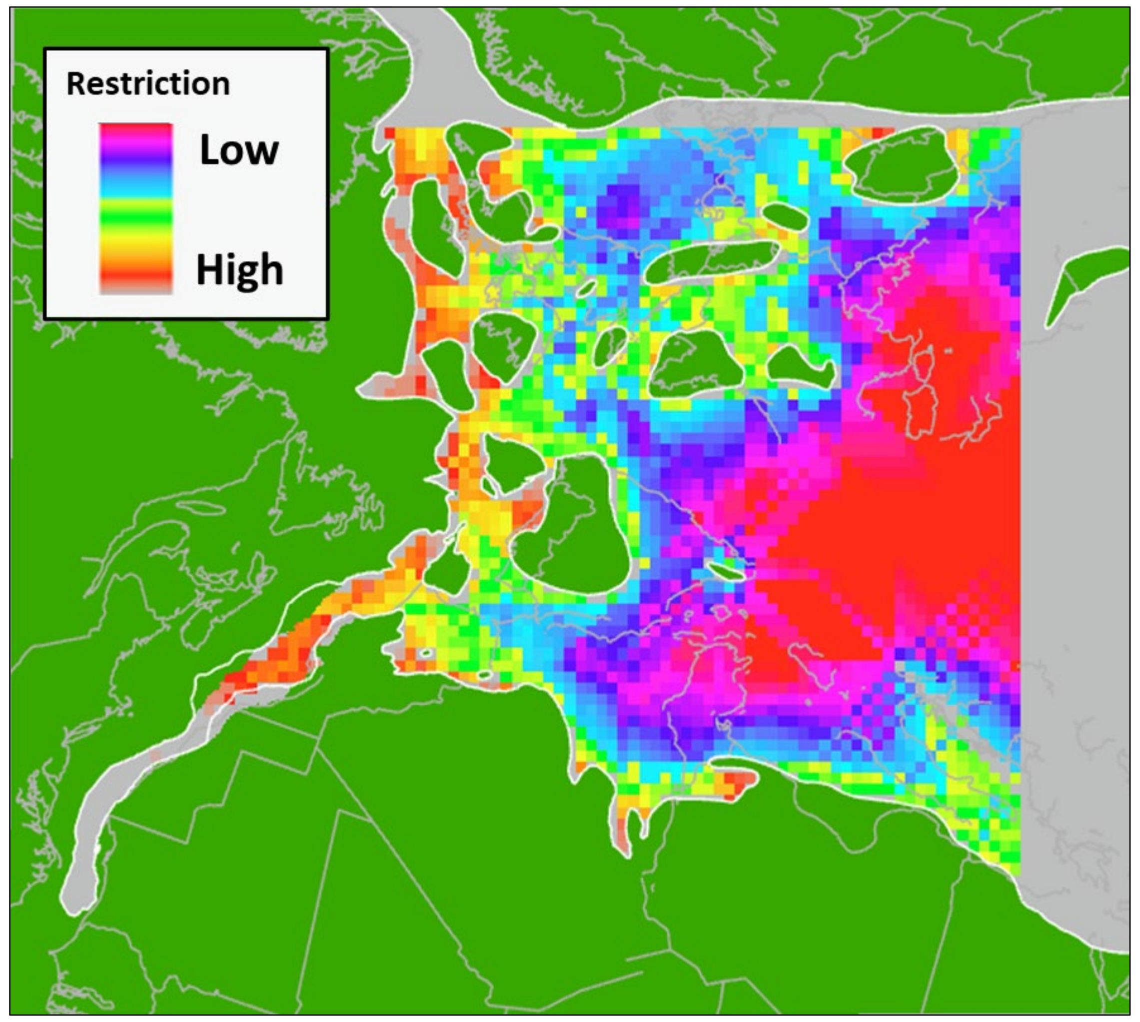

Figure 51: Calculated restriction for the central Atlantic during the Pliensbachian. Base paleogeography from Getech study (Scougal et al., 2021) (Bishop, 2022).

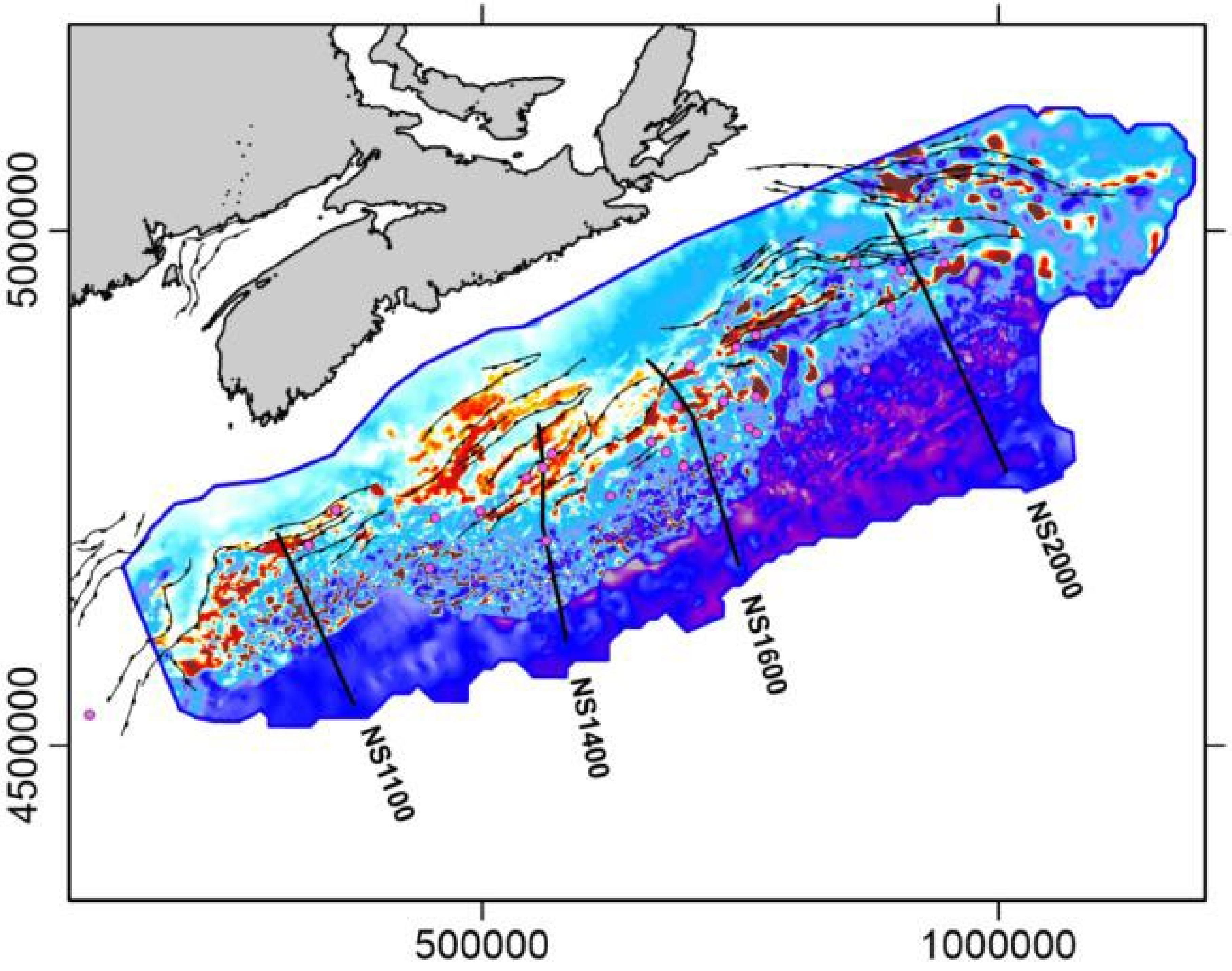

Figure 52: J195 palaeobathymetric reconstruction (Tugend et al. 2023)

LOWER JURASSIC SOURCE ROCK PRESENCE RISK MAPS

Methodology

The final step in this synthesis was to model source rock presence maps for the margin. Modeling was completed by superimposing the hydrocarbon occurrence map with EMAG2 magnetic data to use any lineaments to help subdivide the areas. It took into account the previous modeling and data synthesized throughout this chapter. Each distinct polygon was assigned one of the three source rock types, with a blanket of SR1 (i.e. non-source), covering the whole area. Three confidence risk maps were created: a P10, P50, and P90. Bishop breaks these down as:

P90 - The P90 map represents the 'minimum risk' scenario. As there is no definitive proof for a Lower Jurassic marine source rock therefore SR3 is not assigned to any polygons. It appears likely that the areas of hydrocarbon indications on the slope are due to Lower Jurassic sourcing, thus SR2 is assigned accordingly. The lack of oil shows in preference to gas shows, is the basis for the assignment of SR2.

P50 - This map reflects the 'coin-toss' scenario. SR2 is now more broadly assigned, covering essentially the entirety of the Scotian Basin where hydrocarbons are observed, including part of the shelf. Additionally, SR3 is assigned to the region where the Mic Mac J-77 putative Lower Jurassic carbonate oil signature is reported, inferring the presence of an oil-prone source.

P10 - In this 'least likely but possible' scenario, the most optimistic perspective of Lower Jurassic source is presented. The primary difference is the assumption that a marine source rock is essentially ubiquitous across the slope, with the lack of oil observations to date perhaps being the result of maturity rather than original source rock kerogen type.

With no direct evidence, indirect indications such as the potential Lower Jurassic facies and oil geochemistry were relied upon to address source rock risk. Also, based on maturity grounds, some of the hydrocarbon observations are difficult to explain if only relying on an Upper Jurassic source, and thus are most likely due to a Lower Jurassic. The confidence rating was highest at the location of the Mic Mac J-77 well with its carbonate oil. Risking is based on the premise of one Lower Jurassic source rock horizon occurring (however probably distributed through several Lower Jurassic stages). This study concluded that this would most likely be Sinemurian or Pliensbachian (Bishop, 2022).

Three potential source rock end-members considered were:

SR1 - Type IV (non source), mean TOC of 1.5% and HI of 150, ~100m thick

SR2 – Type III/II, TOC of 3.0% and HI of 300, ~50m thick

SR3 - Type II marine, mean TOC of 4.0% and HI of 500, ~ 30m thick

Key Uncertainties

Bishop identified five key uncertainties in the modeling and potential presence of a Lower Jurassic Source in offshore Nova Scotia. These were:

1. Paleobathymetry
2. Local Early Jurassic Paleoclimate
3. Timing of Salt Tectonics
4. Break-up Unconformity
5. Hot Spot Duration

KEY CONCLUSIONS

Despite absence of direct evidence of both Lower Jurassic marine facies and source rock, Bishop concluded that there is a ***considerable amount of circumstantial evidence*** which suggests that such a source rock may exist. Some hydrocarbon occurrences on the shelf and slope, such as that of the Mic Mac J-77 oil, are difficult to account for unless a Lower Jurassic source rock is inferred. Optimum source rock conditions would naturally be expected in distal basin locations, for which data is currently unavailable (Bishop, 2022).

There is a considerable amount of circumstantial evidence which suggests that such a source rock may exist.

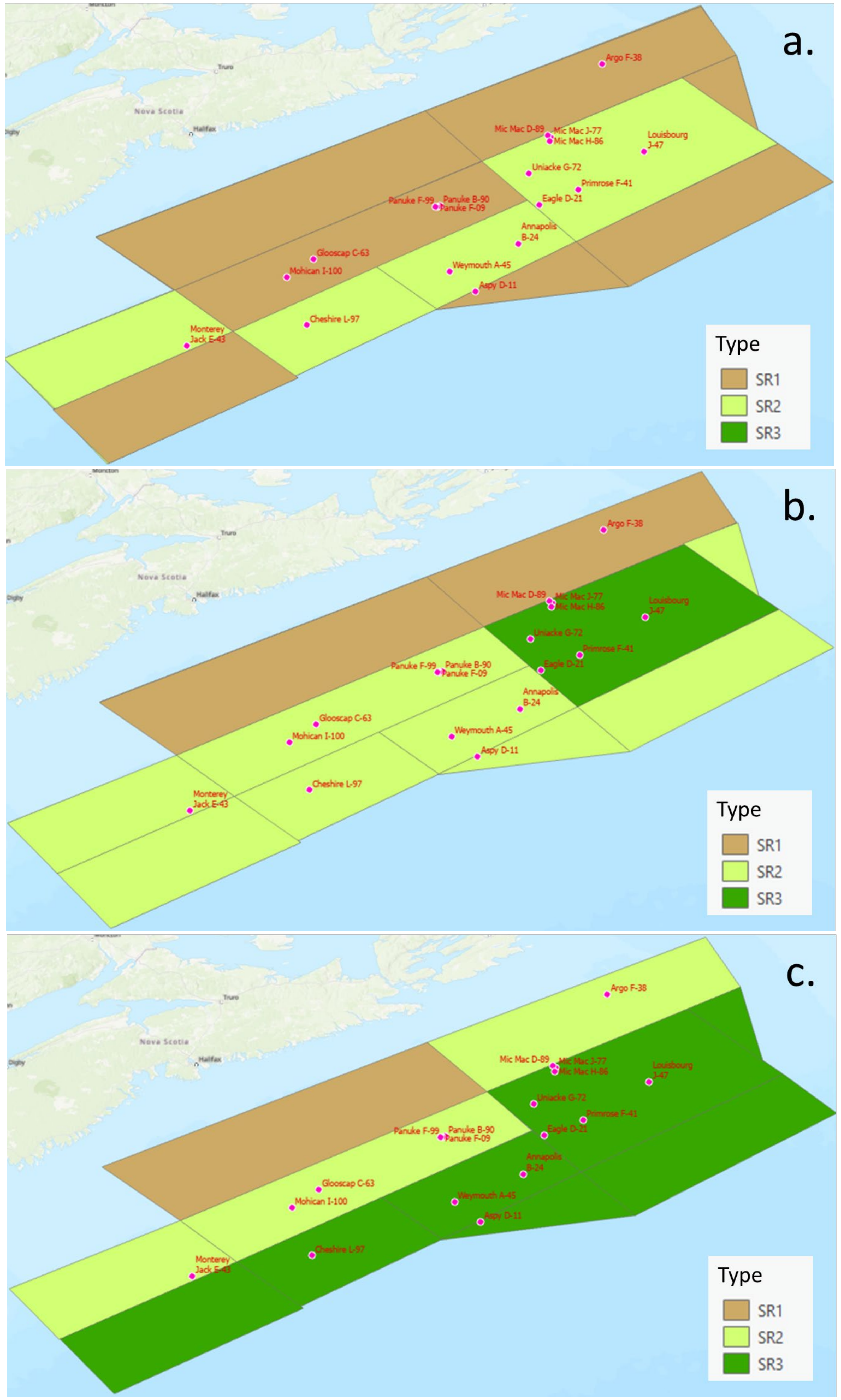

Figure 53: Bishop's modeled source risk presence maps a) P90 scenario, b) P50 scenario, and c) P10 scenario (Bishop, 2022).

CONCLUSIONS

Since 2011, the research and subsequent synthesis studying source rock in offshore Nova Scotia has both decreased the exploration risk and created a simpler, but much stronger, understanding. The original, as well as subsequent, PFAs tested a variety of source rocks (Figure 54)). This current update has produced a more confident set of conclusions about the two most likely source rocks, namely Tithonian and Pliensbachian (Lower Jurassic). These have a high confidence and moderate confidence level, respectively.

2011 PFA

Source rock	Type	TOC (%)	HI	Thickness
Aptian	III	2 %	235	0-100 m
Valanginian	III	1 %	235	0-200 m
Tithonian	II-III	3 %	424	0-50 m
Callovian	II-III	2 %	424	0-20 m
Pliensbachian (L. M. Jurassic)	II	5 %	600	0-20 m

2023 Integration Project

Source rock	Type	TOC (%)	HI	Thickness
Tithonian	II-III	3-5	424	20 m
Lias (~ Pliensbachian)	III/II	3.0	300	30 m
Lias (~ Pliensbachian)	II	4.0	500	10 m
Lias (~ Pliensbachian)	II	4.0	500	30 m

Figure 54: Comparison of source rocks and corresponding parameters from the 2011 PFA to the current integration project. The three variations of the Lias represent the different end members tested.

Returning to the four pillars on investigation, each of the questions asked have been answered in the subsequent pages (examples in Figure 52). These answer's aided in concluding the source parameters in Figure 51 and in the creation of new Common Risk Segment (CRS) maps of both intervals. The two key parameters used in the source rock risking in this project are presence and effectiveness. Studies such as the Moroccan Reconstruction and Getech's modeling both directly support the presence of a Pliensbachian source rock, while the geochemistry, piston coring and seismic analysis all support its potential effectiveness.

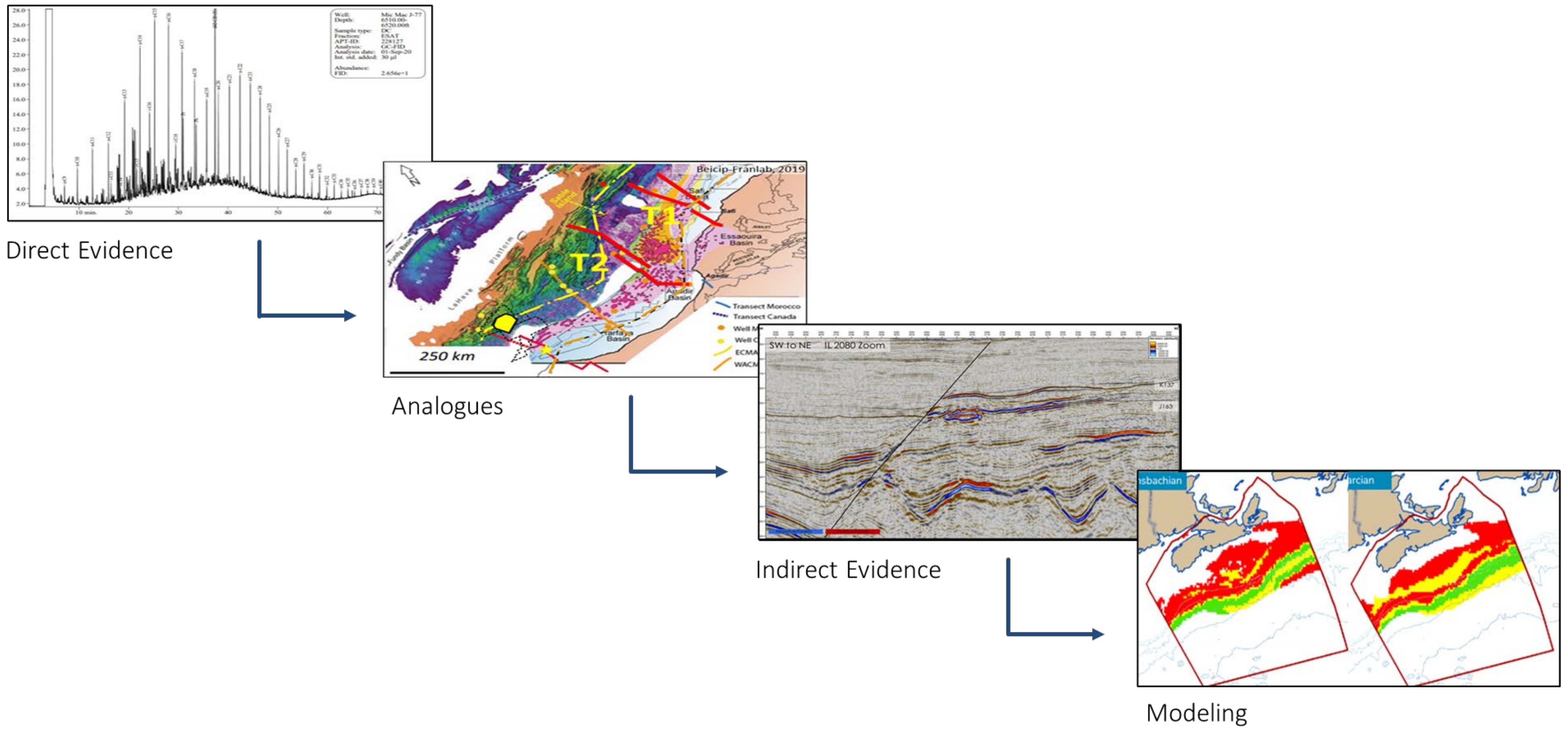

Figure 55: Examples of each of the four pillars of source rock research.

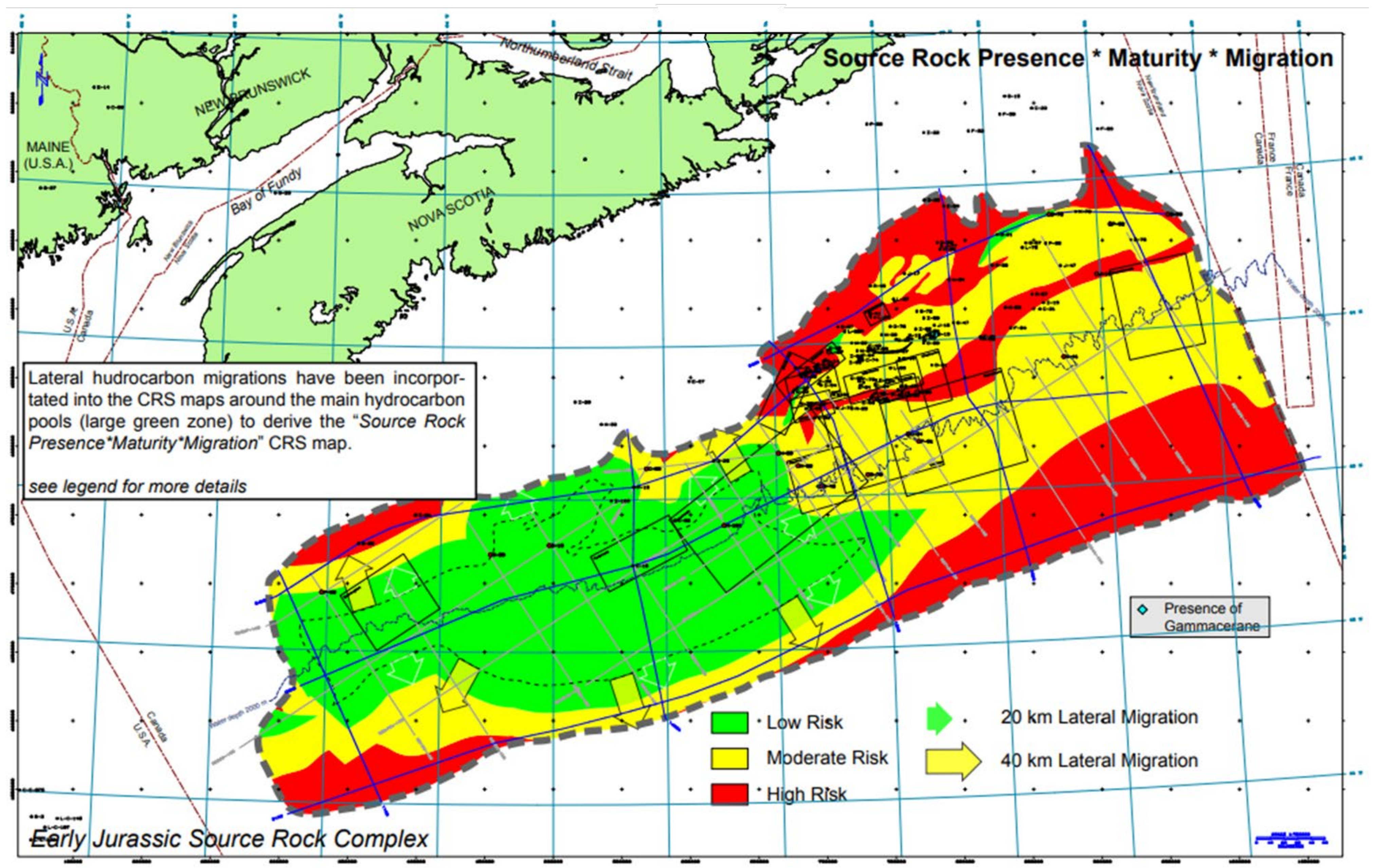

Lateral hudrocarbon migrations have been incorporated into the CRS maps around the main hydrocarbon pools (large green zone) to derive the "*Source Rock Presence*Maturity*Migration*" CRS map.

see legend for more details

Figure 56: Originally modeled Early Jurassic Source Complex CRS Map (Beicip et al. 2011).

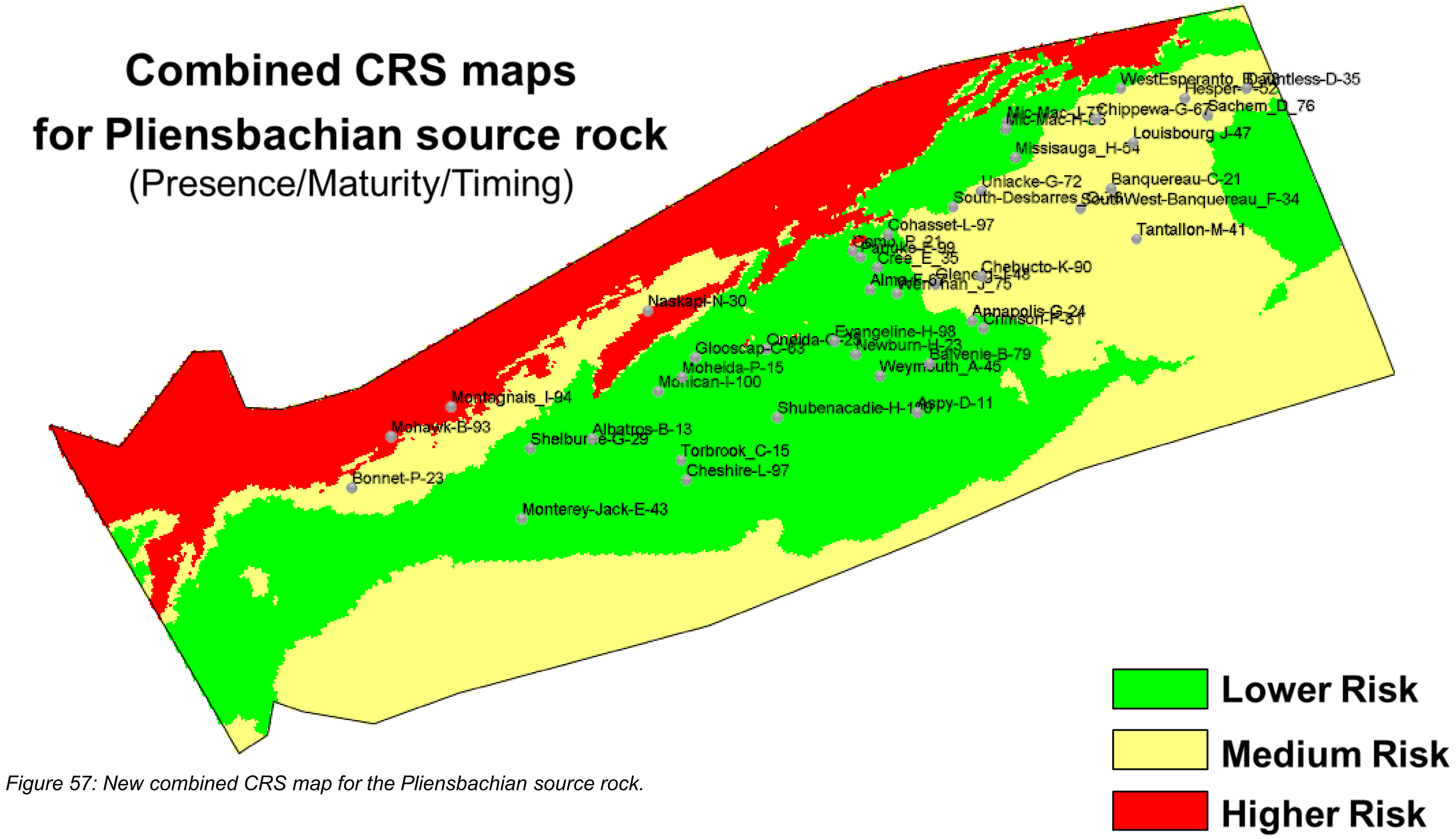

Figure 57: New combined CRS map for the Pliensbachian source rock.

CHAPTER 2.4

ADVANCED GEOPHYSICS: ROCK PHYSICS AND BARRINGTON 3D AVO STUDY

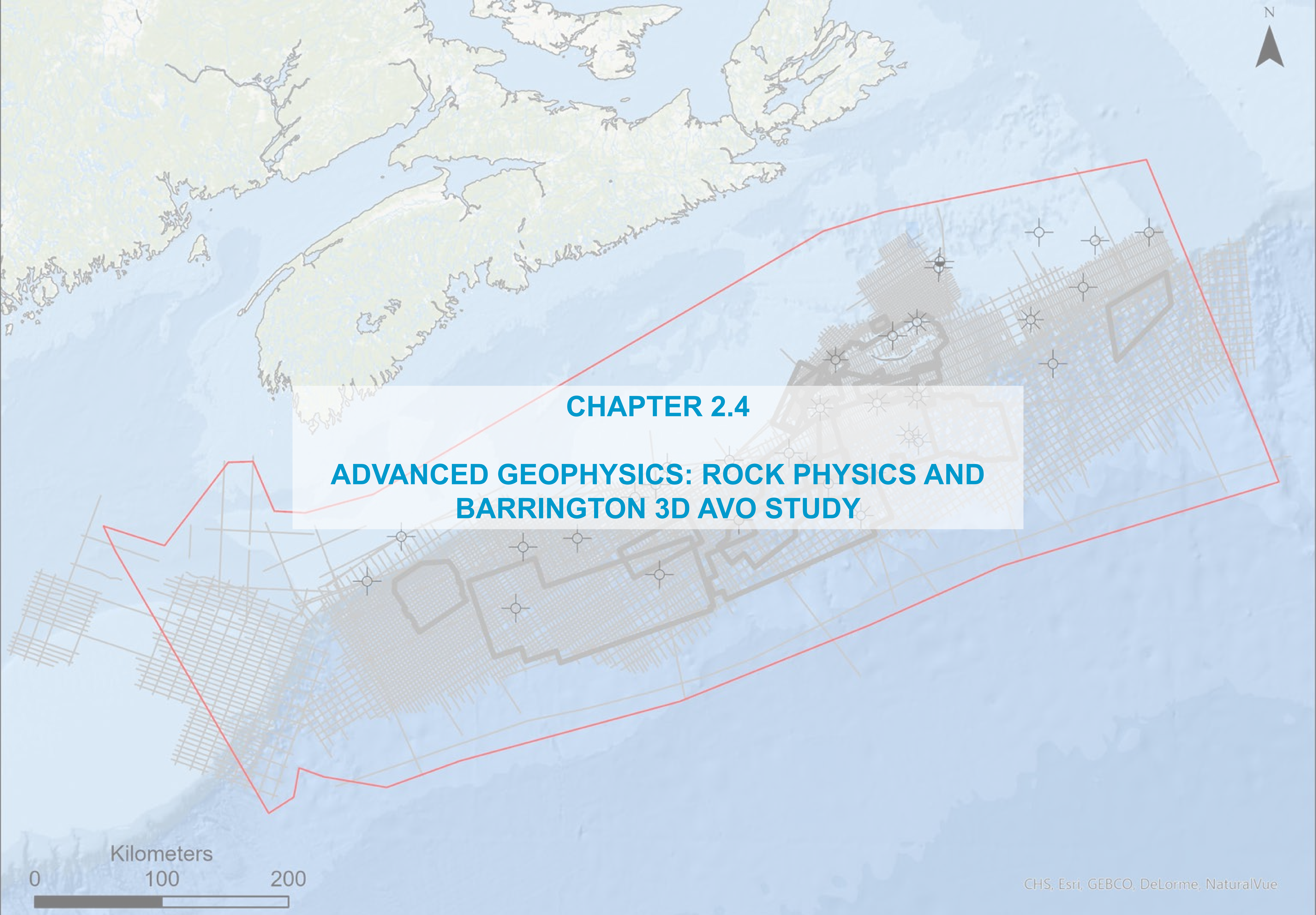

CHS, Esri, GEBCO, DeLorme, NaturalVue

Advanced Geophysics

ADVANCED GEOPHYSICS

There have been two advanced geophysical projects completed since 2011 on the limited pre-stacked seismic available to the NSDRR. Though limited, these projects have had significant risk reduction potential from the advances seismic work.

NOVA SCOTIA ROCK PROPERTIES MODELLING

In 2013, in support of the Nova Scotia Call for Bids NS13-1, the Nova Scotia Department of Natural Resources completed a Rock Physics project with ERC Equipoise on 14 wells on the Scotian Shelf. This was the initial attempt at understanding rock properties in the basin, focusing specifically on forward modeling as no 3D AVO data were available.

The Database

Fourteen wells were chosen to represent a 400 x 150 km area of the Nova Scotian shelf .

- Most basic logs were available
- Shear wave logs available for three wells: G-24, H-23, H-59.
- A contiguous set of tops were created using composite plots, online Nova Scotia tops database, and interpolation (three tops).

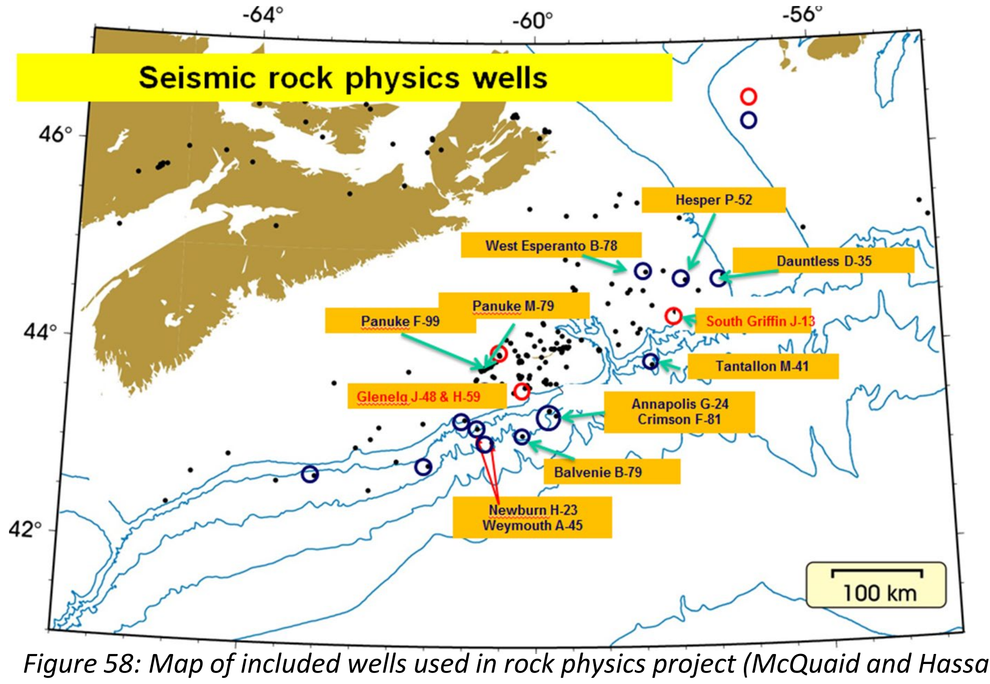

Figure 58: Map of included wells used in rock physics project (McQuaid and Hassan, 2013).

Approach

The approach to this project consisted of four main steps:

1. Identify the key regional parameters. Sensitivity was tested against overpressure, cementation, and facies variation.
2. Develop a background rock physics model with parameters easily definable at any location.
3. Develop a sand rock physics model again with easily definable parameters.
4. Use Aki and Richards and Gassmann equations to develop specific half-space AVO models

There was very limited data available for the sandy intervals in these wells. Additionally, with the diverse water depth (shelf versus deep water) data and subsequent facies variations, analysis of the sand was quite difficult. However, Vp, Vs and AI trends in deep water were still able to be predicted for both non-reservoir (shales) and sands. This concluded that the Poisson's ratio was function of effective stress for sands with porosity as function of depth below mud line (McQuaid and Hassan, 2013)

Forward Modelling and General Conclusions

Forward modelling was completed using a single interface (top reservoir) and, using the derived rock physics model, analyzed the following synthetic examples:

- Water filled
- Oil filled (25 API – GOR ~300 scf/bbl)
- Cemented sands
- Uncemented sands
- Water depth (300m or 1500m

This modeling highlighted AVO anomalies for both the water and oil filled sands. The AVO exhibited a progressive change from Type IV, through III and II, to Type 1 with increasing depth. A similar effect was observed with increasing cementation which is likely a function of temperature (not tested in this study). AVO response was concluded to be depth dependent. The reflectivity across all angles generally moves up (becomes more positive) for a given depth below mudline when we:

I. Go from oil to water

II. Go to deeper water because the background shale trend for AI becomes lower.

III. Go from uncemented to cemented sands.

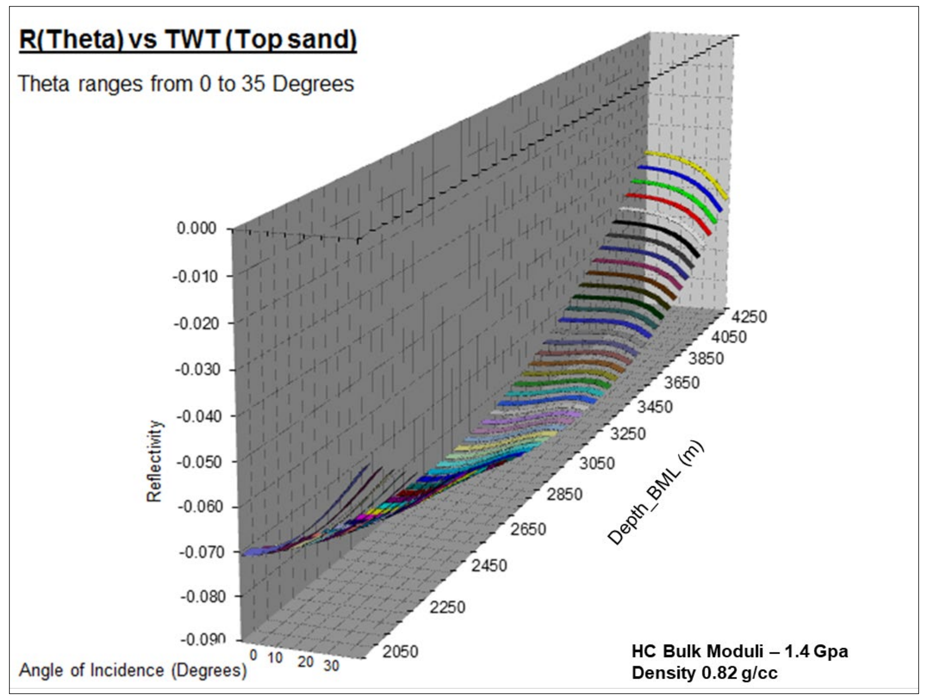

Figure 56 Forward model result at 1500m water depth for Water Filled Uncemented Sands (McQuaid and Hassan, 2013).

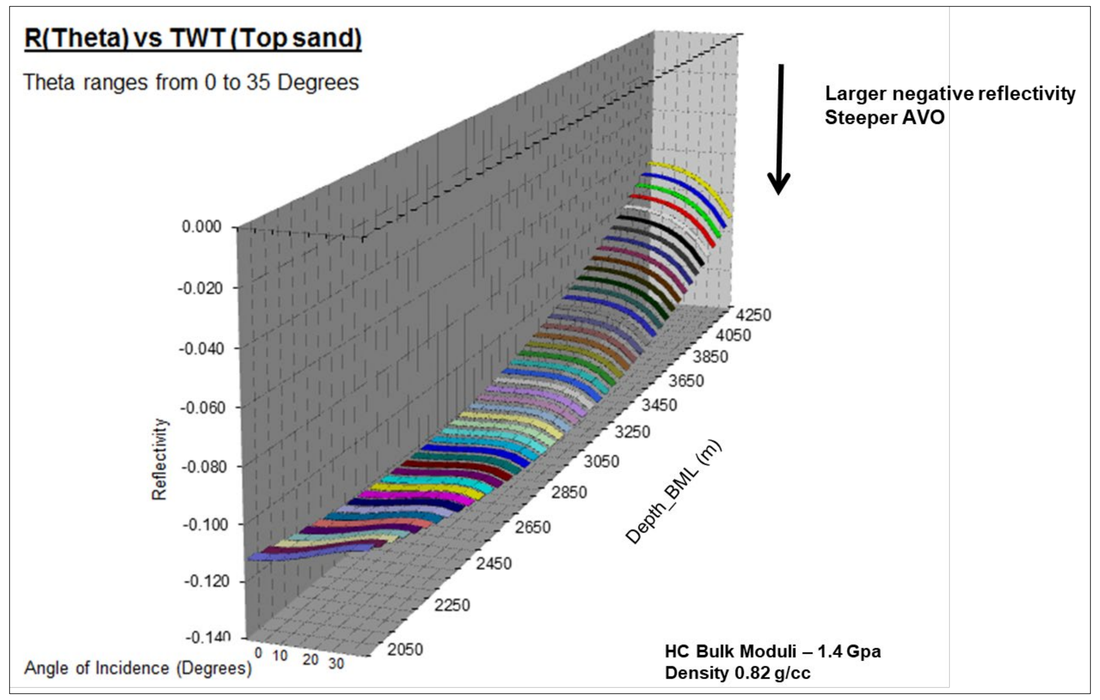

Figure 57 Forward model result at 1500m water depth for 80% Oil Filled Uncemented Sands (McQuaid and Hassan, 2013).

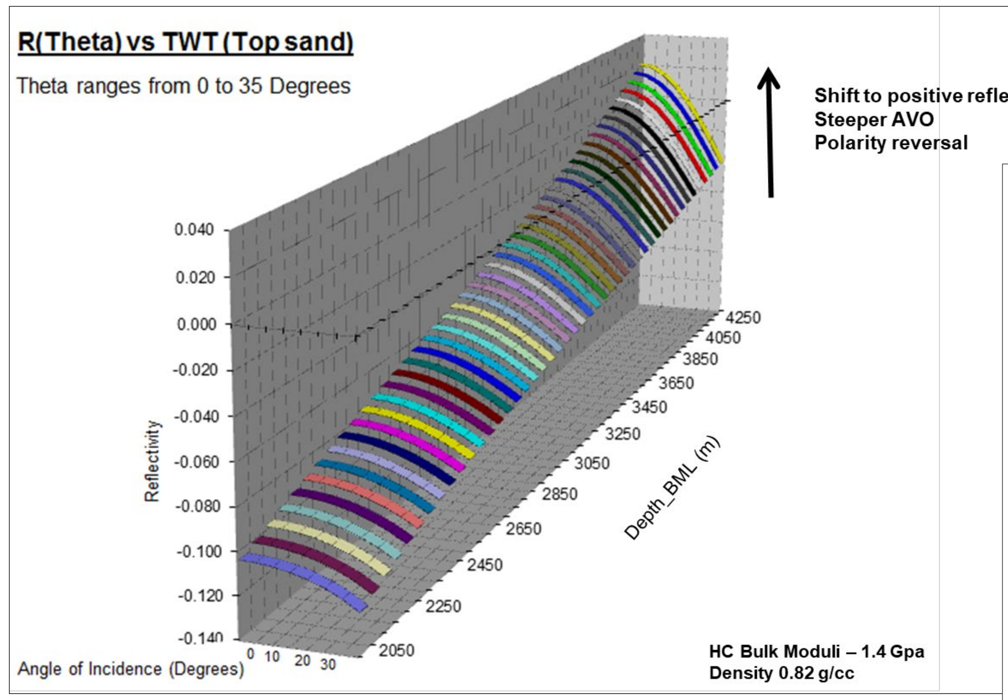

Figure 58 Forward model result at 1500m water depth for 80% Oil Filled Cemented Sands (McQuaid and Hassan, 2013).

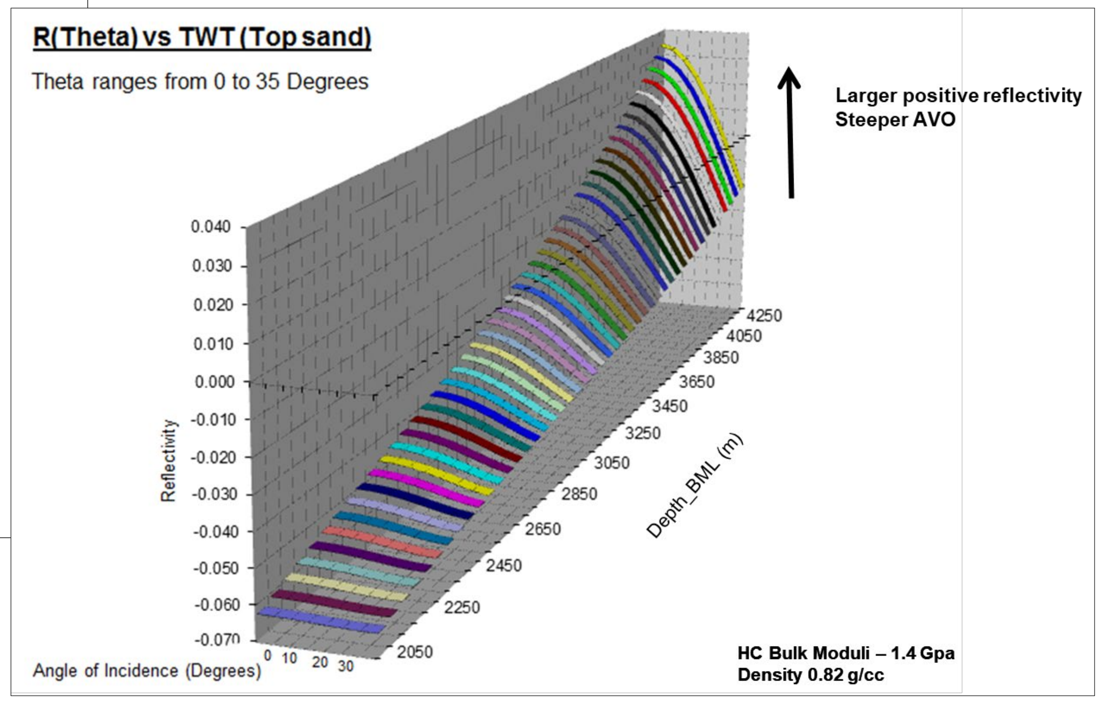

Figure 59: Forward model result at 1500m water depth for 80% Water Filled Cemented Sands (McQuaid and Hassan, 2013).

Annapolis G-24 Synthetic Seismogram Modelling

The single gas example was modelled in the M sand reservoir in Annapolis G-24. This indicated that analysis should show a Type 3 anomaly and that the presence of gas, under these conditions, should exhibit a direct hydrocarbon indicator (DHI). This modelling applied the rock properties model derived by this study, however an attempt to verify using 2D data failed. Future work is needed to check with 3D pre-stack migrated data (not available for this study (McQuaid and Hassan, 2013).

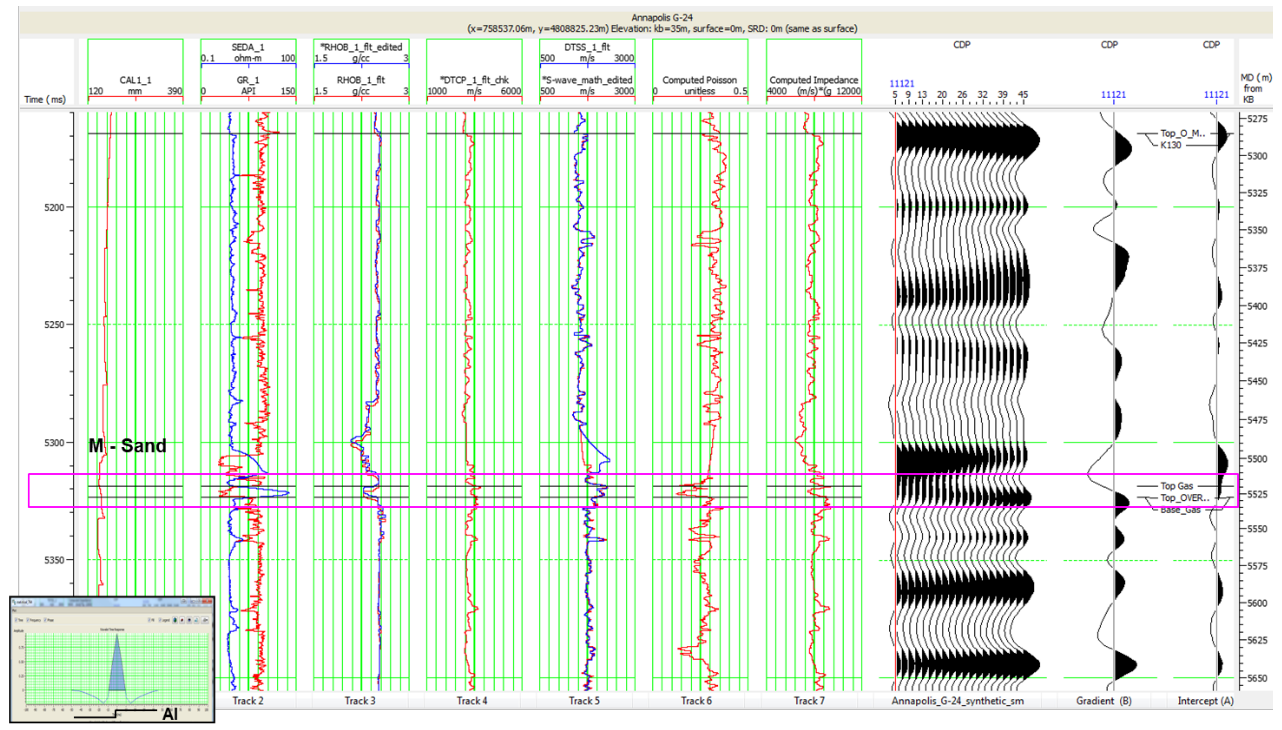

Figure 60: Angle Synthetic for Annapolis G-24 highlighting the M sand and top of gas (McQuaid and Hassan, 2013)

BARRINGTON 3D REPROCESSING & INVERSION

Beginning in 2020, the Department of Natural Resources and Renewables began a project with WesternGeco (Schlumberger) to reprocess the legacy Barrington narrow-azimuth, 3D survey. The Barrington 3D survey was originally acquired by WesternGeco for PanCanadian (now Ovintiv) in 2001. It covers approximately 1,800 km^2 of the shelf to slope transition, in water depths ranging from 530 – 2,200 m (Figure 61). New reprocessing and analysis described here included modern techniques such as adaptive deghosting, full tilted transverse isotropy Kirchhoff pre-stack depth migration and litho-elastic inversion (as described in the source rock chapter). This represented the first dataset available to the province that allowed for this rigorous, in-depth analysis.

Reprocessing

The reprocessing workflow, based on Western's extensive Atlantic Canadian experience, was tailored to include modern processing techniques such as adaptive deghosting, true-azimuth multiple elimination and matching pursuit Fourier interpolation. These time processing tools, combined with high resolution tilted transverse isotopy (TTI) modeling and migration to depth, resulted in a major data improvement in with improvement in the imaging of shallow faults, increased bandwidth, and higher resolution deeper events (eg. Morrison et al. 2021). The smooth 3D velocity field use is this modeling was obtained by combining a legacy, single-function velocity profile with regionally interpreted 2011 PFA horizons. The salt was modeled through a series of flood and body migrations, encapsulating both allochthonous and autochthonous salt features, to an observed clean velocity of 4500 m/s. (Raj et al., 2021). All data was processed to full AVO compliance.

The processing workflow can be found in Tables 2 and 3 below. Maximizing signal to noise ratio, achieving increased bandwidth through deghosting techniques, attenuation of multiples, and accurate velocity model building were critical to the success of the reprocessing. These objectives were all attained while preserving amplitude balance across all offsets for the subsequent AVO analysis. Due to the high complexity of the geology, much of the pre-migration work focused on this preservation of signal while implementing noise removal (Raj et al., 2021).

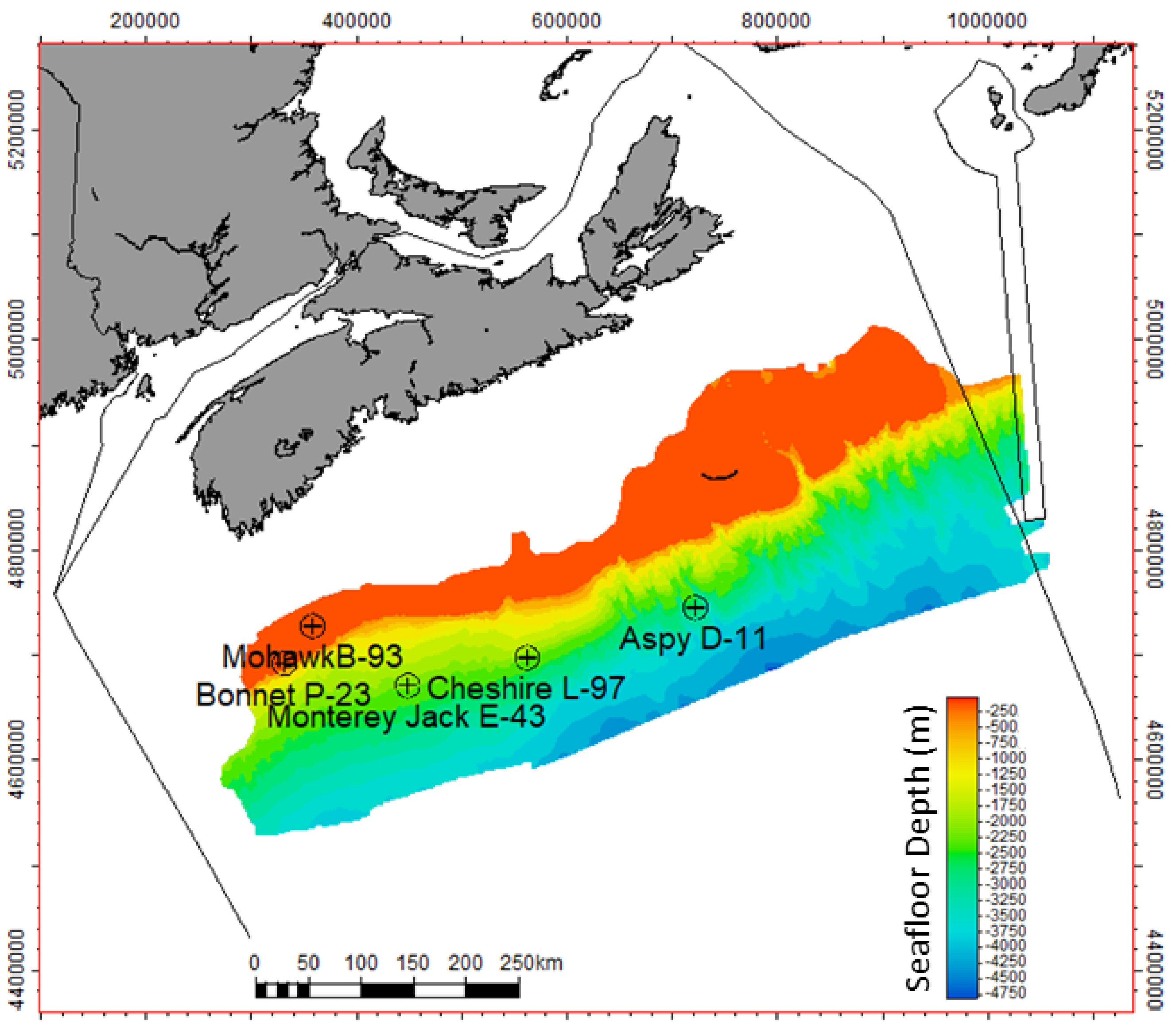

Figure 61: Location of the Barrington 3D survey, wells used in the study, and extent of the legacy basin model.

Table 2.1: Time Processing Sequence

Time Processing
SEGY Reformat
Navigation Merge
Despike
Lo-Cut Filter
Singular Value Decomposition (SVD)
Anomalous Amplitude Attenuation (AAA)
Cable Jerk Attenuation
Adaptive Noise Attenuation (ADNA)
Source and Receiver Amplitude Correction
Receiver Motion Correction
Resample to 4ms
Adaptive Deghosting
Residual Debubble
Residual Noise Attenuation
3D Surface Related Multiple Prediction (SRME)
Least Squares Adaptive Subtraction
Water Bottom Radon Demultiple
Post-Radon Isolating Multiple Algorithm (PRIMAL)
Matching Pursuit Fourier Interpolation (MPFI)
Time Variant Filter (TVF)
Inverse Q Phase Compensation
Coordinate Transformation

Table 2.2: Depth Processing Sequence

Depth Imaging
Initial Model Build
Tomography Iteration 1
Tomography Iteration 2
Tomography Iteration 3
Tomography Iteration 4
Tomography Iteration 5
Salt Interpretation
Final Kirchhoff Prestack Depth Migration (KPSDM)
Common Image Point (CIP) Residual Moveout (RMO) Fit
Weighted Least Squares Radon Residual Demultiple
Curvelet Domain Noise Attenuation
Full Offset Residual Trim (FORT)
Inverse Q Amplitude Compensation
3D Structural Smoothing
Angle Mute
Stack
Bandwidth Extension (BWXT)
Acquisition Footprint (AFA)
Residual Amplitude Analysis / Compensation (RAAC)

The depth imaging utilized a general reflection tomography method which used residual moveout analysis of the prestack depth migrated common image point gathers to update a velocity model. This method was chosen due to the complex geology of the area as it is globally optimized instead of using localized updates, thus allowing for dip. This method also makes no assumptions about the smoothness of the velocity model with respect to cable length (Raj et al., 2021).

A total of five iterations of tomography were completed. A global solution of optimum velocities was sought that aligned events over all offsets while minimizing residual move out. The initial model build was quite challenging due to the lack of wells within the survey area and the legacy 3D time migration velocity model being unavailable. A smooth 3D velocity field was obtained by combining a legacy, single-function velocity profile with regionally interpreted 2011 PFA horizons (Raj et al., 2021). The salt interpretation throughout the area was generated through a series of flood and body migrations that encapsulated both allochthonous and autochthonous salt features, with an observed clean velocity of 4500 m/s (Raj et al., 2021). Initial salt interpretations were provided, for reference to the Western team, by Mark Deptuck at the CNSOPB.

Depth processing results achieved a major data improvement in comparison with the legacy data. There is clear improvement in the imaging of shallow faults, increased bandwidth, and higher resolution deeper events. Figure 62 shows the uplift in XL4000 (A & B) and a zoomed in, deeper portion of XL 4800, exhibiting immense uplift in detail through the Jurassic and pre-salt section (C & D). The reprocessing team noted the structural imaging improvements and high-resolution stratigraphy were achieved due to the robust Tilted Transverse Isotropy (TTI) model and through the signal processing workflow (Raj et al. 2021).

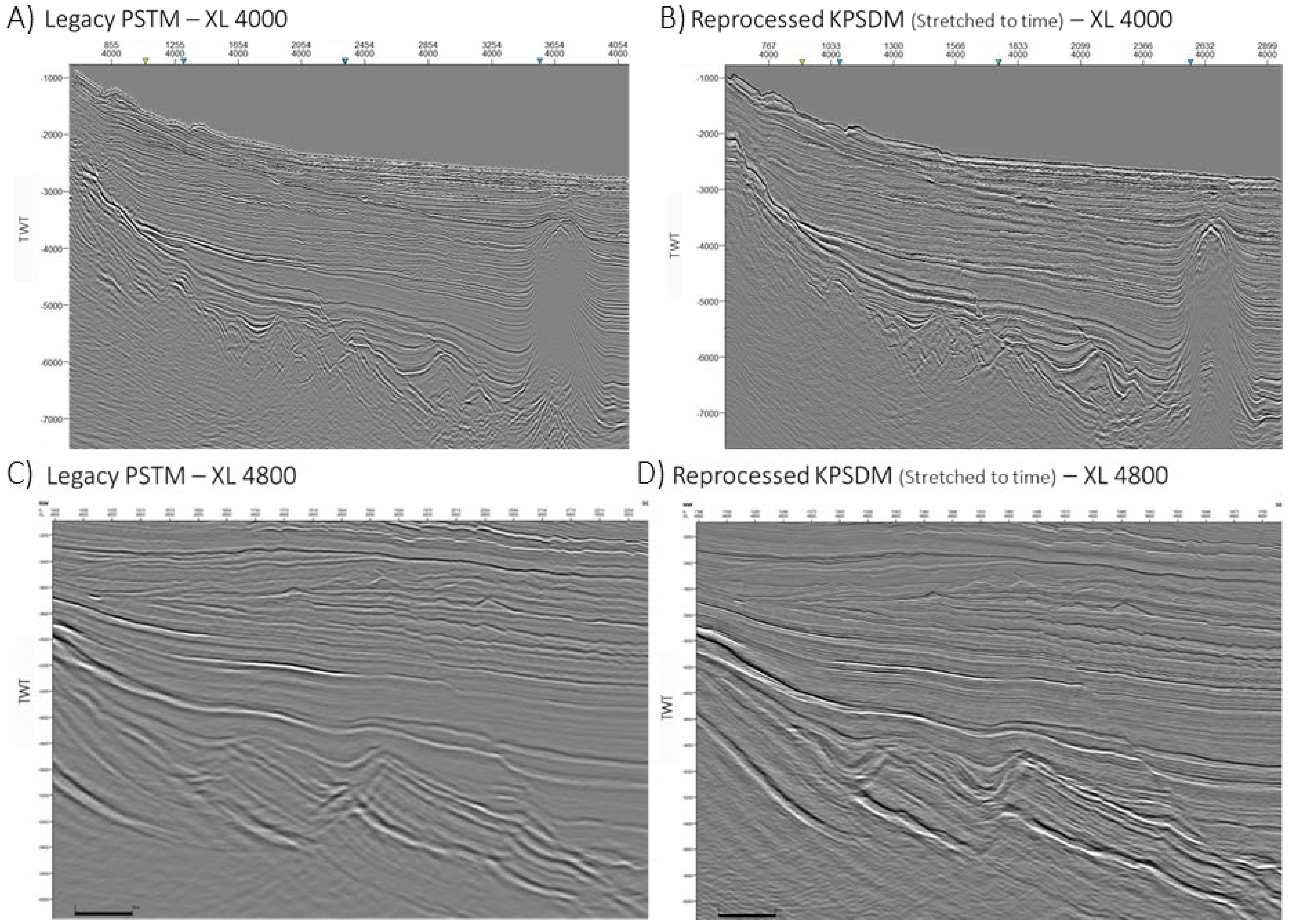

Figure 62: A) XL 4000 of the Legacy KPSTM, B) XL 4000 of the reprocessed KPSDM stretched to time, C) Cretaceous and Jurassic zoom of XL 4800 of the Legacy KPSTM, D) Cretaceous and Jurassic zoom of XL 4800 of the reprocessed KPSDM stretched to time..

Rock Physics and AVA Modeling

Seismic reservoir characterization (SRC) in the form of rock physics modeling and litho-elastic inversion was carried out on the Barrington 3D reprocessed PSDM seismic data with the goal of investigating the possibility of directly imaging reservoir and charge to identify potential hydrocarbon exploration leads and prospects. The workflow used the Litho-Petro-Elastic (LPE) technology developed by Schlumberger, which incorporated rock physics and lithology modeling using seismic amplitude versus angle variations (AVA). LPE inversion provided a single-loop approach to reservoir characterization based on rock model and compaction trends(Dasgupta et al. 2021). In the case of the Barrington 3D survey, the LPE technology integrated the effective stress and temperature predictions from the basin modeling completed by Beicip-Franlab in 2011 for the Play Fairway Analysis (Beicip-Franlab, 2011), a factor not taken into account in the first rock physics study. This was a very important innovation in that it allowed the estimation of the potentially significant impact on rock properties due to regional variations in stress and temperature. Figure 61 on the previous page displays the wells used in the study, as well as the extent of the legacy basin model.

The rock physics modeling was completed using a 3-step workflow that included exploratory data analysis, deterministic and stochastic rock physics modeling. There are no wells drilled within the boundaries of the survey, therefore, the rock physics modeling used data from nearby offset wells (Cheshire L-97, Monterey Jack E-43, Bonnet P-23, Mohawk B-93, and Aspy D-11). Of the five wells chosen, three have measured shear slowness.

This modeling uniquely integrated the effective stress and temperature from the legacy 3D petroleum systems model, completed by Beicip-Franlab in 2011. Three main lithology classes were observed, carbonates (including limestone, dolomite, and marl), shales and sands. Further data exploration analysis showed the correlation between the compressional sonic and the density trends and both the basin model's effective stress and temperature at the well locations.

The stochastic rock physics modeling clearly exhibited a strong dependence of shale trends on effective stress and temperature. This dependency has a strong impact on acoustic impedance and Vp/Vs for the key rock classes analyzed in this study (sand, shale, and carbonate). The rock physics models formed the a priori information that was used as an input to the litho-elastic inversion (Dasgupta et al. 2021). Fluid sensitivities (brine, gas, and oil) for the sands were also analyzed in the study with fluid properties estimated using Batzle and Wang equations and parameters shown in Table 2.3.

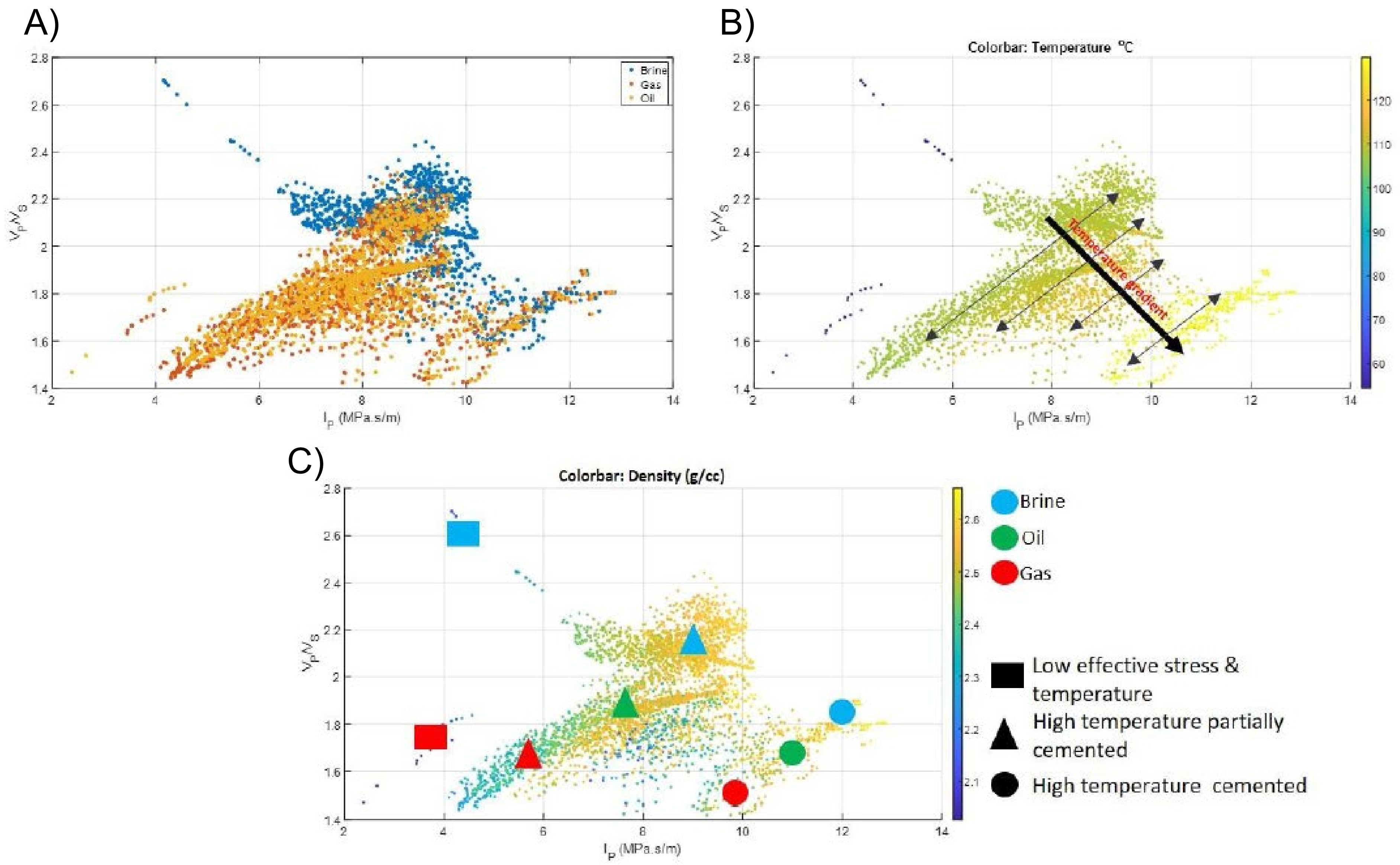

Figure 63 VP/VS ratio as a function of P-impedance of brine sands, modeled oil sands, and modeled gas sands color-coded by (a) sand type, (b) temperature, and (c) density.

Table 2.3: Parameters Used for Fluid Substitution, estimated using Batzle and Wang 1992.

Water Salinity		Oil Property		Gas Gravity		[redacted]	
10000 ppm		25 API		0.5			
		300 scf/bbl					
Pressure (Mpa)	Temperature (DegC)	Water		Oil		Gas	
		Bulk Modulus (GPa)	Bulk Density (g/cc)	Bulk Modulus (GPa)	Bulk Density (g/cc)	Bulk Modulus (GPa)	Bulk Density (g/cc)
1	19.34	2.2368	1.0044	0.4636	0.6588	0.0014	0.0072
2.5	47.63	2.4075	0.9968	0.3480	0.6457	0.0036	0.0165
4.5	85	2.4098	0.9793	0.2293	0.6294	0.0072	0.0267
6.5	122.5	2.2430	0.9540	0.1426	0.6141	0.0112	0.0348
8	150	2.0584	0.9310	0.0963	0.6036	0.0144	0.0400

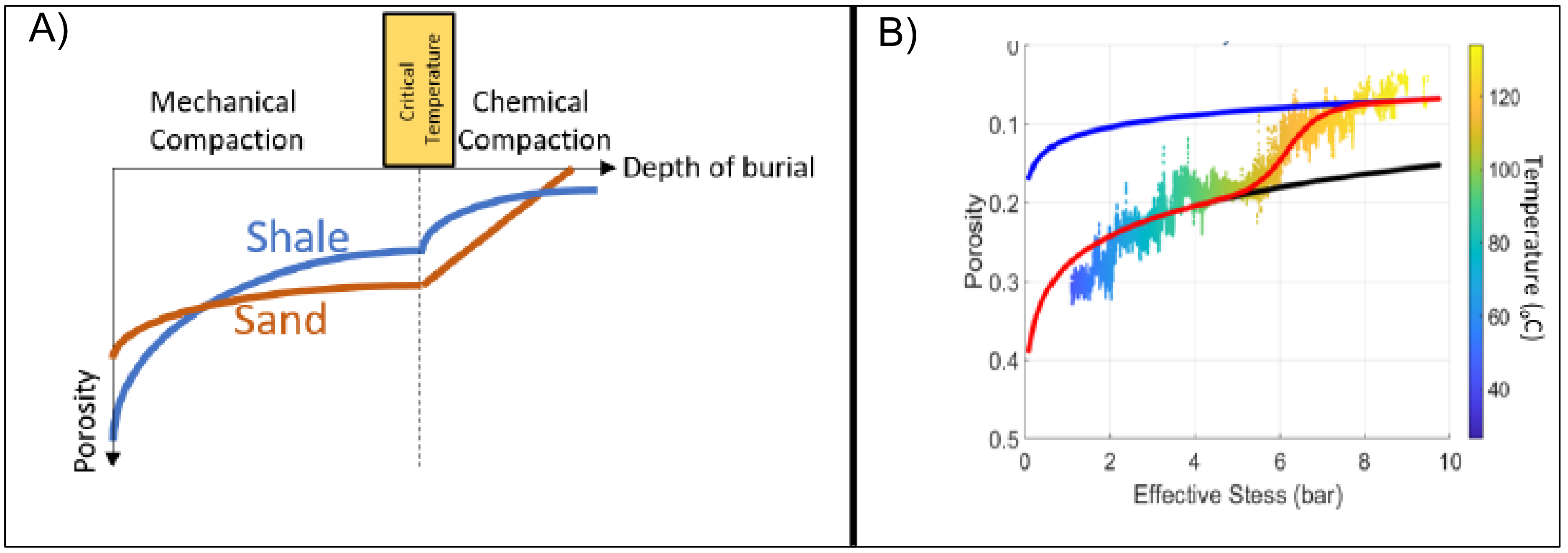

Figure 64 (a) schematic compaction trend of clean shale and clean sand and (b) shale measured porosity and fitted trends assuming temperature below 90oC (black line), assuming temperature above 130oC (blue line), and a fitted curve including a transition zone (red line).

Litho-Elastic Inversion

The Litho-Elastic inversion workflow was completed in 3 main steps:

- Seismic input preparation
- Model prior preparation
- Inversion.

The rock physics modeling was used to create a series of multidimensional probability density functions (PDFs) or "litho-brains" (e,g, Bachrach and Gopher, 2019). These PDFs (Figure 66) relate the observed elastic property values to a specific lithology at a given stress/temperature (Dasgupta et al, 2021). The LE inversion was carried out on nine PSDM partial angle stacks (for the 0-7, 5-12, 10-17, 15-22, 20-27, 25-32, 30-37, 35-42, and 40-47 degree angle bands). A schematic diagram of this process can be seen in Figure 65. During the inversion itself, the 3D basin model was also used to ensure that the elastic background model stayed geologically consistent (Gofer et al., *in prep*).

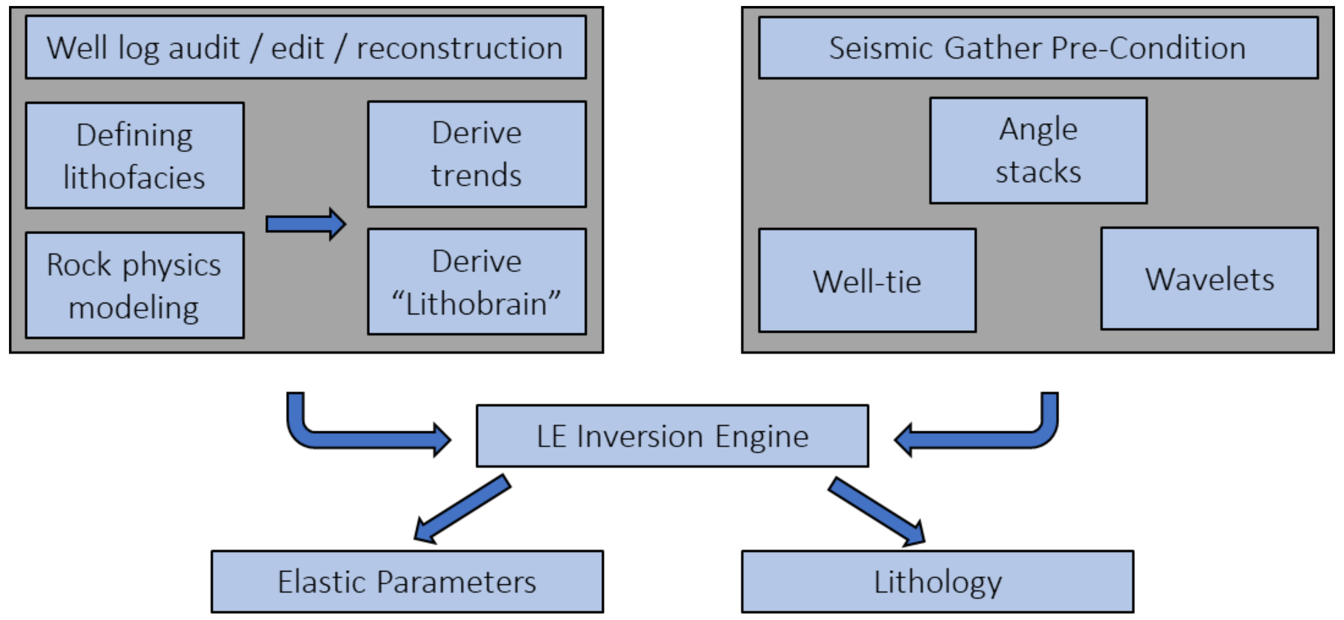
Well log audit / edit / reconstruction
Defining lithofacies
Derive trends
Rock physics modeling
Derive "Lithobrain"
Seismic Gather Pre-Condition
Angle stacks
Well-tie
Wavelets
LE Inversion Engine
Elastic Parameters
Lithology

Figure 65: Diagram of the LE Inversion workflow. Modified from Dasgupta et al. 2021.

Three iterations of the inversion were run using the shale trend for the initial model with the lithoclass and elastic background model being updated with each iteration. Results exhibited hydrocarbons in zones with low P-impedance and anomalous Vp/Vs ratio. Examples of the inversion results can be seen in Figure 3.4 and 3.5.

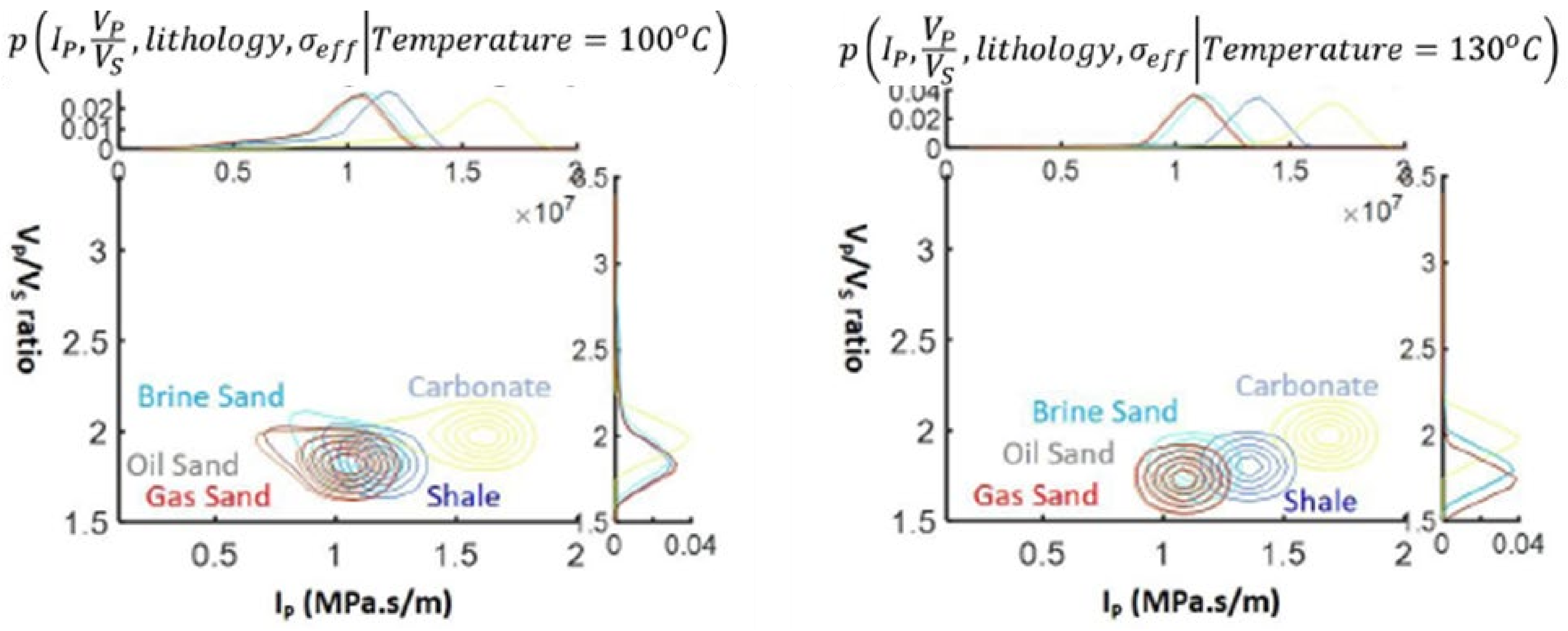
$$p\left(I_P, \frac{V_P}{V_S}, lithology, \sigma_{eff} \middle| Temperature = 100^oC\right)$$
$$p\left(I_P, \frac{V_P}{V_S}, lithology, \sigma_{eff} \middle| Temperature = 130^oC\right)$$

Figure 66: "LithoBrain" contour plot and projected marginal PDF at 100°C and 130°C temperature.

The initial lithoclass estimations and probabilities are equiprobable. This means no specific lithologies are preferred over another a priori. Probabilities in the range 0.4 to 0.6 result in ambiguities, with the possibility of more than one lithoclass being present in a given area. Probabilities over 0.8 indicate the highest confidence of a specific lithology (Gofer et al., *in prep*). Outputs of this inversion included elastic properties (P-Impedance, Vp/Vs Ratio, and Density – both relative and absolute) and lithoclass probabilities (estimated lithoclass and shale, carbonate, brine, gas and oil sands). The inversion concluded that the dominant lithologies were shale and brine sands.

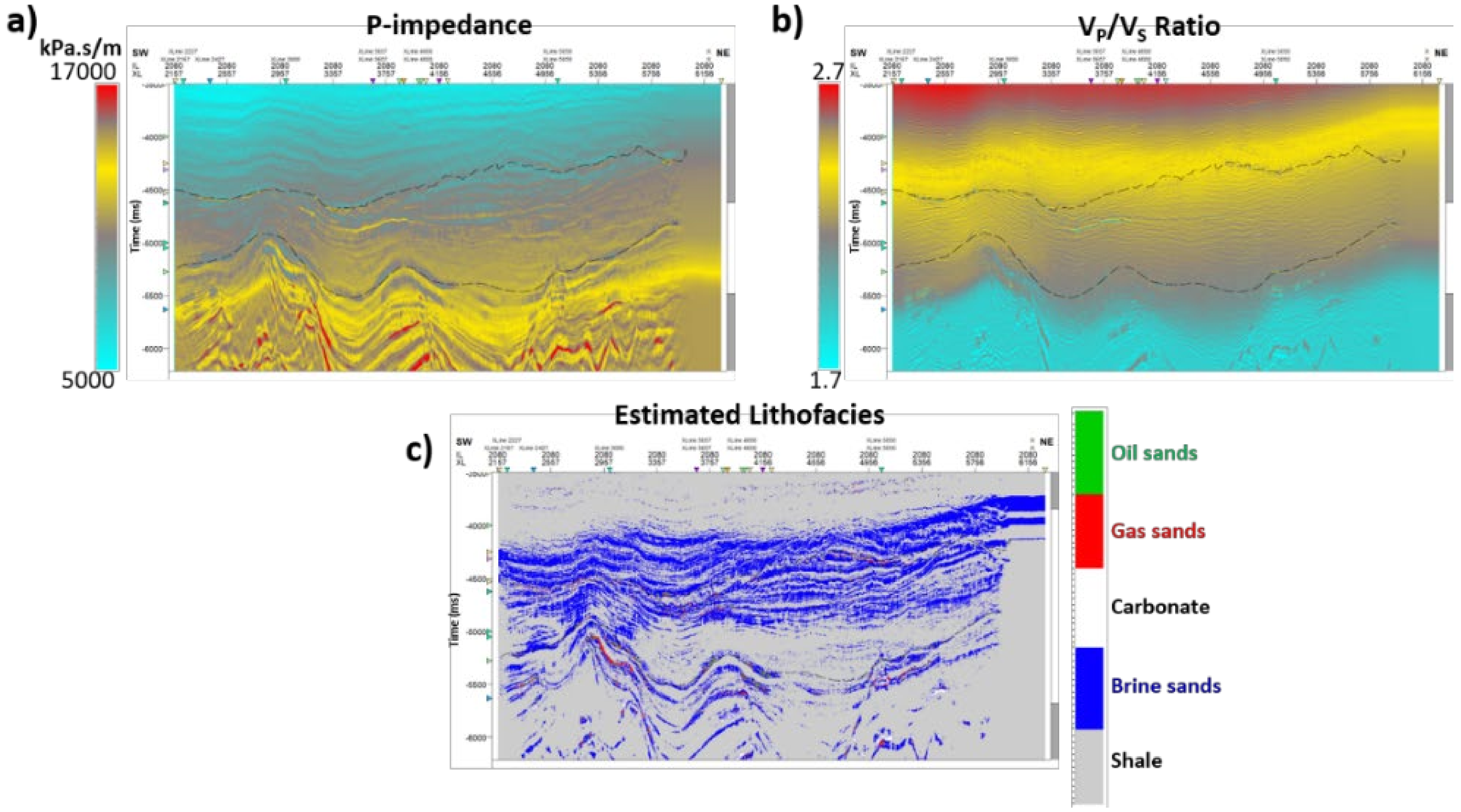

Figure 67: LE inversion results along inline 2080. (a) P-impedance, (b) VP/VS ratio, and (c) estimated lithology.

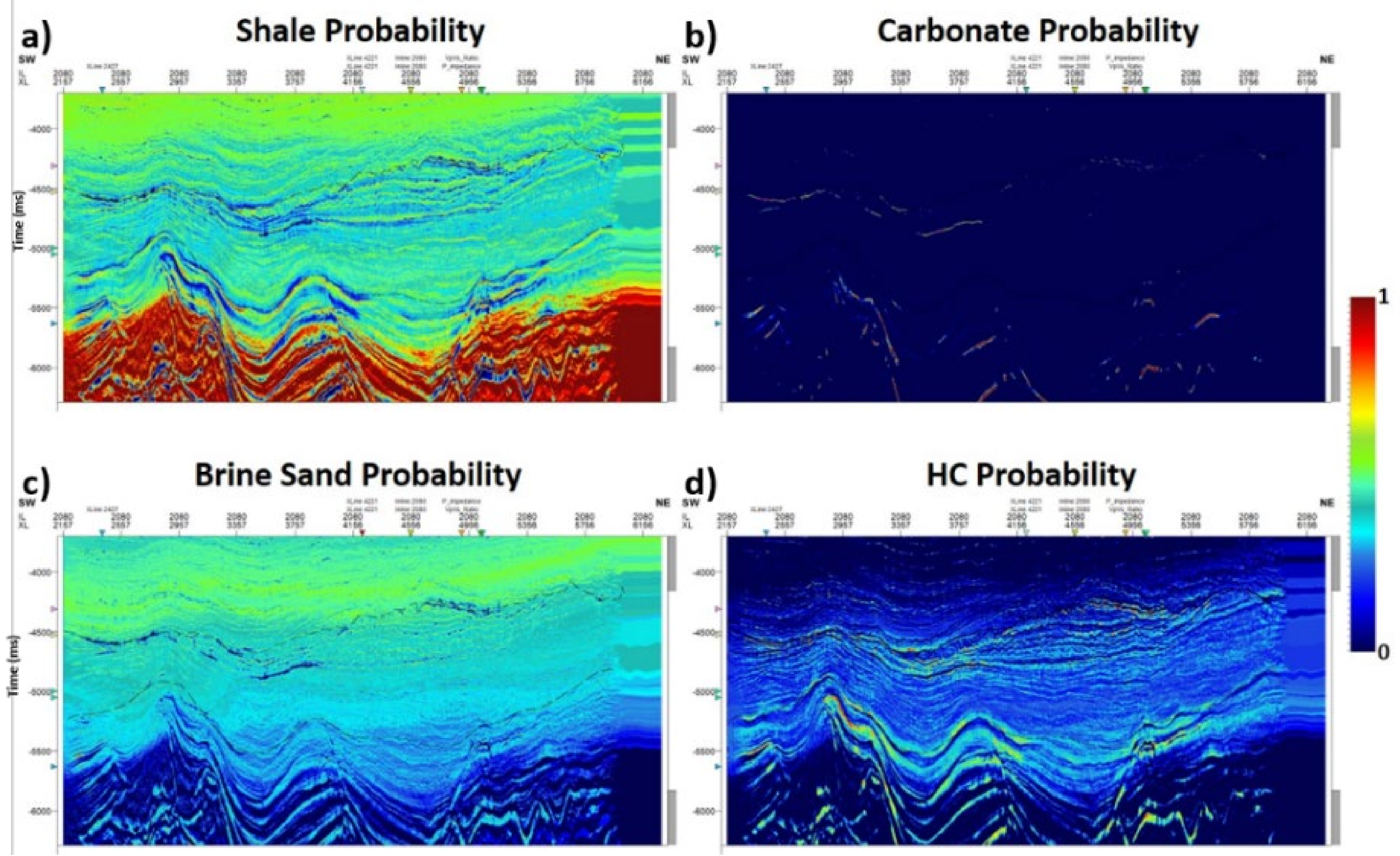

Figure 68: Estimated lithology probability of (a) shale, (b) carbonate, (c) brine sand, and (d) HC sand along inline 2080.

Conclusions

The following section outlines the potential leads (Figure 69) found through a preliminary evaluation of the reprocessing, AVA, and inversion data. Examples of this data, for each of the leads, are available in the figures below. The uplift in data resolution has provided significant data quality improvement, specifically within the deep Cretaceous and Jurassic sections. The LPE imaging, combined with the use of the legacy pressure and temperature model, proved a successful test case of the technology in offshore, Nova Scotia. It has reconfirmed the Cretaceous and Tertiary Cayuga amplitude anomalies and revealed some new interesting anomalies in the Jurassic, that are encouraging from a source rock perspective. The main characteristics present in these anomalies are summarized in Table 3.4 This section will review two of the above leads; (1) the Jurassic reefal build-up and (2) Cayuga turbidite onlap.

Table 3.4: Table summarizing the main characteristics, ages, and depths of the five potential leads..

	Lead	Characteristics	Lead Age	Lead Depth	Water Depth
1	Jurassic Reefal Build-Up	•Flat spot within a reef morphology •Clean internal seismic character • Phase reversal at edges • Lensoid in shape • Type 4 anomaly with a strong negative intercept and a positive gradient • High P-impedance rock overlaying compliant zone with anonymously low VP/VS ratio	Pre J-163	5425 m	1750 m
2	2nd Jurassic Reefal Build-Up	• Flat spot • Phase reversal at its edges • Negative intercept with a positive gradient • Gathers exhibit peak with overlying trough, dimming with offset	Pre J-163	5100 m	1640 m
3	Cayuga Turbidite Onlap	• Downdip termination of the amplitudes • Intervals have clear onlap onto a steep margin • Channel like features exhibit clear amplitude shut offs, high P-impedance and high Vp/Vs ratio • Gathers dim with offset	T50 and K94	2900 - 4100 m	1100 - 1650 m
4	Pre-Salt Muskat	• ~ 20 km2 fault-dependant, 3-way closure along the base salt surface • Overlying salt layer welded out or very thin	Synrift Triassic	5100 m	1575 - 1775 m
5	Jurassic Gas Traps	• Two layers of potential gas charged sands trapped by the structure created by the salt, dependant on fault closure to the south • High impedance overlying a low impedance zone. • Gathers dim with offset	Pre J-163	4600 - 5100 m	1800 - 1900 m

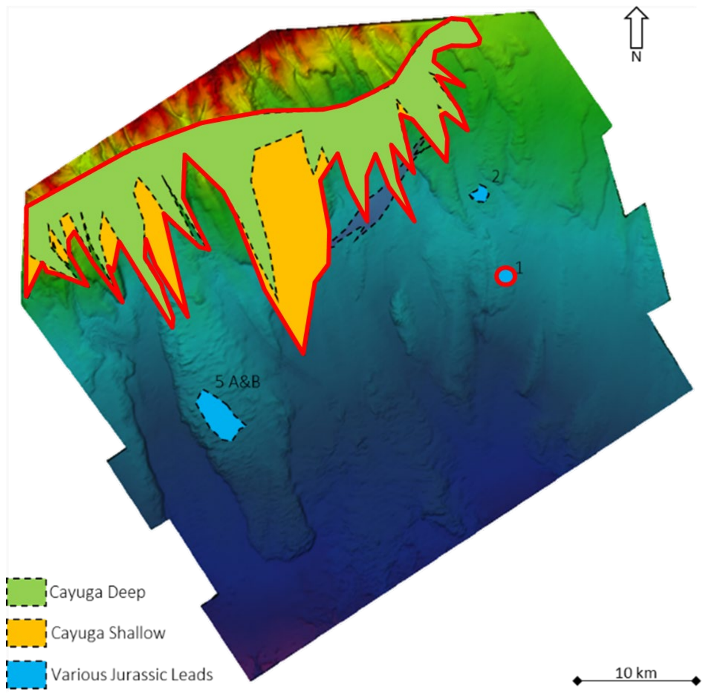

Figure 69: Outline of the 5 potential lead areas atop the seafloor depth structure map. Two leads discussed here outlined in Red.

Jurassic Reef Build-Up

Lead 1 (Figure 69) is a flat spot within a reef morphology. It has a clean internal seismic character and an interesting phase reversal at its edges that may indicate a hydrocarbon contact. In Figure 70, the plan view map indicated the anomaly is lensoidal in shape and consistent geometrically with other deep-water carbonate discoveries such as the Aptian Ranger discovery in Guyana. Interpretation suggests this reef formed during, or before, the Callovian and was deposited at a time of shallow water depths with a nearby well, Monterey Jack providing corroborating evidence for limestones, carbonates and marls at this time. This feature is located on the carbonate foreslope, basinward of the Abenaki carbonate bank. RMS extracts of horizons through the Oxfordian and Callovian (Deptuck, 2020) clearly show the slope morphology and reef margin positions with lower slope isolated features during this time. The gross depositional environment map indicates a dendritic carbonate reef or lagoon being the dominant environment at the time.

This feature exhibited a type 4 AVO anomaly with a strong negative intercept and a positive gradient, as seen in Figure 71. The inverted elastic parameters show high P-impedance rock (Figure 71 D) overlaying a very compliant zone with anomalously low Vp/Vs ratio (Figure 71 E). This is consistent with rock physics model values of a carbonate overlying a charged gas sand (or an analogous carbonate overlying a more porous carbonate). Gathers exhibited a top trough, overlying a peak, with both gathers dimming with offset (Figure 71 C). While this feature would likely not be of commercial size, at ~1.5 km2 and 100 m thickness, it does provide clear and encouraging support for a working thermogenic Jurassic charge system.

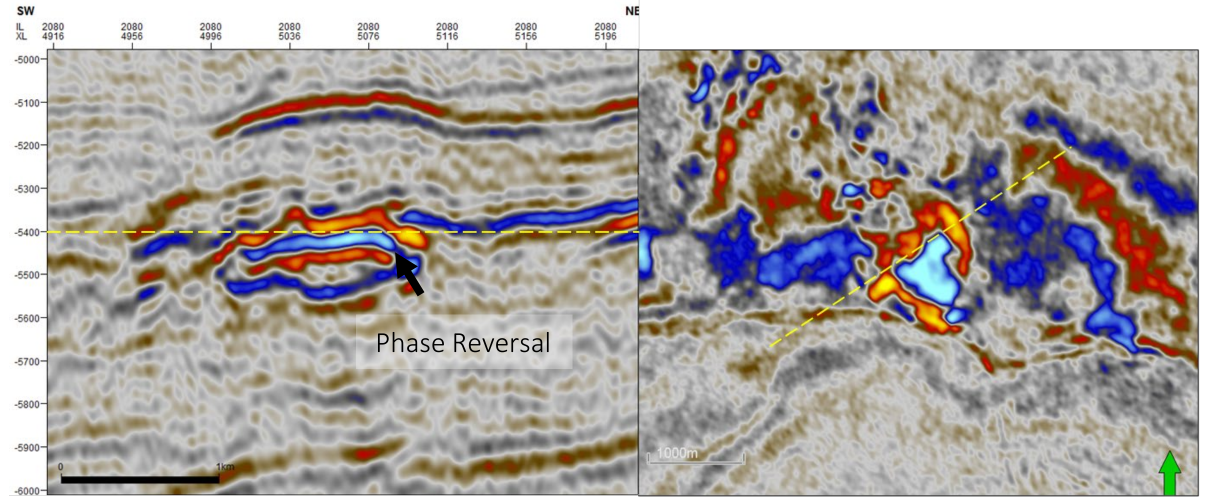

Figure 70: Cross-section along inline 2080 showing the phase reversal potentially indicating a hydrocarbon contact, as well as the lead in plan view at -5400 m highlighting its lensoidal shape. The yellow hatched lines indicate the location of the cross section or time slice on the corresponding image.

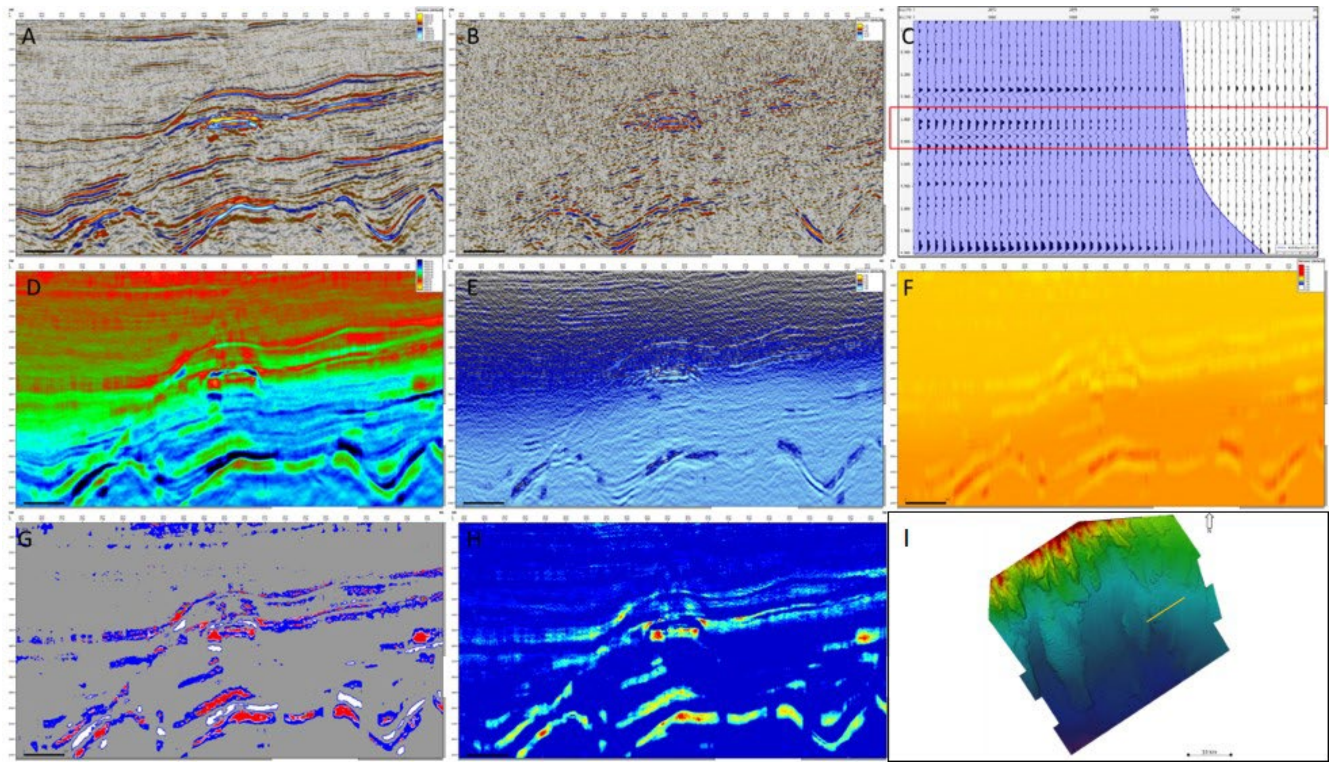

Figure 71: Cross-section along inline 2080 showing (A) KPSDM stack stretched to time, (B) AVA gradient, (C) gathers, (D) inverted P-impedance, (E) inverted V_P/V_S ratio (F) inverted density, (G) estimated lithology, (H) Hydrocarbon Probability and (I) location of seismic line

Cayuga Prospect

The multi-level Cayuga prospect, described in Section 1 above, was first identified by Deptuck et al. in 2015. It occurs throughout the shelf to slope transition along the entire Barrington survey. The downdip termination of the amplitudes corresponding to the Upper Cretaceous K94 and Early Tertiary T50 horizons are still clearly evident on the reprocessed 3D; with the lower Cayuga interval appearing to have two intervals of these terminations, seen in Figure 72. The intervals have clear onlap onto a steep carbonate margin, with these channel like features exhibiting clear amplitude shut offs, especially within the Cayuga Deep (K94) interval. Given the ages of these sediments, these lower anomalies are likely associated with the Logan Canyon Member channel turbidites, a part of the long lasting Sable Delta.

Observing the amplitudes closest to the shelf in Figure 73 A, there is a scour surface potentially creating a lateral seal across these amplitudes. In addition, the amplitude termination below this interval could infer there is an adequate bottom seal as well. These potential trapping geometries within the onlapping features could help reduce the lateral and top seal risk. Cayuga is analogous to the Jubliee discovery offshore Ghana and has a similar regional setting and charge/trap configuration. Small pods of Early Jurassic sediments could potentially provide charge to the Cayuga turbidite channels, if a source is present.

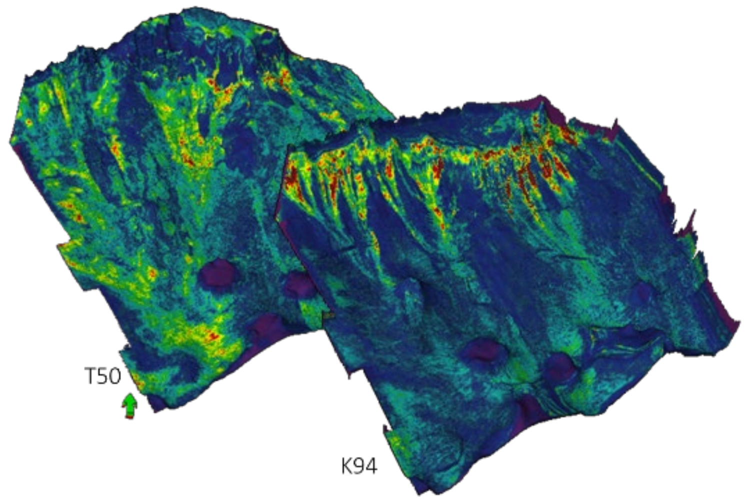

Figure 72: RMS extracts from the reprocessed seismic of the T50 and K94 horizons.

The inversion results along the Cayuga prospect indicate they are associated with high P-impedances and high Vp/Vs ratios (Figure 73 C and D). The gathers dim with offset, with the lithoclass indicating the amplitudes are associated with a high impedance carbonate or shale. The inverted lithoclass cube identifies the sediment below the anomalous amplitudes as potential gas sands. These anomalies need further work to understand the complicated morphologies and AVO response to assess its full hydrocarbon potential. The seismic termination is clear but the predicted lithoclasses for the features do not support reservoir facies being present.

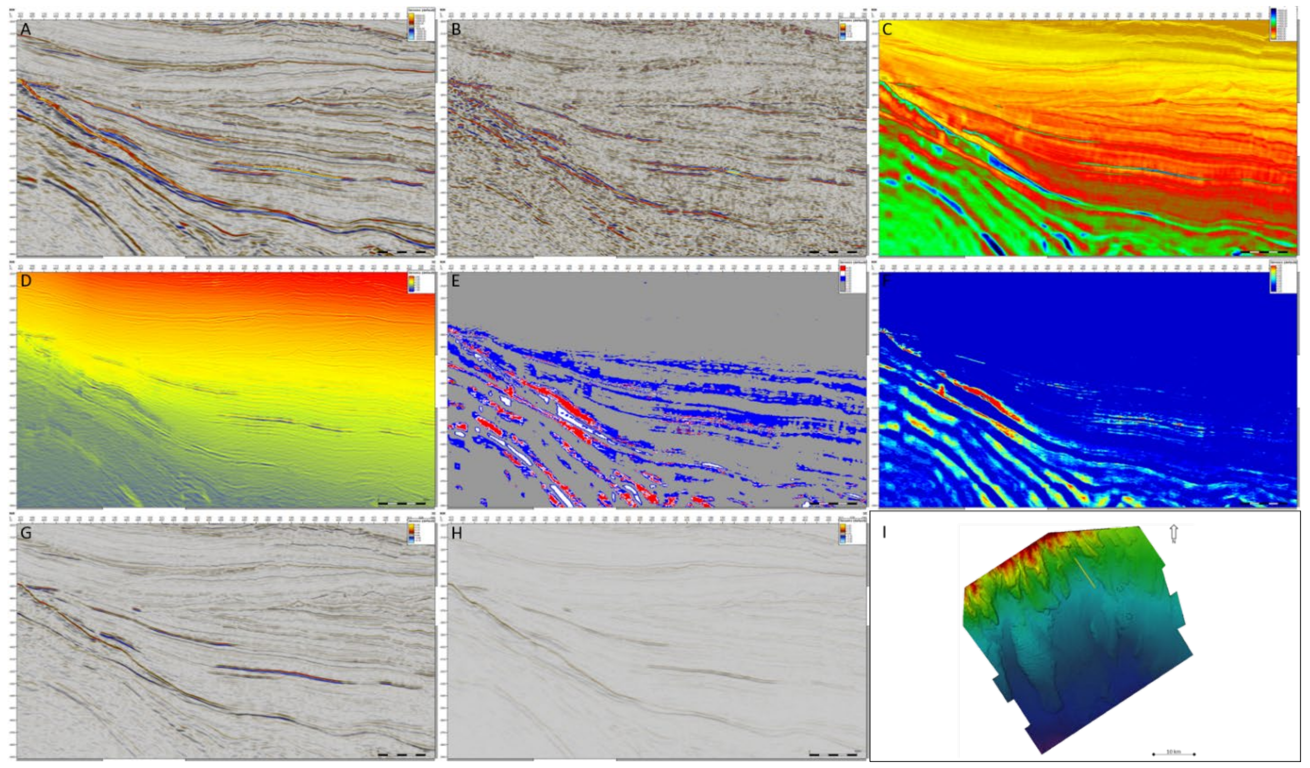

Figure 73: Cross-section along Xline 4800 showing (A) KPSDM stack stretched to time, (B) AVA gradient, (C) inverted P-impedance, (D) inverted VP/VS ratio, (E) estimated lithology, (F) Hydrocarbon Probability, (G) Near stack, (H) Far stack, and (I) location of seismic line